Characterising groundwater-surface water interaction using fibre-optic distributed temperature sensing and validating techniques in Whakaipo Bay, Lake Taupo, New Zealand

Master's thesis

Jelmer Klinkenberg
MSc. Water Science & Management
Faculty of Geosciences
Utrecht University
November 2015

Characterising groundwater-surface water interaction using fibre-optic distributed temperature sensing and validating techniques in Whakaipo Bay, Lake Taupo, New Zealand

In partial fulfilment of the requirements for the degree

Master of Science in Water Science and Management

Final master's thesis

Author:	Jelmer R. Klinkenberg
Student number:	4044843
University:	Utrecht University
Faculty:	Faculty of Geosciences
Study:	MSc. Water Science and Management
Course code:	GEO4-6004
Credits:	45 ECTS
Internship:	Royal HaskoningDHV
Email:	jelmerklinkenberg@gmail.com / j.r.klinkenberg@students.uu.nl
Phone number:	+31 6 17183596

University supervisor:	prof. dr. ir. Marc F.P. Bierkens Chair of Department of Physical Geography at Utrecht m.f.p.bierkens@uu.nl
Supervisor Royal Haskoning:	ir. Floris Verhagen Senior Consultant (geo-) hydrology at Royal HaskoningDHV floris.verhagen@rhdhv.com
Supervisor GNS Science	dr. Stewart Cameron Senior Scientist, Head of Department of Hydrogeology of GNS Science, New Zealand s.cameron@gns.cri.nz

Universiteit Utrecht

Faculty of Geosciences

Royal HaskoningDHV

Enhancing Society Together

GNS SCIENCE TE PŪ AO

ABSTRACT

Lake Taupo, the largest lake of New Zealand, is blessed with good water quality. However, over the last decades the natural system is under pressure from increased dairy-farming. These agricultural activities primarily export nutrients to the groundwater system, which transports it to the lake. This can possibly have detrimental effects on lake ecology, tourism and animal and human health. Since the sources of nutrients around the lake are numerous and diffuse, some of the methods that have been developed under the SMART Aquifer Characterisation Programme are possibly suitable for developing rapid and cost-effective characterization of the groundwater systems around the lake.

This thesis is a follow-up study of Meijer (2014) and will characterize groundwater-surface water interaction using fibre-optic distributed temperature sensing and validating techniques in Whakaipo Bay, Lake Taupo. To map and quantify the seepage flows into the bay, high-resolution spatial and temporal temperature measurements were conducted and linked to direct seepage measurements and a heat transport model. The seepage areas detected by horizontal distributed temperature sensing were validated using seepage flow calculation by vertical temperature sensing. These flows were extrapolated across the shallow part of the bay and the total seepage flow was compared to water balance studies. Ultimately, a direct way was investigated to detect seepage areas and calculate seepage flows by horizontal distributed temperature sensing.

Temperatures on the sediment-water interface near the shore of Whakaipo Bay vary between 15 and 22 °C. The cold spots are characterised by high seepage flows and rates differ notably throughout the bay. The seepage rates measured by vertical DTS range vary between $0.253\ \mathrm{cm^3/m^2/s}$ and $0.736\ \mathrm{cm^3/m^2/s}$, whereas the rates by the seepage meter are factor 4 smaller at high-flow seepage locations and almost similar at low-flow locations. Although the seepage meter might underestimate the high-seepage flows, the heat flux modelling results approximate the vertical DTS flow rates. The average flow for the area shallower than 6.5 meter depth is $0.141\ \mathrm{m^3/s}$, which is 41% of the seepage component in the water balance. However, it is unlikely that the seepage areas examined in this research are the only major source of seepage. Seasonal variability might affect the seepage as well.

Key words: Groundwater surface water interaction; Fibre optic distributed temperature sensing; DTS; SMART; seepage flow; seepage meter; heat transport models; spatial variability; water balance; Whakaipo Bay; Lake Taupo; New Zealand

ACKNOWLEDGEMENTS

This report presents this research done on groundwater-surface water interaction, in order to obtain the degree of Master in Water Science and Management at the faculty of Geosciences of Utrecht University. The research was conducted at GNS Science in Wairakei, New Zealand. I would like to thank everyone from the Hydrogeology Department for their help and other GNS staff who answered questions and helped me with practical aspects. I would like to thank the Head of the Hydrogeology Department, my supervisor Stewart Cameron, for his guidance, tips and feedback. Further I would especially like to thank Abigail Lovett, Katherine Aurisch, Kolja Schaller, Kuini Dewes, Marc Reidi and Rogier Westerhoff for their support in the field and in the office. I would like to thank my supervisor Floris Verhagen from engineering consultancy Royal HaskoningDHV for his valuable suggestions, feedback and help with practical matters. Also, I would like to thank my university supervisor Marc Bierkens, for his ideas and feedback throughout the thesis period. Also, I would like to thank NIWA groundwater scientist Max Gibbs for helping me with the equipment for the seepage meters. Lastly, I would like to thank my friends in New-Zealand and my parents and friends in the Netherlands, who supported me where possible.

TABLE OF CONTENTS

LIST OF ABBREVIATIONS

DTS	Fibre-Optic Distributed Temperature Sensing
GW-SWI	Groundwater-surface water interaction
H-DTS	Horizontal DTS
Q	Flow rate (Q [m^3/s])
q	Flux (q [$m^3/m^2/s$])
RHDHV	Royal HaskoningDHV
SAC	SMART Aquifer Characterisation
SMART	Save Money And Reduce Time
SPM	Seepage meter
SWI	Sediment-water interface
T	Temperature (T [°C])
V-DTS	Vertical DTS

LIST OF FIGURES

LIST OF TABLES

1 INTRODUCTION

1.1 Background

Water quality in Lake Taupo, the largest lake of New Zealand, is very high. Unfortunately, both quality and clarity of the lake have deteriorated during the last 50 years due to increased nitrogen loads by land use intensification (Hadfield, 2007). Historically, low nitrogen loads were measured, but these concentrations are increasing and will cause further deterioration and eutrophication (Hadfield, 2007). Over the last 50 years scrublands and forests have been converted to agriculture in the Lake Taupo catchment, which has caused an increased fertiliser use and higher levels of nutrients leaching to groundwater and waterways (Morgenstern and Daughney, 2012). Because of the arrival of nitrate by groundwater seepage to the lake, nutrient loads are increasing and the water of Lake Taupo is deteriorating (Morgenstern, 2008). A further decline in the quality of the lake is to be expected (Hadfield, 2007), even if adaptations to land use and farming practices are made, due to the long lag time (>100 years) of impacted groundwater discharging into the lake (Hadfield, 2007). Environment Waikato imposed a policy change in order to maintain water quality at its current level. Nitrogen loads to the lake should be reduced with 20% by 2020 by the conversion of pasture to alternative land uses such as forestry, the use of new farming practices or crops and upgrades to wastewater treatment facilities (Wildland consultants, 2013).

As groundwater systems are complex, difficult to understand and generally poorly understood, multidisciplinary approaches are necessary to predict future groundwater nitrogen loads to surface water (Morgenstern, 2007). Improved characterisation of the groundwater in New Zealand is necessary as increasing nitrogen loads in lakes and rivers is recognised as a national issue. Agricultural and consumptive use of groundwater is predicted to increase, which will put additional pressure on the available groundwater and further increases the need to understand the systems (GNS Science, 2011).

Water management decisions are often made with incomplete knowledge of basic characteristics of groundwater aquifers. Hence, in 2011 the project SMART (Save Money and Reduce Time) Aquifer Characterisation (SAC) project was initiated by New Zealand and European Union (EU) research partners (GNS Science, 2011). The New Zealand Crown Research Institute GNS Science, which is involved in geology, geophysics, nuclear science and geohydrology, was awarded funding and lead for this project by the Ministry of Business, Innovation and Employment (MBIE). One of the EU partners is Dutch engineering consultancy Royal HaskoningDHV (RHDHV). Not only in New Zealand, but

worldwide concerns are growing on groundwater and lake water quality because of increasing nutrient rates. RHDHV focuses on sustainable water supply and water management, which can be an inspiration for Dutch or European conditions. Furthermore, it connects New-Zealand's and European researchers and it connects the cultural values of the Maori to protect earth and water (Verhagen, 2014).

SAC aims to develop a set of innovative methods which will help to better understand New Zealand's groundwater systems (GNS Science, 2011). The project focuses on techniques that passively provide data, because traditional methods are too expensive and too time consuming. This means that data is used that already exists or can be retrieved from new cost-effective measurements. The groundwater characteristics that are intended to be measured are volumes, flow rates, directions, age and the exchange between surface water and groundwater. The methods are transferrable to other regions and future application will contribute to improved water management at the national scale.

The focus in this research will be on the interaction between groundwater and surface water. The locations and volumes of flows across the groundwater-surface water interface are unknown, in addition to the interchange of groundwater with streams, rivers and lakes. Traditionally, the interchange of flows of water in or out of a stream are quantified by gauging surveys, which compare the flow rate between two stream reaches, or methods such as salt or dye dilution (Briggs et al., 2012). These methods are time consuming, expensive for widespread use and most importantly, have a low spatial and temporal resolution.

To address the limitations of traditional methods, SAC trialled the use of fibre-optics distributed temperature sensing (DTS). This method uses heat as a tracer for groundwater movement to surface water. The use of heat as qualitative indicator of groundwater flow to surface water was recognised 150 years and has been used as a groundwater tracer ever since (Thoreau, 1854; Anderson, 2005). Horizontal DTS makes use of a fibre optic cable up to 30 km long, which can be deployed on the bed of a water body. The temperature of the water can be determined by the back-scattering of light through the cable (Selker et al., 2006). The temperature at approximately meter interval along the cable is measured, with a thermal resolution of 0.01°C. Groundwater typically is colder than surface water in summer and warmer during winter. This temperature difference can be used to locate and quantify groundwater inflow to a surface water body (Anderson, 2005).

In addition to horizontal DTS, a vertical DTS technique can be applied to further investigate groundwater movement to the surface water (Meijer, 2014). In this technique a frame, around which a fibre-optic cable is wrapped, is temporarily installed on the bottom of a water body, to detect the smallest temperature anomalies in the water layers closest to the sediment-water interface. Horizontal DTS is able to detect groundwater seepage zones by temperature differences in a horizontal direction, whereas vertical DTS can further investigate and quantify the seepage flux using a displacement method or heat-conduction modelling. The vertical and horizontal DTS can be combined to provide an estimate of spatial fluxes and flow rates.

One case-study site, Whakaipo Bay, Lake Taupo, was selected to test and validate temperature sensing techniques. Groundwater inflow measurements were undertaken previously in this bay, but this project also aimed to improve knowledge of groundwater-surface water interaction processes in the bay.

Research has been previously conducted in Whakaipo Bay by Hector (2004), Gibbs et al. (2005) and Meijer (2014). Hector (2004) researched the shallow lake-edge seepage rates by seepage samplers and benthic chambers. Gibbs et al. (2005) examined Whakaipo Bay by manually detecting seepage areas by divers and installing seepage meters. Meijer (2014) examined Whakaipo Bay using horizontal- and 18 vertical DTS measurements to detect groundwater seepage areas. The research in this study builds directly on Meijer (2014).

Hector (2004) and Gibbs et al. (2005) produced the initial water balance for the Mapara Stream catchment, which was later validated by Blume et al. (2013). Hector (2004) estimated that shallow groundwater seepage, which was defined as the area with a water depth of <1 meter, accounts for 5% of the groundwater derived water volume of Lake Taupo. This leaves an estimated 95% from deep (water depth >1 meter) groundwater seepage. Diffuse areas of deep groundwater inflow were found between 2 meters and 6.5 meter depth and the size of these areas varies heavily (Gibbs et al., 2005). The water depths correspond with the water depths of the large groundwater inflow area identified by Meijer (2014). Hector (2004) estimated that the deep groundwater inflow rates are $0.25\ \mathrm{m^3/m^2/s}$. Because colder groundwater is heavier than warmer surface water, the groundwater flows in a thin layer down the slope of the bed of Lake Taupo and pools in depressions (Gibbs et al., 2005).

1.2 Research questions

The following research questions have been proposed for this study to further characterise the groundwater-surface water interaction using fibre-optic distributed temperature sensing and validating techniques in Whakaipo Bay, Lake Taupo:

1 **Horizontal temperature profiling**

To what extent are seepage areas in Whakaipo Bay detectable by horizontal DTS?

2 **Vertical temperature profiling**

To what extent is vertical deployment of DTS, validated with a numerical model, temperature loggers and seepage meters, able to quantify the seepage flow in different parts of Whakaipo Bay?

3 **Improving DTS**

To what extent could horizontal DTS be improved to directly detect seepage areas and quantify seepage flows in lake environments?

4 **Spatial variability**

To what extent is DTS able to calculate the seepage component of the water balance by extrapolation of seepage inflow into Whakaipo Bay?

1.3 Aims

The following aims underlay the research questions, described in the paragraph 1.2.

1. **Horizontal temperature profiling**

   Meijer (2014) used horizontal DTS in combination with vertical DTS in Whakaipo Bay to assess the applicability and suitability of DTS in locating groundwater seepage areas in lakes. The goal of this sub-research is to get a better overview of the usability of horizontal DTS in detecting groundwater inflow zones and to get an insight in the spatial variability of seepage in Whakaipo Bay.

2. **Vertical temperature profiling**

   The goal of this sub-research will be to get better insight in the usability of vertical DTS in quantifying groundwater inflow zones and to get a better overview of the spatial variability of groundwater inflow in Whakaipo Bay.

A notable presence of pockmarked depressions and accumulated algae exists in Whakaipo Bay, as explained by Gibbs et al. (2005) and Meijer (2014). These pockmarked depressions might be indicators of groundwater seepage areas because of the nutrient needs of the algae. Within this sub-research will be examined whether these depressions are hotspots for groundwater seepage.

Meijer (2014) developed a 1D flux determination model to model groundwater flow from the lakebed to the lake, using temperature change over time and depth. Both DTS data and the model would be more trustworthy if the outcomes are compared with traditional proven methods, such as the comparison of DTS fluxes with seepage meter fluxes that was made by Lowry et al. (2007). To increase the applicability of the model, the DTS measurements will be compared to the results of

- Vertical DTS temperatures
- Temperature logger measurements, another temperature-based method.
- Seepage meters, which are able to directly measure groundwater flows.

3. **Improving DTS**

   Vertical DTS measures temperatures at groundwater inflow locations that are detected by horizontal DTS. The aim of this research is to examine to what extent these techniques could be linked to make horizontal DTS able to allow an informed estimate of seepage inflow using a correlation between temperature and flow rate.

4. **Spatial variability**

   The aim of this sub-research is to examine the spatial variability of groundwater inflow areas into Whakaipo Bay and to estimate the seepage flow into the whole bay. The quantified seepage flow can be useful for local authorities. Aimed is to give an interpolation of the measurements between the V-DTS locations, to show the flows along the cable, whereas a further extrapolation of the flows into the bay estimates the total seepage flow over Whakaipo Bay. Aimed is to compare the extrapolated seepage rate to a water balance based seepage rate in an uncertainty analysis.

2 THEORY

2.1 Groundwater-surface water interaction

Surface water and groundwater used to be considered as separate entities. It was common to study these entities independently from each other for a long time (Kalbus et al., 2006). Groundwater is defined as *"water below the earth's surface (subsurface) in the pore spaces between rocks and soils"* (Hamblin and Christiansen, 1995).
Surface water is defined as *"the waters of all sources, flowing in streams, canyons, ravines or other natural channels, or in definite underground channels, with the exception of effluent, whether perennial or intermittent, flood, waste or surplus water, and of lakes, ponds and springs on the surface"* (Rahman et al., 2009). Interaction between surface water and groundwater occurs by *"subsurface lateral flow through the unsaturated soil and by infiltration into or exfiltration from the saturated zones"* (Sophocleous, 2001). The ecological status of an open-water body is crucially dependent on the transition zone between surface water and groundwater, which is known as the hyporheic zone (Vogt et al., 2010). The outflow of nutrients and pollutants occurs within this zone.

There are two important pathways that nutrients use to reach a surface water body, or a lake, in the context of this study. Groundwater-fed streams indirectly reach the lake surface, whereas groundwater seepage through the lakebed occurs directly (Briggs et al., 2012). Seepage through the soil to the lake occurs through the sediment-water interface (SWI). The seepage zone is defined as the area in which groundwater enters other water bodies (Hector, 2004). Highest seepage rates into a lake are generally found on lake edges (Blume et al., 2013). When seepage is mentioned throughout this report, seepage into the lake is meant. Since the 1960's, the interaction between lakes and groundwater has been studied as a consequence of concerns about acid rain and eutrophication (Sophocleous, 2001). Eutrophication is defined as *"the increase in trophic condition of a water body resulting from increased levels of plant macro-nutrients in both freshwater and marine ecosystems"* (Wetzel, 2001). Eutrophication happens naturally, but can be influenced by human activities. The way water bodies respond to eutrophication depends on its physical, chemical and geological characteristics (Steckis et al., 1995).

Water always moves from locations with a high hydraulic head to locations with a lower hydraulic head (Stronestrom and Constantz, 2003). Hydraulic head is defined as elevation head summed with pressure head. At the surface water level the pressure head, with respect to the atmospheric pressure, is zero. Therefore the elevation of the water table relative to the lake surface indicates the direction of the subsurface flow. Blume et al.

(2013) uses DTS to validate that highest seepage rates in a sandy lake environment are found on the lake edges (McBride and Pfannkuch, 1975; Winter et al., 1998).

The process of exchange between the surface water and groundwater varies over time and space (Vogt et al., 2010). Studying groundwater-surface water interaction (GW-SWI) has been limited by the lack of possibilities to measure on a larger spatial scale. If point measurements would be used, this requires hundreds of thousands of sensors to only cover a small area (Selker et al., 2006). In the past decade many new technologies for this hydrological research have been developed, e.g. remote sensing and DTS.

2.2 Research on groundwater-surface water interaction

Several methods exist to examine seepage flows to water bodies. Traditionally, these flows have been estimated using a water balance and meteorological approaches. When subtracting stream discharge and actual evapotranspiration from the incoming precipitation, the seepage component could be estimated for a specific area (Rudnick et al., 2015; Yang et al., 2015). Other techniques that are used to investigate groundwater-surface water interaction are seepage meters and flow gauging (Lee, 1977; Lowry, et al., 2007; Rosenberry, 2008, González-Pinzón et al., 2015). A relatively new method to investigate GW-SWI is DTS, a method which uses heat as tracer and which can be used to further investigate possible seepage locations and flows. Groundwater temperatures remain quite stable during the year in the Lake Taupo region, at approximately 12 °C. In contrast, surface water temperatures fluctuate daily and seasonally. As a consequence, differences in groundwater and surface water temperatures can be used to research GW-SWI. In New Zealand, surface water temperatures are highest in summer and are approximately 20 °C (Gibbs et al. 2005). Water temperatures in Lake Taupo are not related to its age, but amongst other to its origin (Morgenstern, 2008). The summer months are the best months to measure GW-SWI using heat differences as a tracer, as this is the period when the temperature contrast between groundwater and surface water in greatest.

2.2.1 Fibre-Optic Distributed Temperature Sensing

Heat has been used as a tracer in hydrological systems for a long time (Anderson, 2005). Using temperature as a natural tracer for the purpose of examining GW-SWI is attractive as temperatures are easily to measure. The last 40 years fibre-optic temperature sensing methods have been developed (Tyler et al., 2009). Normally, temperature measurements are taken at several depths at one location. The seepage flow then is calculated by using

an analytical solution, time series analysis or a groundwater flow and heat transport model (Lowry et al., 2007).

DTS helped to increase the spatial and temporal coverage of temperature measurements in hydrogeological investigations (Selker et al., 2006). The differences in groundwater and surface water temperatures help to identify spatial patterns of groundwater seepage by tracing temperature anomalies at the sediment-water interface (Blume et al., 2013). Temperature measurements at a high resolution in both space and time are possible with DTS. DTS systems send a light pulse down to the end of a fibre and determine the temperature along the fibre by measuring the ratio of temperature independent Raman backscatter (Stokes) to temperature dependent backscatter (anti-Stokes) of the light pulse (Selker et al., 2006; Lowry et al., 2007; Tyler et al., 2009). The delay of the returning backscatter yields the location of the measurement. To reduce instrument noise, measurements along each meter of fibre are averaged over a specific time period.

Horizontal deployment of DTS cables (H-DTS) has led to insights into hydrological processes occurring on the local scale, which were not possible to resolve with traditional temperature-measurements (Mwakanyamale, 2013). The quality of the measurements depends on the DTS instrument, field-deployment configuration and instrument calibration (Hausner et al., 2011). Instruments for DTS are available with a thermal resolution of 0.01 °C and a spatial distribution of 1 meter up to lengths of 30 km (Selker et al., 2006).

Vertical DTS (V-DTS) measurements can be placed on distinctive colder spots detected by horizontal DTS, to acquire a vertical temperature profile of that specific location and to examine the seepage flow rates. Many researches use a convection-conduction equation to calculate the flow rate retrieved from temperature data (Anderson, 2005; Vogt et al., 2010).

It may be hard to determine the exact extent of seepage areas in lakes using temperature tracing techniques (Meijer, 2014). Seeping groundwater flows downwards on the sediment-water interface following the bathymetry. This is due to density differences between the cold groundwater and the warmer lake water. As a consequence, cold groundwater can be present at locations where no seepage occurs (Figure 1). If H-DTS measures low water temperatures at a location, this does not necessarily mean that this area is a seepage area. Besides, this complicates the relation between groundwater temperature and seepage flux. Hence techniques other than DTS are necessary to validate seepage rates.

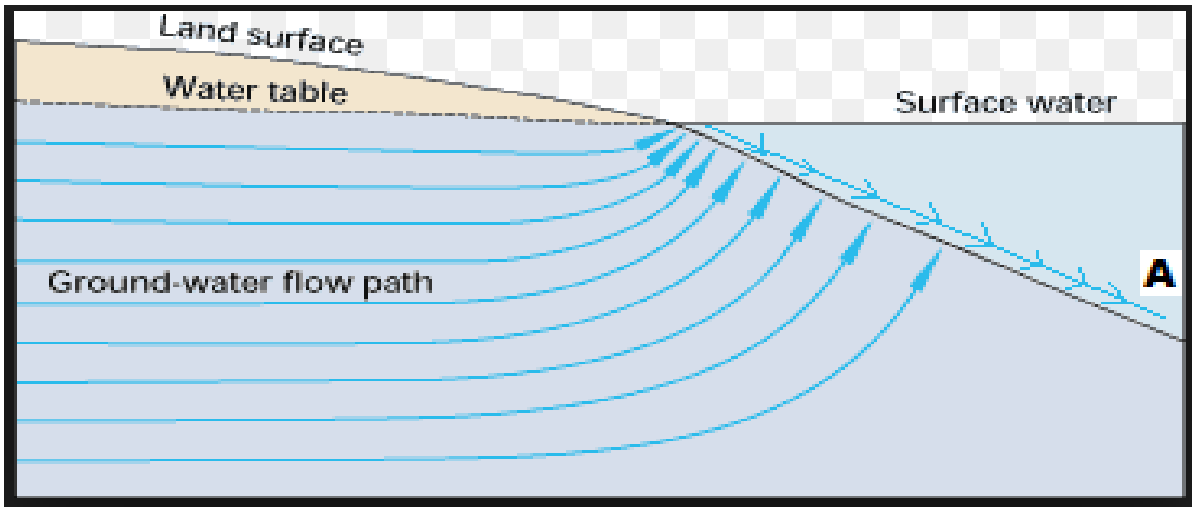

Figure 1: Groundwater flow in subsurface and lake (Winter et al., 1998, adjusted by Meijer, 2014)

2.2.2 Loggers

Temperature loggers can be used to measure temperatures at a fixed location for a set period. Loggers can be deployed in several ways to measure temperatures. One option is measuring vertical temperature profiles of a water column by fixing loggers on a rope, anchored on the bottom and using a buoy to keep the rope in its place. A way to directly measure temperatures of the groundwater is by using water level loggers in piezometers or monitoring wells. These simple and inexpensive instruments can measure the hydraulic head that drives the GW-SWI (Martinez, 2013b). This approach has the advantage of using a simple technique, which is not time-consuming and provides information on the groundwater table. However, it takes quite some effort to install and de-install them and the instruments only measure the temperature at one location.

2.2.3 Seepage meters

A common and direct way to measure GW-SWI is by using a seepage meter (SPM). They can be constructed inexpensively (Lee, 1977; Martinez, 2013a). Flow measurements from a SPM can be combined with hydraulic head measurements from piezometers to calculate hydraulic conductivity of the bottom sediments. A SPM usually consists of a bottomless cylinder vented to a deflated plastic bag (Kalbus et al., 2006). The cylinder is twisted into the sediment and collects groundwater that seeps into the surface water. The seepage flow is calculated using the collected volume of water, the cross-sectional area of the cylinder and the duration of the measurement by Equation 1:

Equation 1: Seepage flow (Brodie et al., 2009). Q is the seepage flow, V_0 is the initial volume and V_f the final volume of water in the bag, t is the duration of the measurement and A is the cross-sectional area of the chamber.

$$Q = \frac{V_f - V_0}{tA}$$

Although the use of a SPM is attractive because of its simplicity, it has drawbacks, e.g. they only measure the flow at one point in space. To be able to meaningfully interpolate flows, many measurements are necessary (Brodie et al., 2009). Additionally, in low flow environments, a long time measurement period is required to obtain a satisfactory change in bag volume in order to make reliable estimates. In lake environments, the most sensitive parameter affecting the accuracy of SPM estimates is the spatial variability of seepage flow within a small area of lakebed (Shaw and Prepas, 1990). Lastly, problems related to water flowing over the bag exist, which could fold the bag and lead to measurement errors (Isiorho and Meyer, 1999; Gibbs et al., 2005; Gibbs, personal communication, 2015;). Usually this happens in streams rather than lakes (Kalbus et al., 2006). Briggs et al. (2012) pointed out that the use of condoms as seepage bag is an appropriate way to measure seepage. However, many researches emphasize that measuring the seepage flow by using small-volume seepage bags such as condoms can cause large errors and uncertainties (Harvey and Lee, 2000; Schincariol and McNeil, 2002; Rosenberry et al., 2008).

2.3 Modelling

Groundwater seepage in a lake environment has been often modelled. The usability of the found results differs considerably between the used modes. Shaw and Prepas (1990) modelled the seepage flow to a hypothetical lake to simulate SPM measurements, using log-normally distributed seepage velocities within a small area of lakebed, and a variance which is positively correlated with mean seepage flow. However, directly modelling the seepage flow can also be done, which was done by Elsawwaf et al. (2014), who used the two dimensional groundwater flow equation by Edelman to estimate groundwater discharge to the Egyptian Lake Nasser. Meijer (2014) used a basic convection-diffusion equation to model groundwater flow based on temperature differences between water and soil.

2.4 Water balance

Water balances have been used for a long time, to get an overview of the ingoing and outgoing flows from a catchment. However, many studies neglect the input path of groundwater to lakes as a consequence of methodological difficulties in its determination (Siebert et al., 2014; Rudnick et al., 2015). Direct measurements are too labour-intensive and error prone. However, water balance studies lack a lot of adequate information about local conditions and spatial patterns.

2.5 Spatial variability

An improved way of estimating the “total” seepage flux would be to combine a water balance with insight of the spatial variability. Vertical seepage measurements such as SPM measurements and the calculated seepage from the temperature measurements of V-DTS do not give much insight of the spatial distribution of groundwater seepage across a water body. The identification of the spatial variability of the seepage flows and the quantification of GW-SWI in a lake environment is difficult to characterise (Blume et al., 2013). Interpolation can provide estimates for areas between observations (Stein, 1999). Contrary, extrapolation can estimate unknown values for areas beyond the range of known observations. Both interpolation and extrapolation can be done in various ways. Using a linear extrapolation, the known information from measurements could be extended to a larger area. However, extrapolation is a much harder problem than interpolation as the absence of nearby known data causes high uncertainty.

3 SITE DESCRIPTION

3.1 Topography

Lake Taupo is located on the central high volcanic plateau of North Island and is the biggest lake of New Zealand, having a surface area of 623 km² (Matheson et al., 2011). The lake has several river or stream inlets, of which the Tongariro River in the south is the biggest. Whakaipo Bay is situated on the north side of the lake. The only river flowing into this bay is the Mapara Stream in the northeast. The catchment of this stream is 21.6 km² in size of which 88% is in pasture. After heavy rainfall events, four ephemeral streams discharge into the bay (Lovett et al., 2015). There is one outlet of Lake Taupo: The Waikato River, which leaves Lake Taupo at the town of Taupo, flows north to 40 km south of the city of Auckland where it discharges into the Tasman Sea. The deepest point of the lake is 186 meter below the lake water surface level. Lake level fluctuates between 356 and 357 meter above sea level and is controlled for hydropower generation by control gates at Taupo township.

3.2 Geology

Lake Taupo is situated on the Taupo Volcanic Zone, a 250 km long volcanic depression which stretches from Mount Ruapehu in the south to White Island in the north on the North Island (Newson, 1993). This zone reflects the position of New Zealand on the boundary of the Australasian and Pacific tectonic plates (Hector, 2004). Multiple eruptions in surrounding vents in the area formed Lake Taupo. The lake, as it exists today, was formed approximately 26,000 years ago as a consequence of a rhyolitic eruption known as the Oruanui eruption, which was an extremely powerful eruption that blew 1300 km³ of fall deposits, magma and pyroclastic material into the air. This explosion formed the Oruanui Ignimbrite formation (Wilson et al., 2001). The most recent period of volcanic activity in the lake was 1800 years ago. This formed the Taupo Ignimbrite formation. The current Whakaipo Bay is characterised by a gradually sloping pumice beach. A layer if Taupo Ignimbrite occurs on the shoreline of Whakaipo Bay. The peninsula west of Whakaipo Bay is comprised of the 3000 year old Rhyolite lava domes, whereas the higher areas in the north-eastern parts of the catchment consist of Oruanui Ignimbrite. In the Mapara Stream catchment several older geology units occur, the Huka Falls Formation, Rhyolite (dome-related) pyroclastics, basalt, andesite lavas and pyroclastic flows (Wilson et al, 2001). The Whakaipo Bay geology is shown in Figure 2 and Figure 3.

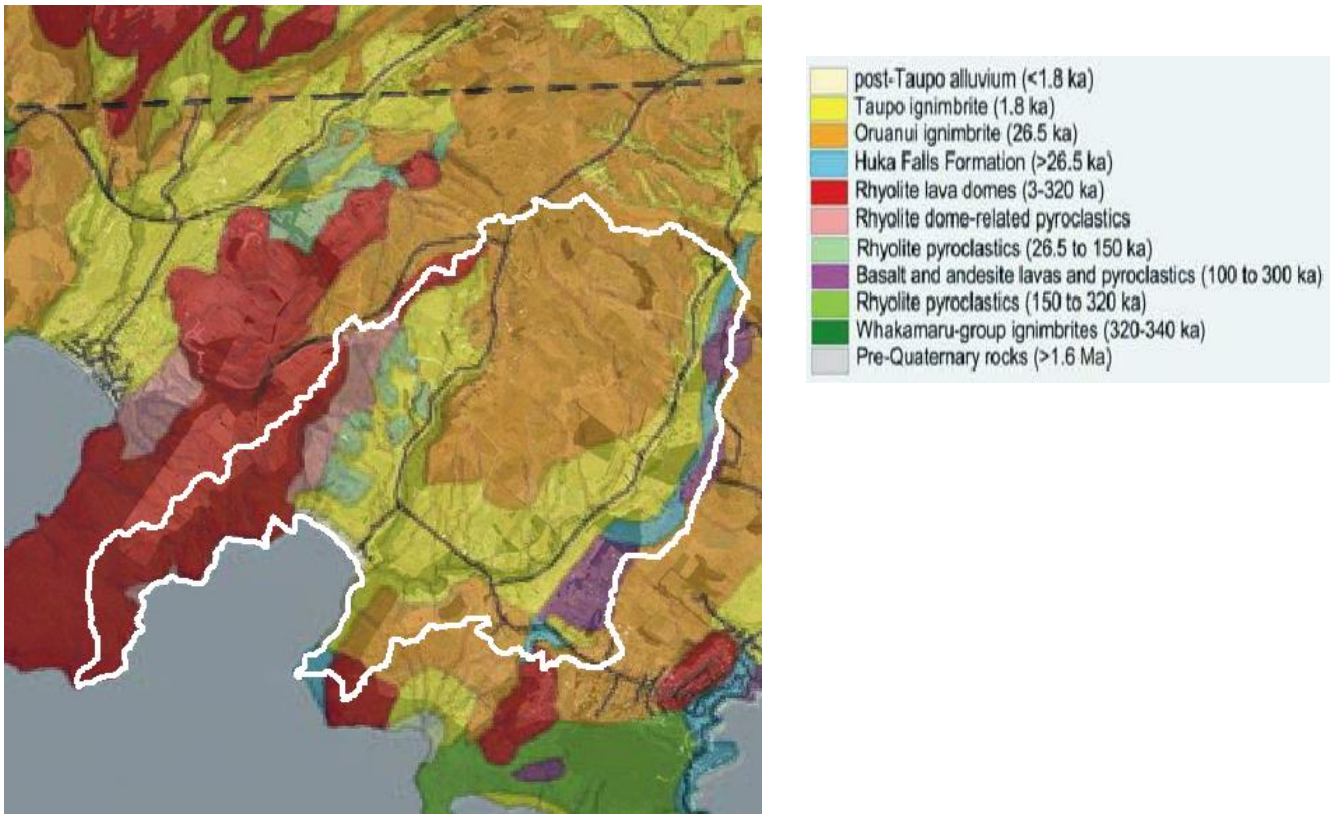

Figure 2: Geology of Whakaipo Bay and the Mapara catchment in the white outlined area (Hadfield, 2007). The dashed black line indicates the location of the cross-section shown in Figure 3

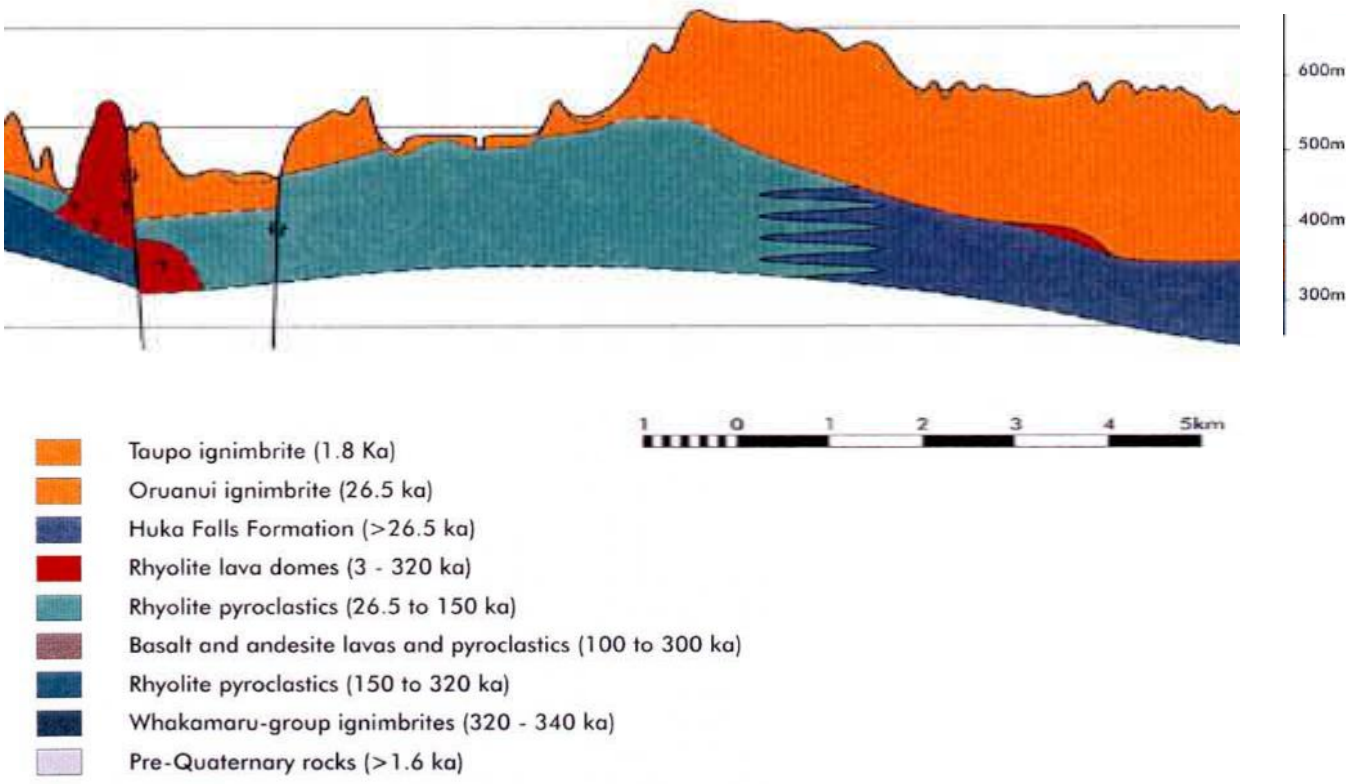

Figure 3: Cross-section of the geology north of the Mapara catchment (Hadfield, 2007)

3.3 Hydro-geology

The geology heavily influences the hydrology of the Mapara Stream catchment. The features which are hydro-geologically most important are the Oruanui Ignimbrite, which has a hydraulic conductivity of 2.91 m/d (Hadfield, 2007), and the underlying rhyolite pyroclastics (*K* = 2.16 m/d). The permeability of these layers causes porous flow (Hadfield et al., 2001). The thick permeable ignimbrite layers allow the largest share of the rainwater to infiltrate into the ground and to seep through the lake bed, causing an enormous groundwater storage reservoir in the catchment (Morgenstern, 2007). The flow in the Mapara Stream consists almost fully of base flow. The majority of flow in this stream originates from the lower part of the catchment. The mean flow rate is 75 L/s (Hadfield, 2007) 85 L/s (Vant and Smith, 2004) at the outlet of the stream into the lake and 90 % of the output comes as base flow, which contributes an estimated 125 mm/y (Piper, 2004). However, 70% of the rainwater of the northern Lake Taupo catchments infiltrates deeper and flows to the lake in deeper aquifer systems, which assumingly discharge at distance from the lake shoreline (Morgenstern, 2008). 81% of the rainwater in the Mapara Stream catchment is estimated to discharge to the lake via lake bed seepage (Piper, 2004).

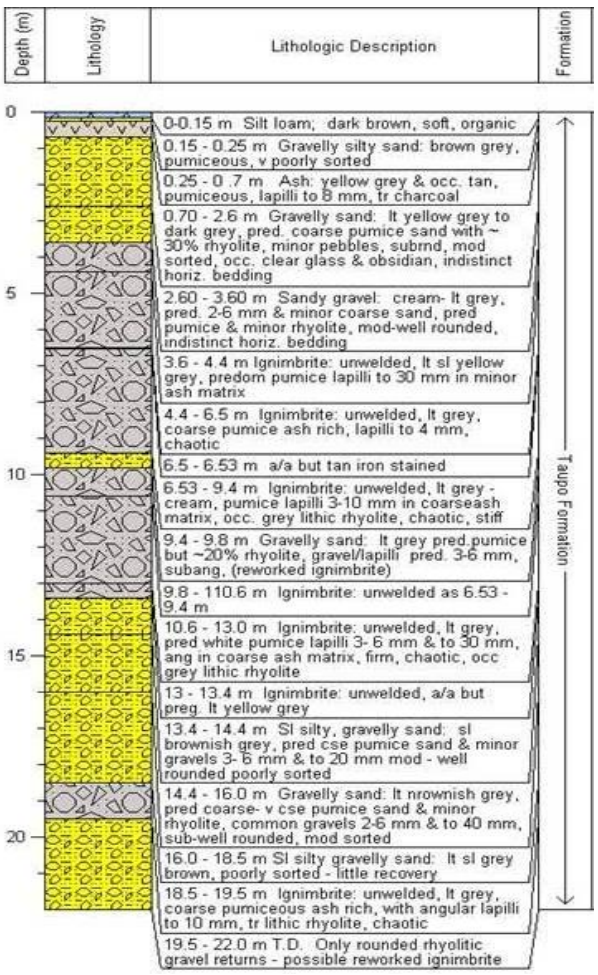

Figure 4: Bore log of June 2010 at the western monitoring well in Whakaipo Bay (Hadfield, 2010)

The borehole displayed in Figure 4 is located in the western part of the bay and is 22 meter deep. The yellow sand and gravel layers can be interpreted as more permeable than the grey ignimbrite layers (Hadfield, 2007). The spatial distribution between these layers can explain why seepage is not equally distributed across the bay.

3.4 Water quality

Natural factors influencing the chemistry and water quality in Lake Taupo catchment are rainwater chemistry, aquifer geology, soil type, geothermal influence, climate and geomorphology. Anthropogenic activities increase the leaching of nutrients to the lake, i.e. due to land use change, such as the conversion from native forest to dairy-farming. Other factors that increase the nitrogen load in groundwater, rivers and lake are the use of septic tanks, outdated municipal waste water treatment plants and run-off from towns (Hadfield et al., 2001; Environment Waikato, 2003; Wildland Consultants, 2013). Inorganic nitrogen (nitrates, NO3-) and ammonium (NH4+) concentrations in rivers have risen and are currently at least factor four higher than in the 1970's (Vant & Smith, 2004). Toxic algal blooms occured in late summer during last decades (Petch et al., 2003; Matheson et al., 2011). Nitrogen feeds the growth of free-floating algae, such as chlorophyll, which has increased in numbers since 1994 and is known to reduce water clarity (Environment Waikato, 2003). As groundwater in the Mapara Stream catchment has an estimated mean residence time of almost half a century, the nitrate and nitrogen loads in recharging groundwater will continue to increase in the short to medium term, even if further nutrient input into the groundwater stops immediately (Wildland Consultants, 2013).

3.5 Earlier research

Hector (2004) stated that most seepage in Whakaipo Bay occurs in water that is shallower than 30 centimetres. Highest seepage rates were found close to the shore, with rates ranging between $0.00067\ \mathrm{m}^3/\mathrm{s}$ and $0.128\ \mathrm{m}^3/\mathrm{s}$. The average seepage rate was $0.021\ \mathrm{m}^3/\mathrm{s}$. No seepage was identified in depths greater than 1 meter.

Gibbs et al. (2005) found locations where deeper diffuse seepage occurs in a part of Whakaipo Bay where the water depth is between 2 and 6.5 meter. The seepage measurements of Gibbs et al. (2005) accounted for a combined groundwater flow into the bay of $0.24\ \mathrm{m}^3/\mathrm{s}$ in this area. When these rates are combined with the shallow seepage found by Hector (2004), a total seepage of 0.261 m³/s results, which is 80% of the expected groundwater inflow by Piper (2004). However, it must be noted that Gibbs et al. (2005) extrapolated seepage over the bay by just using the results of four benthic flux chamber measurements. Estimates of extrapolated local point measurements across a

lake body encompass a high degree of uncertainty (Blume et al., 2013). At the moment impossible is to calculate useful seepage rates, because only a few measurements, which show that the bay is characterised by heterogeneous temperatures, were undertaken.

In 2014, two H-DTS measurements were taken in Whakaipo Bay. On 18 February, a near-shore horizontal measurement was undertaken, as seen in Figure 5.

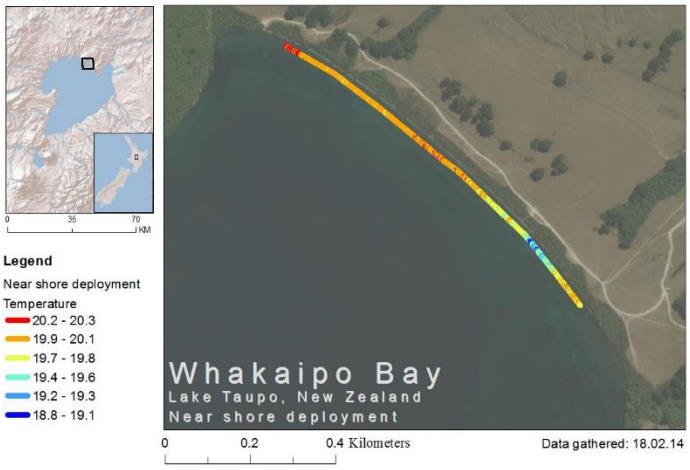

Figure 5: Near-shore H-DTS retrieved temperatures on 18 February 2014 (Meijer, 2014)

The measurement was conducted during 7 minutes and the temperatures in this period ranged between 17.90 ℃ and 21.30 ℃ (Meijer, 2014). One cold area can be identified in the south-east part of the bay.

A off-shore DTS measurement was undertaken in March 2014 and shown in Figure 6.

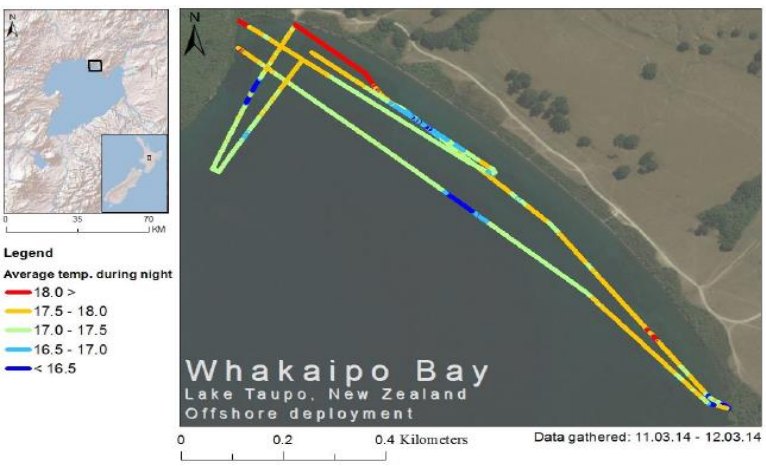

Figure 6: Off-shore H-DTS retrieved temperatures on 11 and 12 March 2014 (Meijer, 2014)

The measurement was taken during overnight and the temperatures in this period ranged between 13.70 ℃ and 18.50 ℃ (Meijer, 2014). Three cold areas can be identified: 80 meter off-shore in the mid-western deep part of the bay, in the middle of bay 160 meter off-shore, and close to the western shore of the bay.

4 MATERIALS AND METHODS

4.1 General approach

Techniques of data collection and data analysis are described in this chapter. First a methodology of the data collection, which occurred between February and May 2015, is given; starting with the DTS equipment, subdivided into the H-DTS and V-DTS procedures. Following, the set-up for the logger instruments and SPM measurements is explained. The data analysis methodology is subdivided into modelling, the calculation of the water balance using regression, interpolation and extrapolation of flows over the bay.

4.2 Data collection

4.2.1 Fibre-Optic Distributed Temperature Sensing

A consistent method was used during all DTS measurements, both horizontal and vertical, in order to have the most reliable data possible. All measurements were single ended with the same configuration of the software and DTS operation system. For each measurement, a four-channel Sensornet Oryx DTS remote unit was used, powered by a 24V battery array. The cable resolution was set at 1.015 meter. A data collector laptop was connected to the Oryx to upload the configuration file and store each new temperature measurement sent by the Oryx. To make sure only absolute temperatures were acquired, ongoing dynamic calibration was applied (Sebok et al., 2013). This was done by using temperature probes and DTS cable submerged in ice-slush calibration baths of ~0º Celsius. Depending on the measurement, the length of the DTS cable chosen and practical matters, different lengths of DTS cable were submerged in the calibration baths (Figure 7), with length never less than 20 meter. An aquarium bubbler kept the water temperatures in the calibration baths consistent within the bath. The configuration and system are shown in Appendix A and B.

Although the use of Oryx DTS channel 2 was preferred as a result of earlier experiences with using the Oryx DTS, problems arose in the field while using this channel. Hence, one measurement was done using channel 1. Data collected on channel 2 before the start of the official start of the measurement showed no difference and thus results of both channels are assumed to be same. All other factors that could have influenced the results were constantly monitored and kept the same as far as possible. This included the internal temperature of the Oryx, the temperature of the probes in the two (ice-) cold calibration baths and the temperature in the air-conditioned car where all electronic gear was housed. The aquarium bubbler was constantly monitored to keep the water in the calibration baths in constant movement. Close attention was paid to possible

measurement errors on the cable due to human interference. Chosen was to take a temperature measurement along the cable every minute.

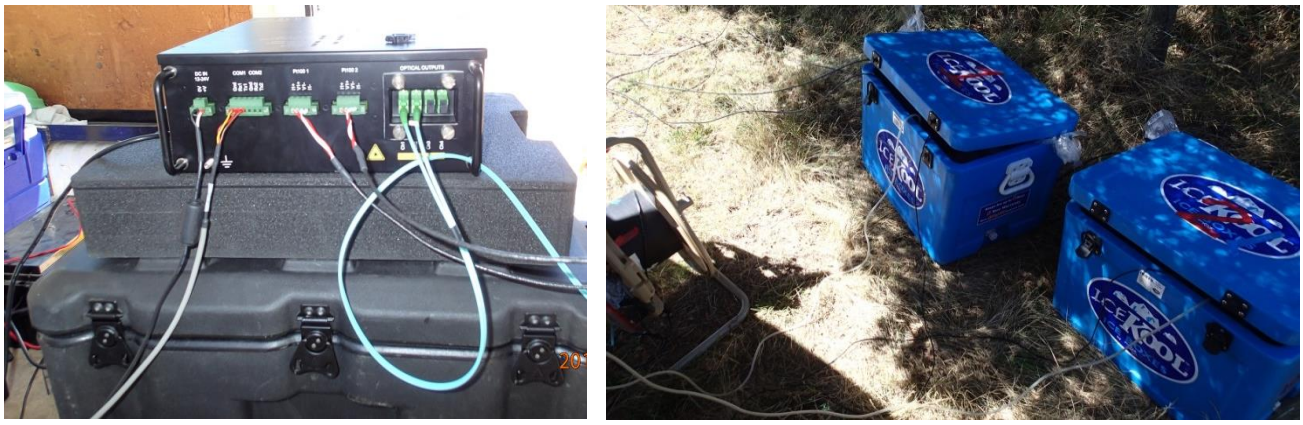

Figure 7: A) Oryx DTS and B) Calibration baths in chilly bins

During the DTS measurements a Global Positioning Unit (Garmin Inc.) was used to reference the location of the cable or notable observations. For V-DTS measurements, the location was a single point and for H-DTS measurements a series of point locations were taken at approximately 100 meter interval along the cable. At these locations, the temperature was also measured with a handheld thermometer.

4.2.2 Horizontal DTS measurement

A near-shore horizontal DTS was conducted to repeat the near-shore survey undertaken by Meijer (2014), as Meijer's measurement period only lasted for a period of 7 minutes. The new near-shore measurement was conducted for 24 hours on the same stretch in Whakaipo Bay where Meijer had measured (Figure 8 and Figure 9). The cable was deployed slightly further in a south-eastern direction compared to Meijer's deployment, as this was expected to be a likely seepage area, based on the vertical measurements done in 2014.

For this measurement, a black OCC (Optical Cable Corporation) Military Grade Fibre Optic Cable with a core/cladding diameter of 50/125 µm and protection armour with a total diameter of 5 mm was used. This cable has inscribed cable length markings every meter.

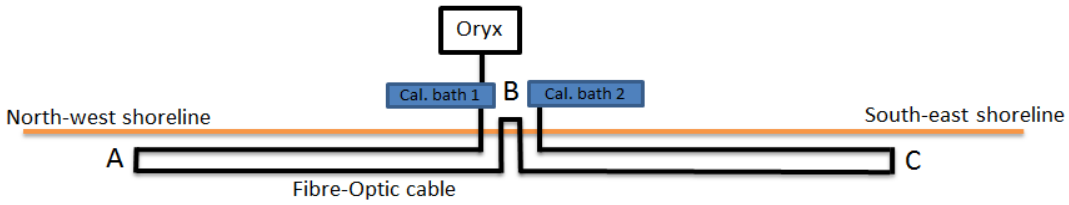

Figure 8: Schematic set-up for horizontal near-shore DTS measurement in Whakaipo Bay. For clarity of the figure, the distance between the cables in both loops is exaggerated.

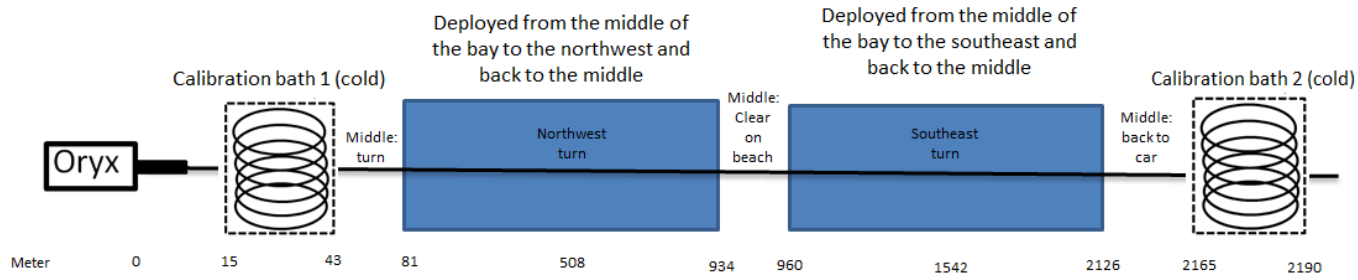

Figure 9: Detailed set up for horizontal near-shore DTS measurement in Whakaipo Bay

The deployment of the cable was done by a kayak on which the 2.3 km DTS cable, coiled on a reel, was installed (Figure 10). From the middle of the bay, the cable was deployed in north-western direction. Weights on the cable were used to make sure the cable stayed in its place and maintained contact with the lake bed. Temperature loggers were used to measure temperature after every 200 m (Figure 11). In the northwest, the cable was turned to the opposite direction and in the middle of the bay it was cleared from the water. Twenty-seven meters of cable was laid out on the beach, before the cable was deployed back in the water in south-eastern direction, where a turn was made at the end. Finally, the cable came back to the middle of the bay back to the measuring instrument, which was situated in the car. The beginning and end of the cable were submerged in two cold calibration baths. As can be seen in Figure 8 the way the cable was deployed enabled one to take two temperature measurements at each location along the bay shore. For each location these temperatures were averaged to obtain an average temperate for each location for each minute of the measurement.

Figure 10: Deployment of the horizontal 2.3 km DTS cable by kayak in Whakaipo Bay

No new off-shore H-DTS temperature measurements was conducted in the first half of 2015, as this is a project that demands much availability of material, transport and people and the 2014 measurement yielded credible results during the deployment.

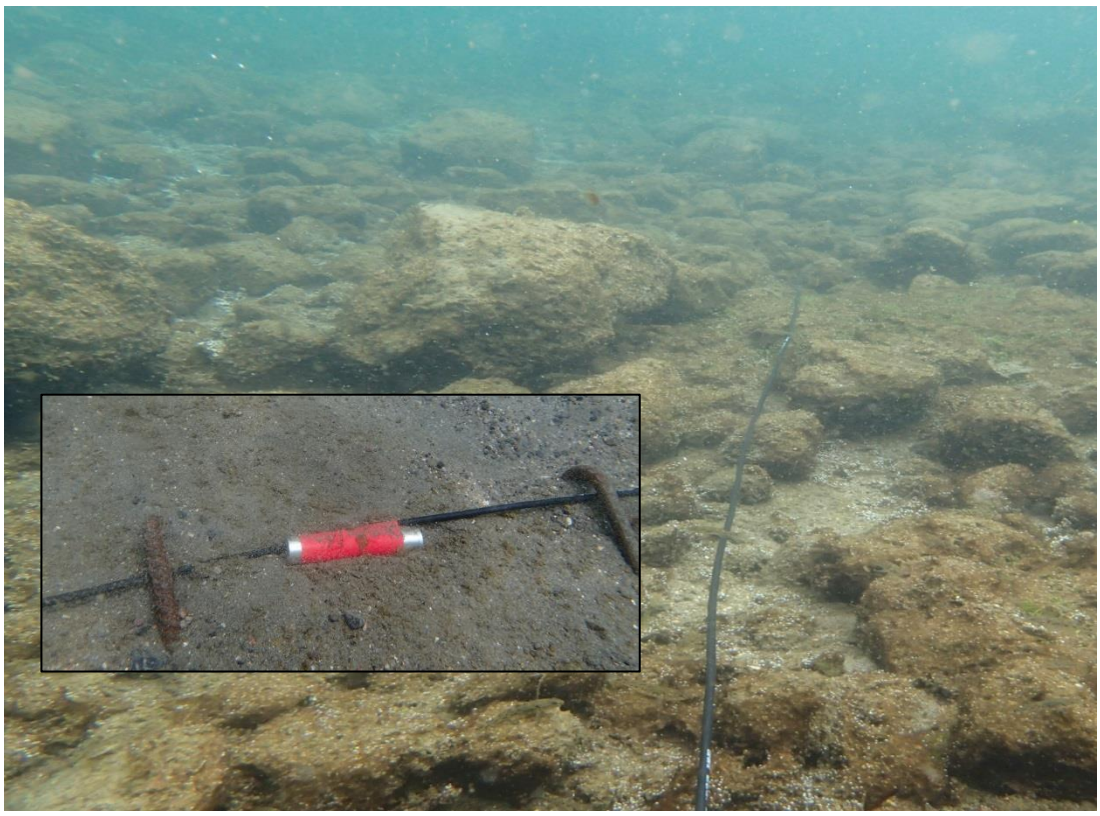

Figure 11: A) Big photo: Deployment of horizontal DTS cable in rocky area in south eastern part of the bay B) Small photo: Deployment of H-DTS cable at sandy location, including logger and weights

4.2.3 Vertical DTS measurements

To get a better insight into the usability of the horizontal temperature sensing measurements, 11 vertical measurements were undertaken at 1-2 meter deep locations in Whakaipo Bay. Combined with the 3 high-resolution V-DTS measurements by Meijer (2014), provided a total of 14 high-resolution measurements in Whakaipo Bay.

High resolution vertical profiling can detect the smallest temperature anomalies near the lake bed. To increase the likelihood of obtaining meaningful results, groundwater seepage was captured for several hours during the high resolution vertical profiling. The effect of wave turbulence and heating by radiation on the construction was minimised by using a cloth as cover of the cylinder, but which allowed water to flow from the cylinder to the lake. For this type of measurement, the black OCC Military Grade Fibre Optic Cable which was also used in the horizontal deployments was used as the connecting cable between the V-DTS device and the Oryx. 350 meter of this 914 µm fibre[1] was wrapped around a 320 mm high metal/bamboo frame, which was spliced to the black military cable.

[1] The height of the vertical DTS is 320 mm and the radius is 158.5 mm. The circumference 2*π*r is thus 1000 mm. Because the total blue cable is 350,000 mm, it is possible to wrap 350,000/1000 = 350 circles around the device. This causes a resolution of height/circles = 320/350 = 0.914 mm or 914 µm. The area of the cylinder = 1134 cm²

Channel 2 was used for all measurements, except for measurement 8. Brown algae mats were found in Whakaipo Bay, which was considered to be an indication of groundwater seepage (Gibbs et al., 2005). Several V-DTS measurements were undertaken in these depressions to ascertain seepage at these locations. The set-up is shown in Figure 12 and Figure 13.

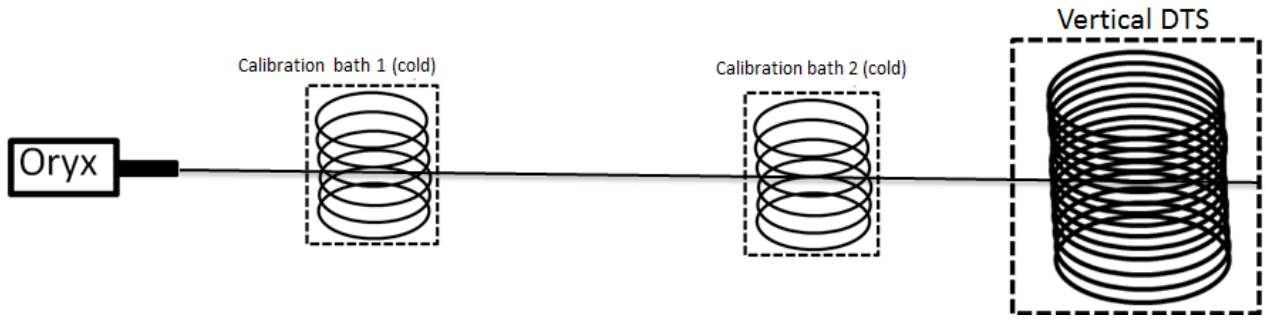

Figure 12: Schematic set-up for single-ended V-DTS measurements in Whakaipo Bay

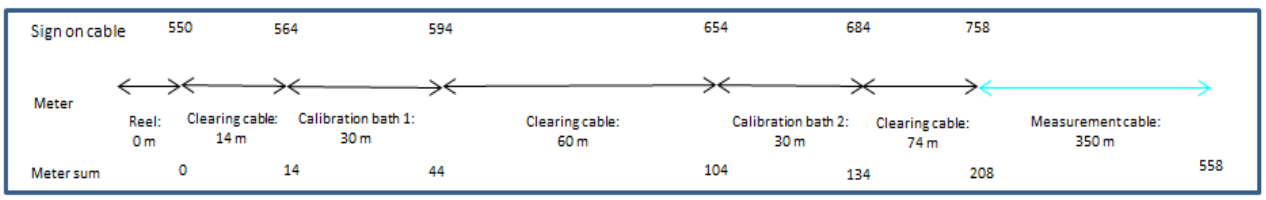

Figure 13: Detailed single-ended set-up for V-DTS measurements in Whakaipo Bay

The V-DTS device was placed in a PVC cylinder with a diameter of 38 cm and a height of 52 cm (Figure 14). The cylinder was fixed to the sandy lakebed by carefully pushing the cylinder several cm into the lake bed. This allowed seeping groundwater to flow from the lakebed through the V-DTS device without horizontal dispersion. At all locations, the device was fully submerged in the water, except for location 12 (LOC12), where a hole was dug in the bank 1.5 meter of the outlet of the Mapara Stream into the lake.

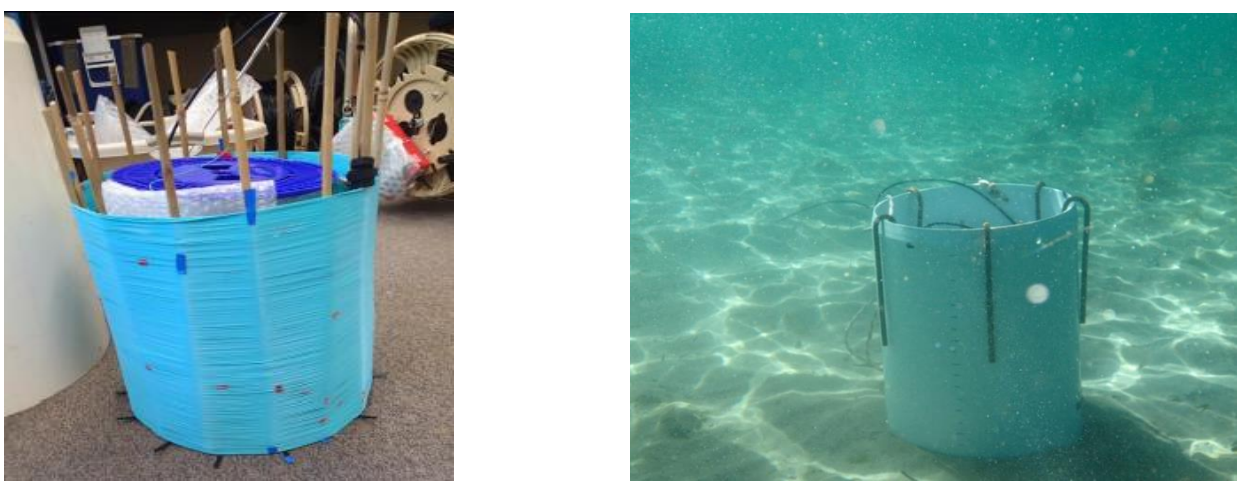

Figure 14: A) V-DTS device in office. B) V-DTS device during measurement in cylinder

4.2.4 Logger measurements

The DTS and SPM measurements in Whakaipo Bay focused on the lake water temperature only. To further examine seepage inflow areas and to compare results with groundwater observations along the shoreline, HOBO Stainless Temperature Data Loggers U12-015 were used. Groundwater temperature measurements were conducted on-shore, by using a logger in a temporary piezometer installed on Whakaipo Bay beach or on a rope in a permanent monitoring well further inland. The groundwater temperatures measured were used as a reference value for the groundwater temperature variable for the 1D flux model. Off-shore, loggers were used at the same locations where a V-DTS measurement was conducted and further off-shore. Furthermore, loggers were used to check temperatures measured by H-DTS measurement and all V-DTS measurements (Table 1).

Table 1: Subdivision of logger measurements

Measurement type	Specific method	Location	Number
Separate measurement	Logger in piezometer	On-shore	1
	Logger on rope in monitoring well	On-shore	1
	Logger device on DTS locations	Off-shore	9 or 10
	Logger device on distant locations	Off-shore	9 or 10
Alongside other measurement	Logger attached to horizontal DTS cable	Off-shore	10
	Logger attached on vertical DTS device	Off-shore	2

The logger measurements in the piezometer were conducted by installing the piezometer, in which the logger was placed, as deep as possible into the pebble beach of Whakaipo Bay (Figure 15). A period of 10 minutes was chosen to let normal groundwater flow conditions to restore. At the groundwater level, the measurement was done by measuring the groundwater level and temperature every minute during at least 10 minutes. This method was also used for the logger measurements in the well.

Figure 15: A) Piezometer location at beach close to shore. B) Logger on rope in a monitoring well

The logger device was constructed from a rope on which the loggers were fixed at interval. An anchor was used to keep the rope in position and a buoy ensured the device remained vertical in the water column. The configuration of the loggers on the rope is displayed in Table 2, whereas the device itself is shown in Figure 16.

Table 2: Configuration of loggers on rope

Logger number	Number	Depth from lakebed
10244110	0	0.00
10244111	1	0.05
10244112	2	0.10
10244113	3	0.15
10244115	4	0.20
10244114	5	0.25
10244117	7	0.30
10244118	8	0.40

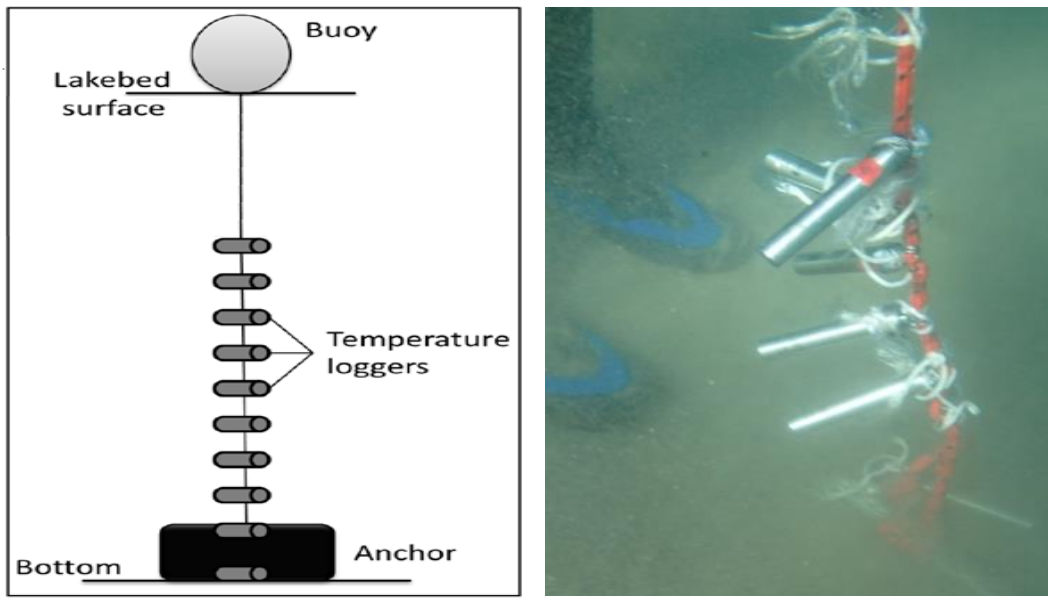

Figure 16: A) Logger device (Meijer, 2014). For convenience, the figure is not on scale. B) Logger device during measurement

4.2.5 Direct seepage measurements

The only vertical profiling technique used that did not involve temperature measurements is the seepage meter. A standard SPM is a bag that fills with water to measure the seepage flow. Although much uncertainty is involved in the use of a SPM, which was explained in the previous chapter, it was chosen as they are a direct, simple and cost-effective way to validate the temperature derived measurements. The SPMs were constructed specifically for this project. They were constructed from the lower third of a 200L plastic drum, on which a valve with a balloon is fixed, as can be seen in Figure 17.

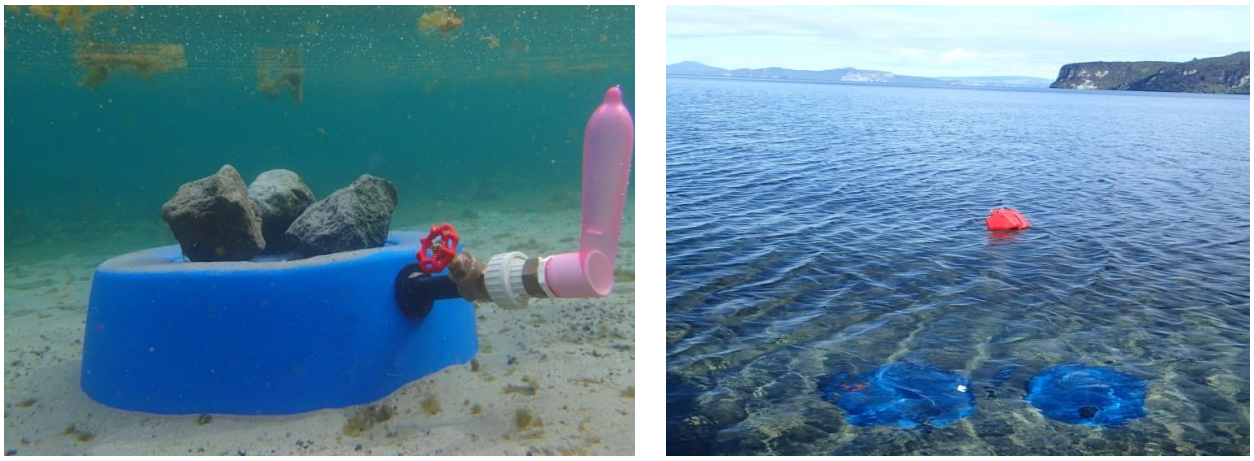

Figure 17: Seepage meter. A) During measurement. B) Two seepage meters. In background the buoy of logger device is visible.

SPM measurements were undertaken at the same locations as the V-DTS measurements. To let the seepage pattern restore, the duration between the emplacement of the SPM and the first installation of the seepage-meter bag was chosen to be 15 minutes. This is slightly more than the minimal equilibration time for Lake Taupo of 5-10 minutes (Rosenberry et al., 2008). This duration is really short compared to studies conducted in other regions where no sandy or gravelly environment was present (Rosenberry et al., 2008). Before the measurement had started, water could freely flow in and out of the SPM. The measurements started once the valve and (prefilled) bag or condom was fixed to the SPM and the valve was opened. At the end of the measurement, the valve was closed and both valve and seepage bag were brought to the beach, where the volume of collected water in the bag was measured. Initially, rocks were used to keep the SPM in place at the locations where the cylinder could not be inserted into the lake bed. As differences in flow patterns might exist in a very small area, two SPMs were installed beside each other and results were compared.

4.3 Data analysis

4.3.1 DTS Analysis

Flow rate

All separate Oryx DTS measurements were compiled and analysed for trends. The seepage flow was calculated at the locations where V-DTS measurements were made. This was based on the depth of the "cold" groundwater layer in the cylinder after a specified time. The depth of the groundwater layer is defined as the water depth above the SWI where the average water temperature at $t_1$is lower than the average water temperature at the SWI at t_0. The V-DTS device measures temperature at 0.9 mm vertical resolution. Each wrap of the DTS cable on the cylinder is 1 meter of cable and the DTS measures temperature at approximately meter interval along the cable and equals the cable diameter of 0.9 mm. Hence, the total depth of the groundwater layer is a multiplication of the number of turns that the average water temperature at t_1< average temperature at t_0. This is called the displacement calculation method (Equation 2).

Equation 2: Groundwater seepage flux (cm/h) displacement calculation based on vertical DTS results

$$Q\ (cm/h) = Depth\ of\ groundwater\ layer\ at\ t_1\ (cm) * \frac{60}{Measurement\ time\ (min)}$$

Subsequently this flux was multiplied by the area of the cylinder, which is 1134 cm², to calculate the flow. A visualization of the temperature layers is provided, which facilitated the comparison with different DTS temperature measurements. These flow rates were compared to the flow rates calculated by the SPM measurements. However, this flow rate calculation is a rather easy one as it does not take heat-conduction into account. In case the displacement calculation results differ much from the modelling results, only the heat-conduction model results were taken for the continuation of this research.

Anomalies

To be able to compare the horizontal temperature measurements of 2014 and 2015 in Whakaipo Bay, the variation of the temperature measurements along the cable relative to the average temperature along the whole cable is used. Since the 2014 measurement lasted only 7 minutes, in the period between 2pm and 3pm, this time period was taken to calculate the averages and anomalies in the 2015 measurement. It should be noted that the 2014 measurement was obtained in February, whereas the 2015 measurement was obtained in the first week of March.

Adjacency

An overview of the effects of adjacent points of a measurement on the horizontal cable was given. This was done by calculating the minimum and maximum values of a certain number of points adjacent to a temperature measurement from the H-DTS cable, which showed the difference. Furthermore, for each temperature measurement, the variance of the adjacent temperatures was calculated. When these temperatures were sorted from the coldest to the warmest temperature measured, an image was acquired of how much the variance of adjacent points along the cable differed from the measured temperature.

4.3.2 Modelling

The 1D finite difference flux model developed by Meijer (2014) was used to test the comparison of techniques. The model is able to calculate the seepage flux after a specified time at chosen locations.

This model is developed using the basic convection-diffusion equation of the explicit scheme of the finite difference method. The approximation for the internal node is shown made in Equation 3, whereas the stability criteria for the model are shown in Equation 4.

Equation 3: Internal node convection-diffusion model (Meijer, 2014). Δz is the mesh step, lower index I indicates position and the higher index f indicates time.

$$T_i^f = \left(1 - \frac{2a\Delta t}{\Delta z^2}\right) T_i^{f-1} + \left(\frac{a\Delta t}{\Delta z^2} + \frac{\epsilon u \Delta t}{2\Delta z}\right) T_{i-1}^{f-1} + \left(\frac{a\Delta t}{\Delta z^2} - \frac{\epsilon u \Delta t}{2\Delta z}\right) T_{i+1}^{f-1}$$

Equation 4: Stability criteria (Meijer, 2014) of convection-diffusion model

$$\Delta z < \frac{2a}{\epsilon u}, \qquad \Delta t < \frac{\Delta z^2}{2a}$$

The model was discretized into two parts, i.e. the lake and lakebed part. The bottom part of the model describes the 10 cm saturated zone below the lakebed, where heat exchange is occurring, whereas the upper part of the model describes the first 30 cm of the water column above the lakebed. Different values for the parameters specific heat, mass density and thermal conductivity were taken for the bottom sediment and the water. The complete MATLAB code and parameters are presented in Appendix C.

The modelling simulates the inflow of groundwater required to induce the measured change in temperature. The measured temperature gradient in time and the temperature of the water that directly neighbours the groundwater layer are the only variables. Based on this input, the heat-conduction model produces the groundwater flux in units of cm/h as output. The lake water temperature is taken to be the average lake water temperature of the layer in which groundwater accumulated in the V-DTS device. An uncertainty analysis

was conducted to investigate the effects of an increased and decreased value for the variables groundwater temperature and lake water temperature. This was done by considering three modelling scenarios, which are explained in Chapter 5.2.4.

4.3.3 Comparison of techniques

The V-DTS, SPM and piezometer results were compared to each other for similarity of results. This analysis is used to see if these techniques give similar results. Errors that have occurred in one of the measurements could be traced by comparing them with other techniques. Furthermore, the locations of V-DTS on pockmarked depressions were compared to temperature profiles at locations which were not situated on or around these pockmarked depressions, in order to investigate whether measurements in these pockmarked depressions result in higher seepage flows than measurements that took place at other locations.

4.3.4 Linking horizontal and vertical DTS

The knowledge gained about the relation between the horizontal and vertical temperature measurements validated against the SPM and logger results was combined to give recommendations for a technique that is able to directly calculate the seepage flow using H-DTS.

4.3.5 Water balance of Mapara catchment

The water balance shows the quantified groundwater flows going in and out of the Mapara Stream groundwater system. Precipitation data were acquired from Tait et al. (2006) and Westerhoff (2015a), whereas potential and actual evapotranspiration came from Mu et al. (2011) and Westerhoff (2015b). Thirty-seven point measurements of precipitation and evapotranspiration, on equal distance from each other, cover the whole Mapara Stream catchment. Equation 5 shows the formula to calculate the seepage component; whereas Equation 6 shows the way the total precipitation and evapotranspiration were calculated.

Equation 5: Seepage component for the Mapara Stream catchment. P = Precipitation, AET = Actual evapotranspiration, Q = Discharge. P-AET is called the precipitation surplus. Assumed is that no water is stored temporarily in the Mapara Stream catchment (S=0). .

$$Seepage\ (\frac{m^3}{y}) = Total\ P\ (\frac{m^3}{y}) - Total\ AET\ (\frac{m^3}{y}) - Q\ Mapara\ Stream\ (\frac{m^3}{y})$$

Equation 6: Total precipitation (Total P) and total evapotranspiration (Total AET) calculation. Note that the distance to the next point measurement squared indicates the area in which the point measurement is valid

$$Total\ P\ \left(\frac{m^3}{y}\right) = Total\ P\ point\ (\frac{m}{y}) * Distance\ to\ next\ point\ ^2\ (m^2)$$

$$Total\ AET\ \left(\frac{m^3}{y}\right) = Total\ AET\ point\ (\frac{m}{y}) * Distance\ to\ next\ point\ ^2\ (m^2)$$

4.3.6 Extrapolation of flows into Whakaipo Bay

As stated before, it is largely unknown how the seepage zones are distributed over Whakaipo Bay. The measurements by Hector (2004) and Gibbs et al. (2005), together with the two near-shore and the off-shore DTS measurements and the logger and seepage meter measurements, show that seepage is not equally distributed. This study aims to improve understanding of the spatial variability of seepage into Whakaipo Bay. By extrapolation of the fluxes retrieved by the displacement calculation over the whole bay, an estimation of the spatial variability of seepage in Whakaipo Bay is made. However, there is still considerable uncertainty in the extrapolation of a seepage flow across a large part of the bay due to the limited number of shallow point measurements. The steps taken to extrapolate the flow over the bay were:

1. Find a linear relation, based on regression, between temperatures (H-DTS) and related flows (V-DTS) at the locations where this is available. A linear regression between temperature and flow rate is assumed according to the convection-diffusion model. The regression is based on Equation 7.

   Equation 7: Linear regression where Y = value of Y for observation, β_1 = mean value of Y when X is zero, β_2 = average change in Y given a one unit change in X, and u, which is the error term

   $$Y = \beta_1 + \beta_2 + u$$

2. Use this relation to calculate the flow for the temperatures observed at meter interval on the horizontal near-shore DTS measurement.
3. Extrapolate the flows for each meter over the bay, for a water depth less than 6.5 meter.
4. Calculate the total flow rate and compare to previous studies water balances and estimates.

The temperatures for the horizontal cable are average temperatures between 14h and 15h to correspond with the measurement time period of Meijer (2014) on the northwest side of the bay.

The extrapolation was done by multiplying the width of the concerned area with the calculated flow at each point on the horizontal cable. The scale of the extrapolation was based on the bathymetry map from LINZ (1966). However, to compare the seepage rates to the extrapolations of Hector (2004) and Gibbs et al (2005), the extrapolation was broken down in three areas of different water depth, which are shown in Table 3. Hector (2004) only calculated the flow for a water depth of less than 1 meter, whereas Gibbs et al. (2005) estimated flow rates for the area with a water depth between 2 and 6.5 meter. Since the area in which the water depth is 2-6.5 meter on the bathymetry map (LINZ, 1966) differs much from Gibbs et al. (2005), Area 3 is subdivided in two sub-regions.

Table 3: Subdivision of extrapolation zones based on bathymetry

Area		Definition	Source
1		Extrapolation across the <1 meter water depth area	Bathymetry map / Hector
2		Extrapolation across the 1-2 meter water depth area	Bathymetry map
3	A	Extrapolation across the 2-6.5 meter water depth area	Bathymetry map
	B	Extrapolation across the 2-6.5 meter water depth area	Gibbs et al.

The flows for each extrapolation step were summed for the whole cable length. This is visualised in Figure 18. The average seepage rates for each extrapolation zone are compared to Hector (2004), Piper (2004) and Gibbs et al. (2005).

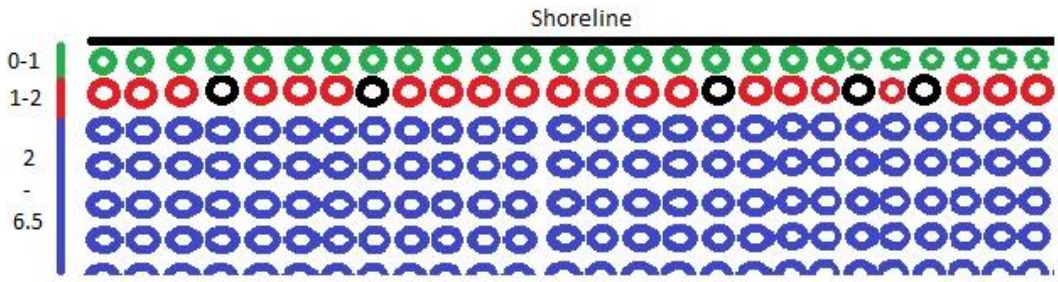

Figure 18: Extrapolation of data sequence. Black circles: V-DTS locations where flow is known and from where is extrapolated. Red circles: First extrapolation across the 1-2 water depth area. Green circles: Second extrapolation across the 0-1 meter water depth area. Blue circles: Third extrapolation across the 2-6.5 meter water depth area

4.3.7 Uncertainty analysis of extrapolation and water balance

In this paragraph an uncertainty analysis is performed, in order to compare the uncertainties in the calculated seepage component for the Mapara catchment by the extrapolation method and the water balance method. This was undertaken to quantify the range of possible seepage flows and to specify differences and similarities in results. An extreme minimum and maximum seepage rate was calculated for both methods, to investigate the range of possible flow rates. Subsequently these minimum and maximum seepage rates were compared to each other.

Extrapolation method

The uncertainty analysis of the extrapolation method is composed of three steps:

1. Use the minimum and maximum modelled flow rate for each of the modelled V-DTS measurements.
2. Calculate regression relations for the minimum and maximum modelled flow rates.
3. Change the extrapolation area width to a minimum value (estimated width – 50%) and a maximum value (estimated width + 50%).
4. Calculate the minimum seepage rate based on the minimum regression relation and the halved width of the deep extrapolation area and calculate the maximum seepage rate based on the maximum regression relation and the doubled width of the deep extrapolation area.

The four steps result in new minimum and maximum seepage rates as calculated by the extrapolation method. This is visualised in Figure 19.

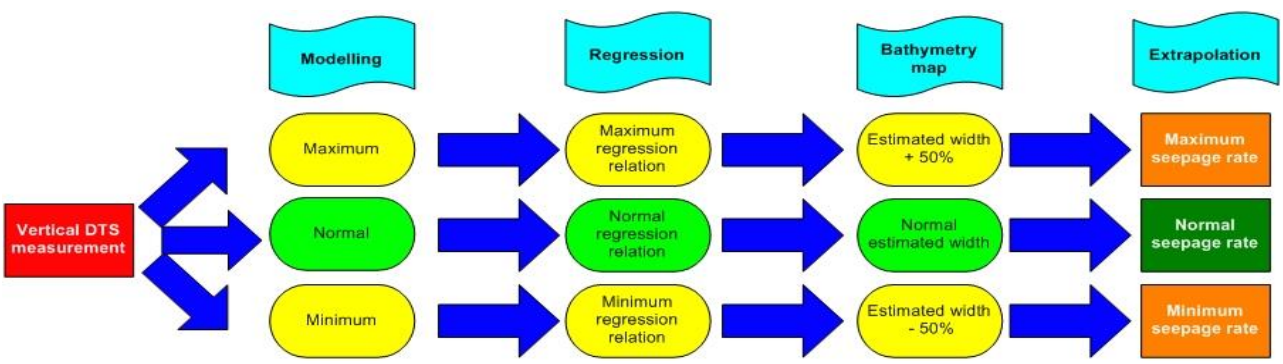

Figure 19: Diagram of steps undertaken in the uncertainty analysis of the extrapolation method

It was chosen to use the minimum and maximum modelling results as basis for this uncertainty analysis, as these values are supposed to specify the absolute range of seepage rates at each location. Besides, it was chosen to increase and decrease the estimated width of the deep extrapolation area by 50%, since much uncertainty is involved in the accuracy of the bathymetry map which dates from half a century ago (LINZ, 1966).

Water balance method

The uncertainty analysis of the water balance method is also composed of three steps:

1. Calculate all the single precipitation rates to the minimum and maximum rates found in the catchment.
2. Calculate all the single actual evapotranspiration rates to the minimum and maximum rates found in the catchment.
3. Change the discharge rate to the minimum and maximum rates of the Mapara Stream found in literature.
4. Subtract the actual evapotranspiration and discharge rate from the precipitation rate.

The four steps result in new minimum and maximum seepage rates as calculated by the water balance method. This is visualised in Figure 20.

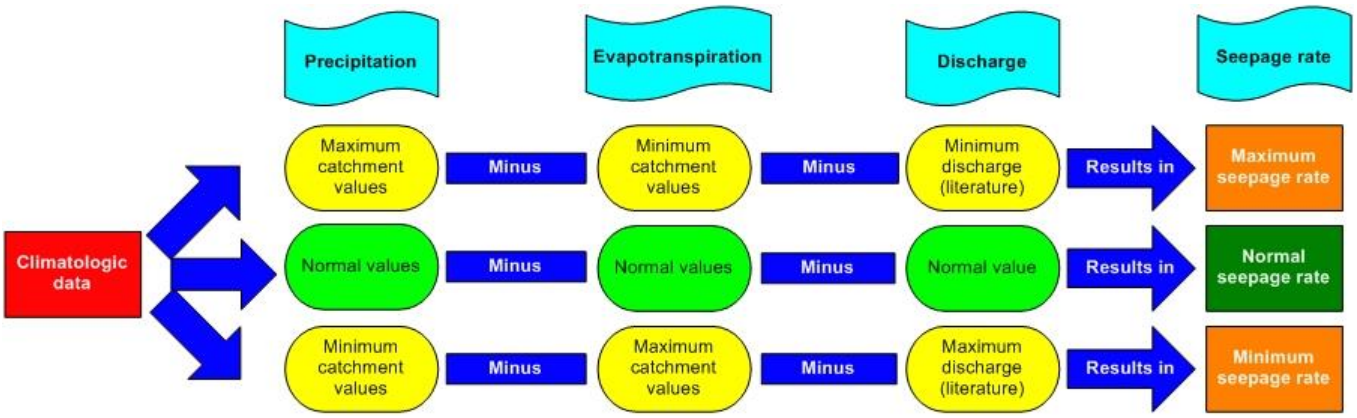

Figure 20: Diagram of steps undertaken in the uncertainty analysis of the water balance

It was chosen to calculate the uncertainty for precipitation and actual evapotranspiration by using the minimum and maximum values, instead of using the original data, for all 37 locations in the catchment area. Differences in point estimates of these climatologic variables exist due to the topographic characteristics and the interpolation method used. However, much uncertainty is involved on the local level (Tait et al., 2006). Besides, it was chosen to calculate the uncertainty of the discharge of the Mapara Stream by using the minimum and maximum values found in literature.

4.4 Revisit of the research questions

To what extent are seepage areas in Whakaipo Bay detectable by a combination of horizontal and vertical deployment of DTS?

The DTS analysis of both horizontal and vertical DTS measurements and the comparison of techniques should give an answer to what extent DTS is able to detect seepage areas.

To what extent is vertical deployment of DTS, validated with a numerical model, temperature loggers and seepage meters, able to quantify the seepage flow in different parts of Whakaipo Bay?

The modelling should give an answer to what extent V-DTS in combination with a numerical model, logger measurements and seepage measurements, is able to quantify the seepage flow in different parts of Whakaipo Bay.

To what extent could horizontal DTS be improved to directly detect seepage areas and flows?

The linkage of H-DTS and V-DTS should give an answer to what extent H-DTS could be improved to directly detect seepage areas and flows.

To what extent is horizontal deployment of DTS able to calculate the water balance and spatial variability of seepage into the whole Whakaipo Bay?

The extrapolation of flows combined with the water balance should give an answer to what extent DTS is able to calculate the seepage flow over Whakaipo Bay.

5 RESULTS AND ANALYSIS

The four research questions are discussed in separate paragraphs. An overview of all measurements is given in Appendix D. Visualisations of the H-DTS and V-DTS measurements that are not displayed in this chapter can be found in Appendix E and F. The temperature data sets of the vertical deployments are analysed using MATLAB software. Both horizontal and vertical datasets are visualised using ArcMap.

5.1 Horizontal near-shore profiling

RQ1: To what extent are seepage areas in Whakaipo Bay detectable by horizontal DTS?

Horizontal profiling using H-DTS took place in March 2015 at near-shore locations in Whakaipo Bay. The lay-out for the 2015 measurement can be seen in Appendix E.

Analysis of surface water temperatures

The water temperature over the cable length ranged between $15.11\ °C$ and $22.31\ °C$, which is a range of $7.06\ °C$ over the 24 hour period of measurement. In the western part of the bay the minimum temperature was much higher: $17.09\ °C$. The average temperature over the bay was $19.38\ °C$ over the 24 hour period. The course of the average temperatures during the measurement can be seen in Figure 21. A colder area in the south eastern part of the bay is evident in the figure and may be a seepage zone. At this location the coldest temperatures are found. The H-DTS temperatures measured on this spot show a large variability: Often the measure before and after a cold temperature measurement, a temperature reading of more than a degree Celsius warmer is gathered. This might be due to measurement noise of DTS. The coldest temperatures were measured in the period between 5am and 8am in the early morning, when temperatures were coldest.

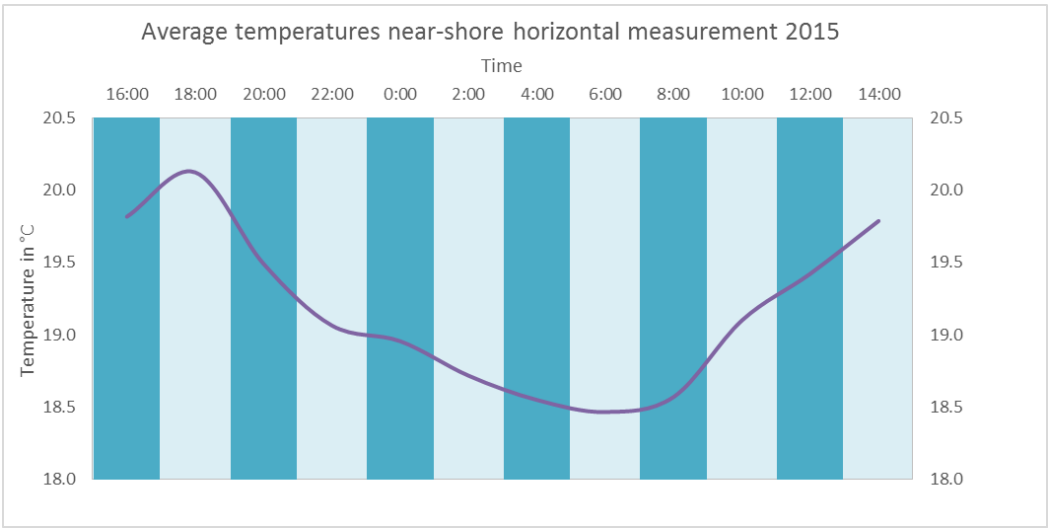

Figure 21: Average surface water temperature at the SWI for each 2 hour period (purple).

The water temperatures along the near-shore are not homogenous, which Hector (2004) and Gibbs et al. (2005) observed as well. This can be seen in Figure 22. The colder part can be seen near the south-eastern end, but there are other sections of the cable where lower temperatures occur, indicated by the light blue locations in the middle and eastern end of the cable in Figure 22. Pockmarked depressions and algae growth were found here, but also at other locations along the cable. Algae growth can be influenced by many factors such as temperature, nutrients, salinity, pH and light (Meijer, 2014). One area of higher temperatures is visible in the western part of the bay whereas another area is visible in the centre of the bay.

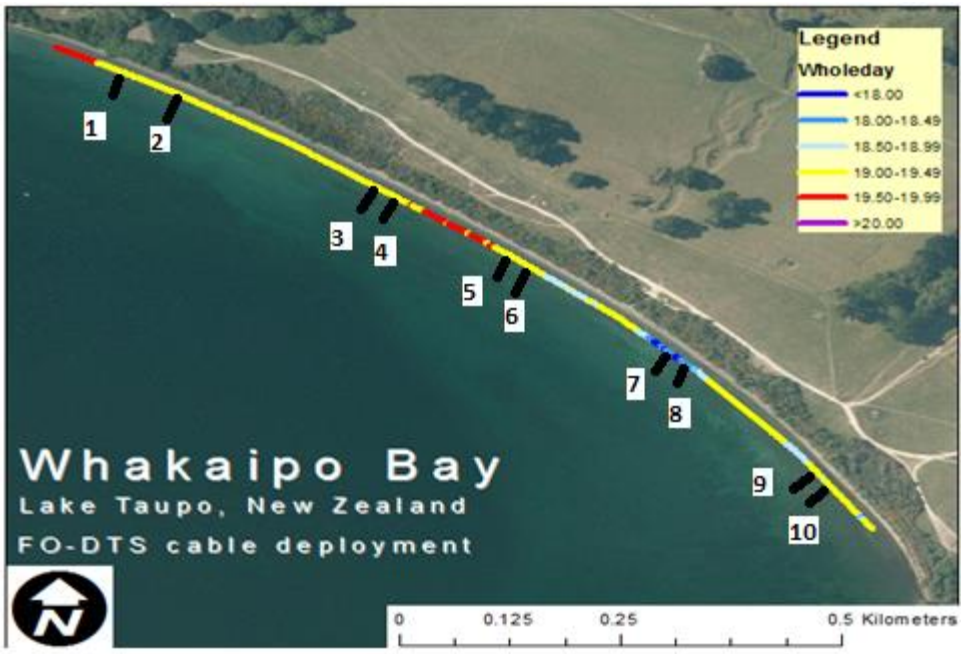

Figure 22: Average H-DTS temperatures by the near-shore H-DTS measurement in 2015. The numbers 1-10 indicate the locations of the loggers that were fixed to the cable.

The water temperature fluctuated during the day. In Figure 23 the average temperatures for the morning, afternoon, evening and night are displayed. The temperatures in the cold-water area in the south-eastern part of the bay, between 600 and 700 meter on the graph, were consistently coldest throughout the measurement period. However, more cold water areas were found, all in the south eastern part of the bay.

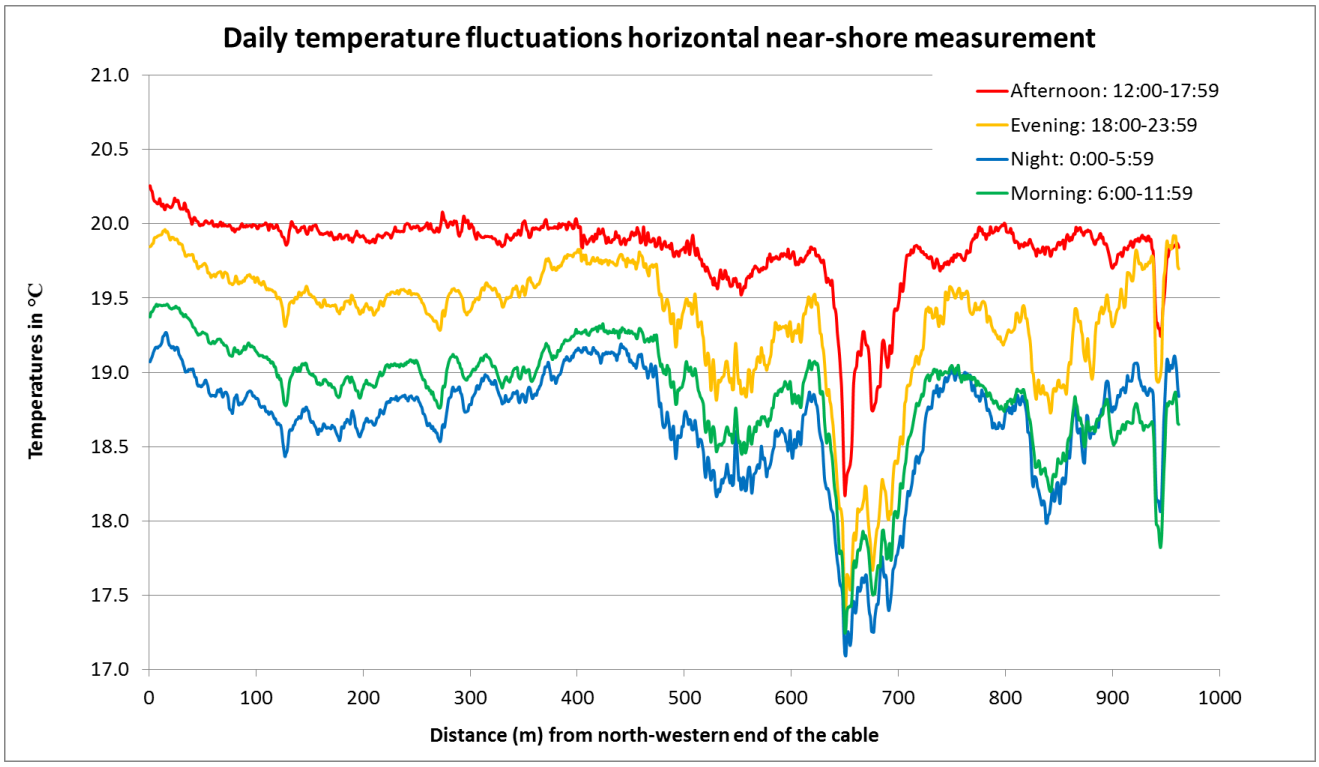

Figure 23: Diurnal temperature fluctuations of the H-DTS near-shore measurement at the SWI

In Figure 24 the temperature differences are visualised between 05-07h, which is on average the coldest period of the 24hr measurement period, and 17-19h, which is on average the warmest period of the 24hr measurement period. Clearly in the warmest regions along the cable, which are in the north-western and middle part of the bay, the temperature differences were smallest. In the colder seepage zones in the south-east, temperature differences were bigger as well.

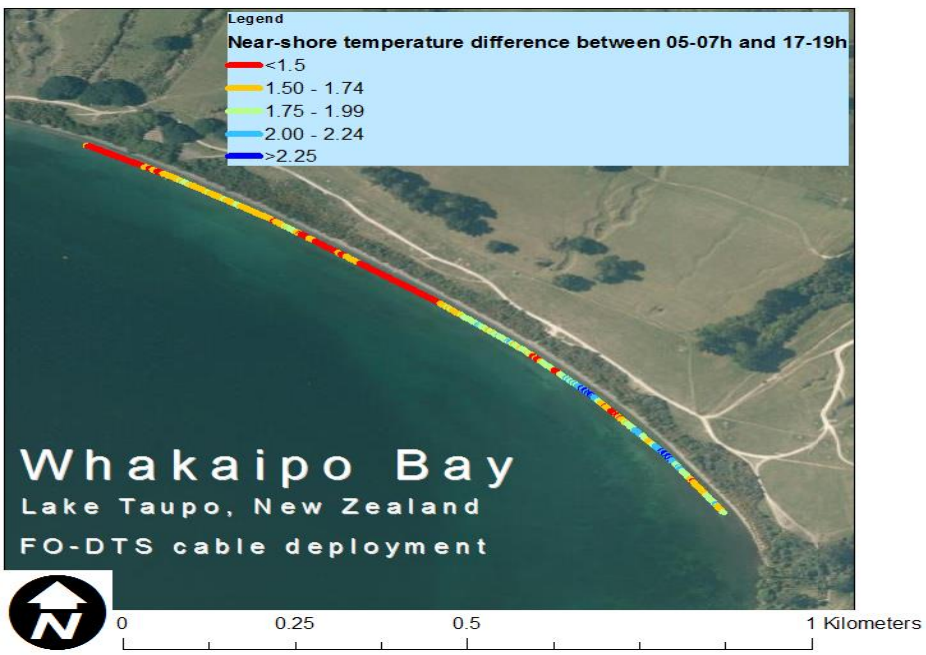

Figure 24: Temperature differences between the coldest (05am-07am) and warmest (17pm-19pm) part of the day

Temperature loggers

To validate measured temperatures, temperature loggers were fixed on the horizontal cable. The average logger temperatures are shown in Figure 25 and Appendix E.

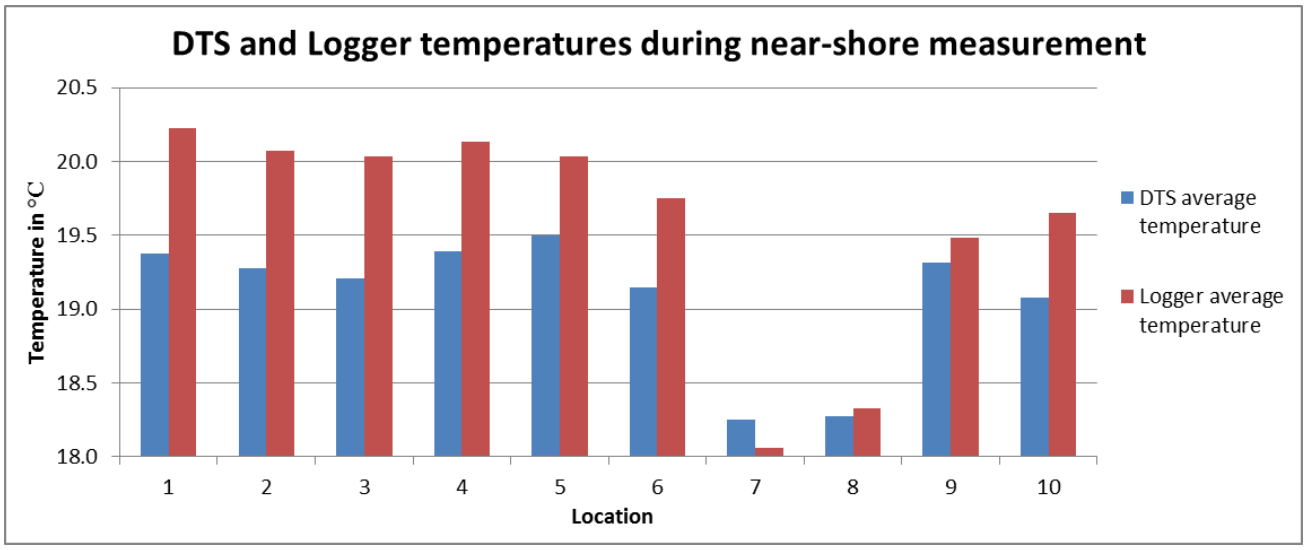

Figure 25: Logger average temperatures and H-DTS average temperatures at the 10 locations along the H-DTS cable which were shown in Figure 22. The loggers at LOC6 and LOC9 were located in the cold area in the south-eastern part of the bay.

The temperature loggers show the same relative temperature pattern as the H-DTS temperatures. At the colder locations of the H-DTS, the temperature loggers also recorded a cold water layer. However, the absolute temperatures differ often much, with the biggest difference being 0.8 °C at LOC1. Differences might be due to a slight vertical difference in the placement of the logger relative to the DTS cable, which caused the loggers to receive more sunlight (Lowry et al., 2007). Furthermore, the loggers measure the temperature at one point, whereas the DTS averages the temperature over 1 meter of cable. Hence, only relative temperature patterns of the loggers are taken into account.

Calibration baths

Factors that might influence the quality of the data are temperatures of the calibration baths and the internal temperature of the Oryx, which both are shown in Figure 26.

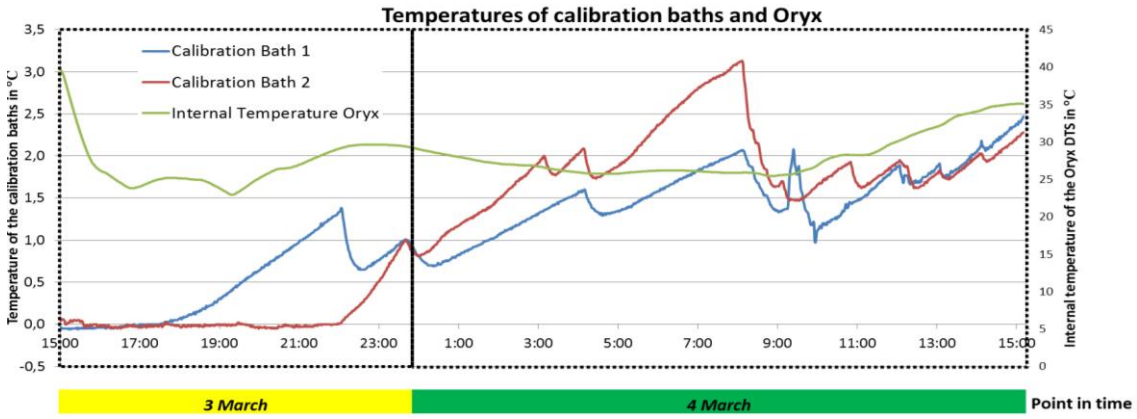

Figure 26: Temperatures of water in the calibration baths and the internal temperature of the Oryx DTS

The temperature of the calibration baths ranged between 0.06 °C and 3.13 °C, whereas the Oryx DTS temperature ranged between 23°C and 40 °C. Before the lake water temperatures dropped, the internal temperature of the Oryx already had decreased and the temperature of the calibration baths had started to rise. All the sudden decreases in temperature possibly influenced the temperatures measured along the cable, as can be seen in some V-DTS measurements. However, it is hard to say what the exact impact of this influence might be.

Anomalies

To compare the 2014 and 2015 datasets, a correction was made for the different season that the measurement was made in. The 2015 measurement was conducted in March, contrary to the 2014 measurement in February, which usually is a slightly warmer month in the Lake Taupo region (Gibbs et al., 2005). Hence temperature differences relative to the average temperature (anomalies) were calculated for each measurement and were compared to each other. In Figure 27 these anomalies can be seen.

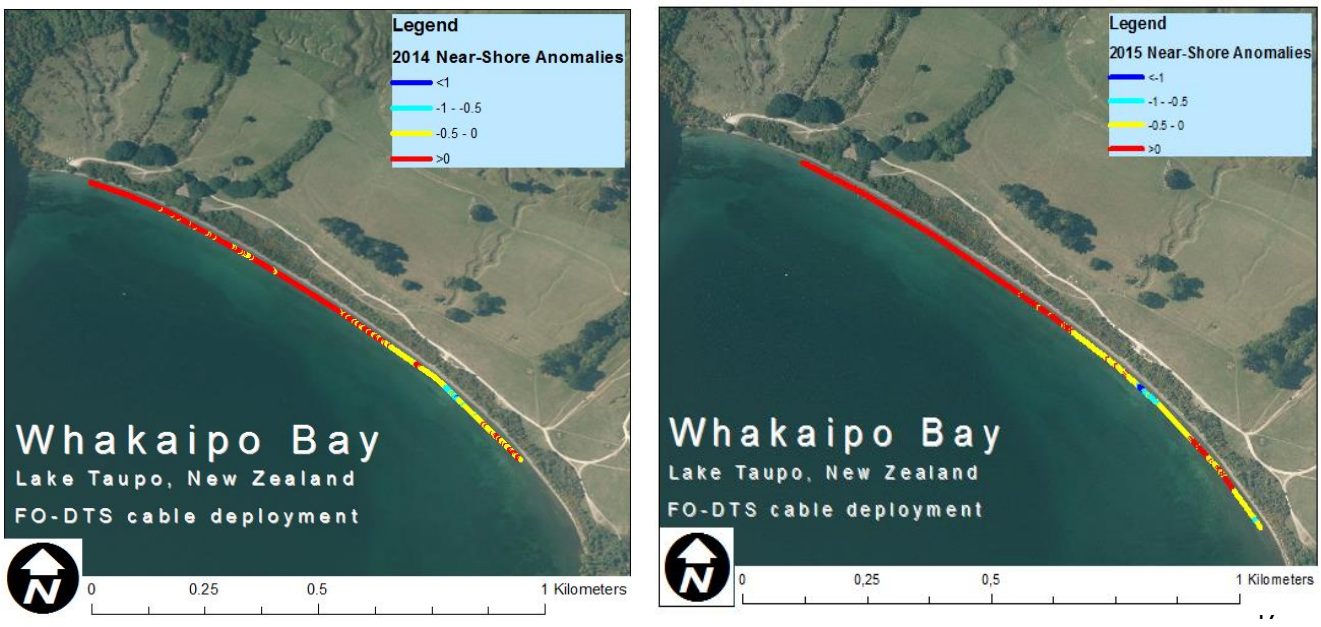

Figure 27: A) Temperature anomalies of the horizontal near-shore deployment of 2014 (Meijer, A) and of 2015 (B)

A few differences exist in the anomalies between the two measurement days. When the anomalies are compared to each other, this becomes even more obvious, as can be seen in Figure 28. The temperature anomalies are quite similar for both measurements. In the cold area, between 700 and 800 meter along the shoreline, the cold area is clearly visible as both measurements show low temperatures. At the end of the 2015 measurement, a cold location can also be found. This suggests there might be a small amount of seepage reaching the lake. However, the temperatures measured in 2015 are colder than in 2014. Although differences exist, the temperature patterns are the same throughout the bay. There can be concluded that the measurement of 7 minutes as done by Meijer (2014) is enough to examine the seepage areas in Whakaipo Bay. The differences in temperatures between the two measurements are assumed to be a consequence of slight differences in location of the cables and a small difference in the measurement season.

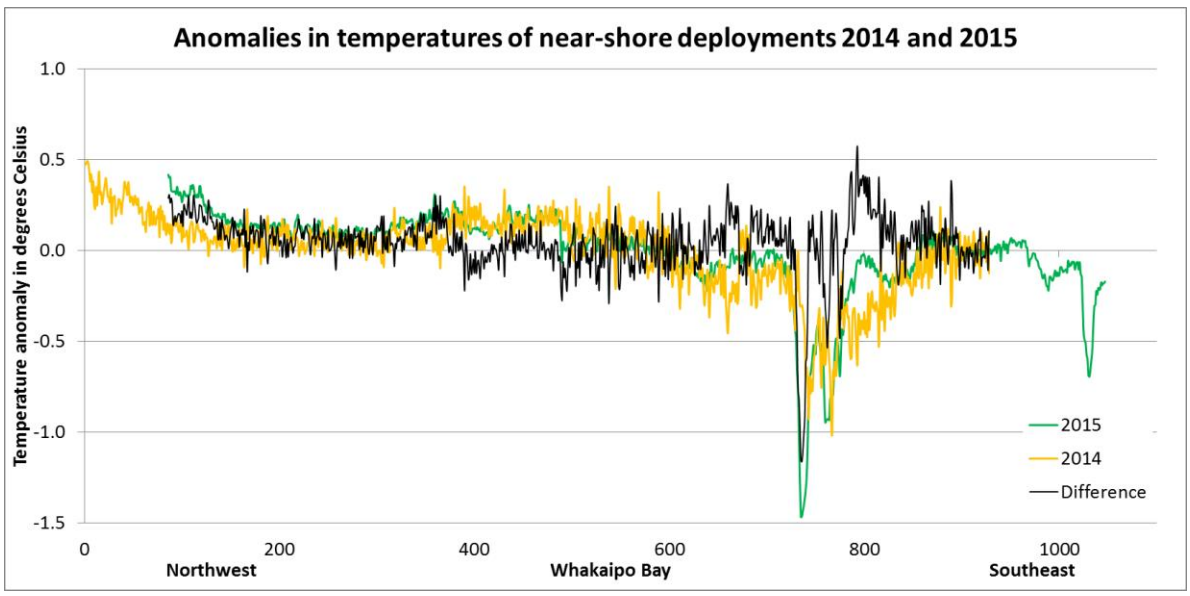

Figure 28: Temperature anomalies of near-shore deployments 2014 and 2015. Positive anomaly difference: Anomaly 2015 bigger than anomaly 2014. Negative anomaly difference: Anomaly 2015 smaller than anomaly 2014.

The differences in temperatures are displayed spatially in Figure 29.

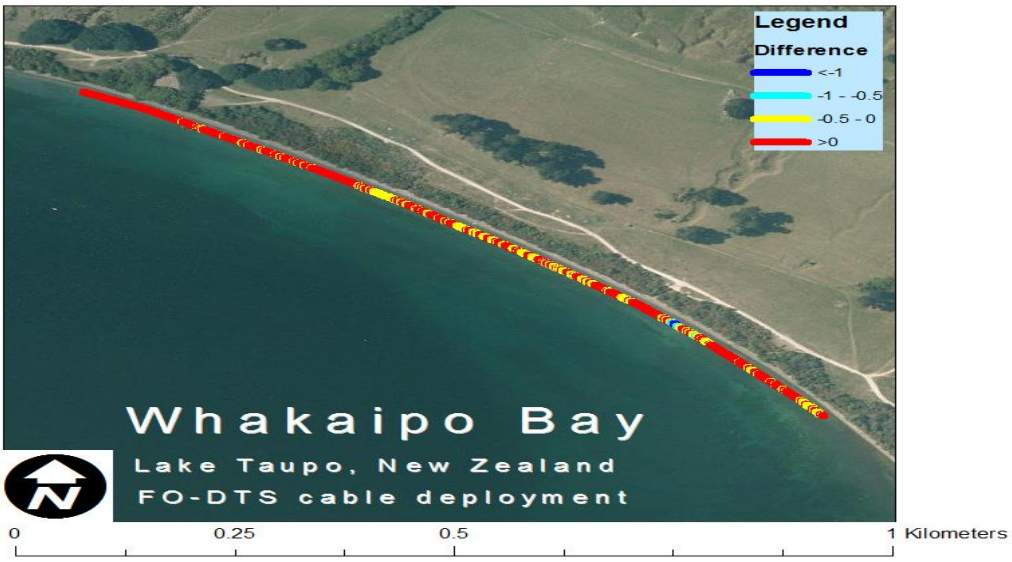

Figure 29: Differences in temperature anomalies between the 18 February 2014 and 3/4 March 2015 horizontal near-shore measurements. Positive anomaly difference: Anomaly 2015 bigger than anomaly 2014. Negative anomaly difference: Anomaly 2015 smaller than anomaly 2014.

The on-shore measurement of 2015 was conducted in the same season as the off-shore measurement of 2014 (Meijer). Hence, absolute temperatures of these measurements are comparable. The temperatures found in the off-shore region were similar to the temperatures found in the cold areas of the on-shore measurement of 2015, albeit slightly colder. To conclude, areas that are significantly colder than their environment are detectable by DTS. Horizontal DTS is useful in distinguishing areas based on different temperatures.

Adjacency

Still unknown is the influence of temperature readings in surrounding areas at a certain point along the cable. The average temperature for each location along the cable was calculated and sorted from low to high. Consequently, the variance for the concerned point was calculated according to Equation 8.

Equation 8: Variance of temperatures, where AT is average temperature, n is the number of adjacent points taken and q is the temperature of the concerned point

$$Variance = ((AT\ of\ n\ locs\ west; AT\ of\ n\ locs\ east) - AT\ loc\ q)^2$$

All variances are shown in Figure 30.

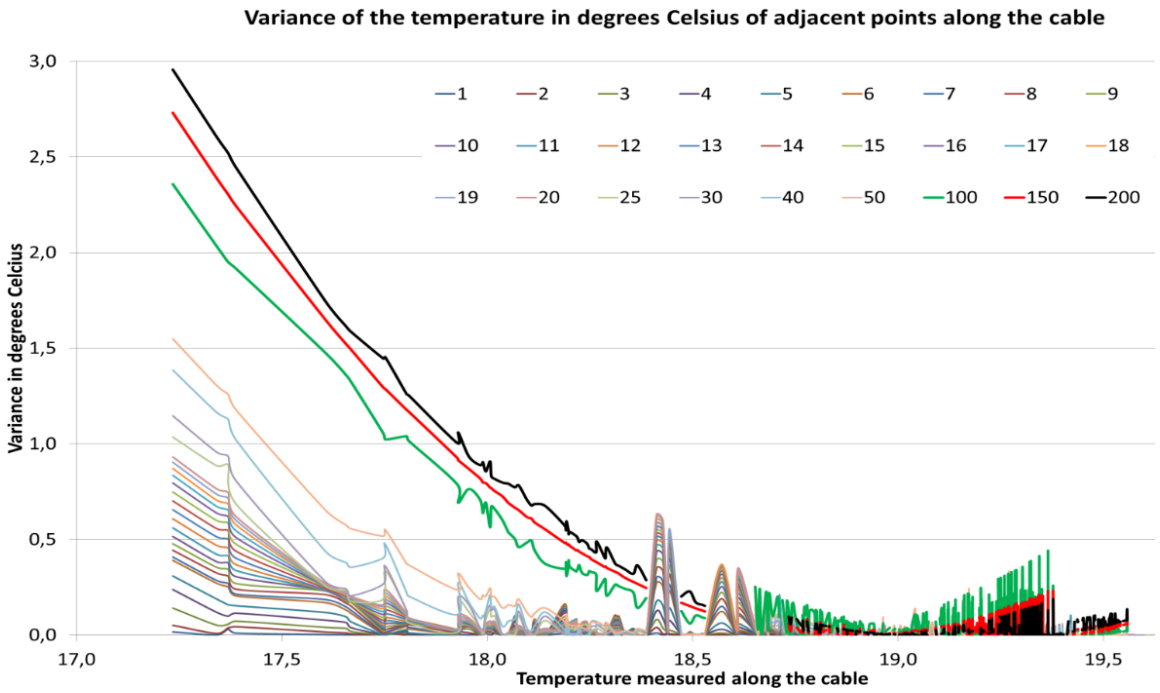

Figure 30: Influence of variance of temperature of adjacent points along the cable on the temperature at a specific location on the cable. The data series with highest number of adjacent points taken (100 / 150 / 200) were given a more distinctive colour

The highest variances in temperature were found at the location where most adjacent points were taken, which was expected. From the graph it appears clearly that the variances in temperature were highest at the locations where the lowest temperatures were measured. To be expected was that the lowest variances were found where highest temperatures were measured by H-DTS, as high temperatures were assumed to indicate lowest seepage rates. However, the lowest variance was found around 19.0 °C, whereas several higher temperatures were measured. Some striking peaks are visible, such as on 18.4 °C and 18.6 °C. This might be due to a sudden decrease in temperature at locations where seepage occurs.

5.2 Vertical profiling

RQ2: To what extent is vertical deployment of DTS, validated with a numerical model, temperature loggers and seepage meters, able to quantify the seepage flow in different parts of Whakaipo Bay?

The vertical profiling consists of V-DTS, logger measurements, direct seepage measurements, modelling and a comparison of the results of these techniques.

5.2.1 Vertical DTS

Vertical profiling using H-DTS took place in April 2014 (Meijer) and in February and March 2015 at near-shore locations in Whakaipo Bay. An overview of the measurements is given in Figure 31. The measurements were located on both horizontal near-shore measurements and observations of algae on pock-marked depressions. The coordinates of these V-DTS locations are given in Appendix F.

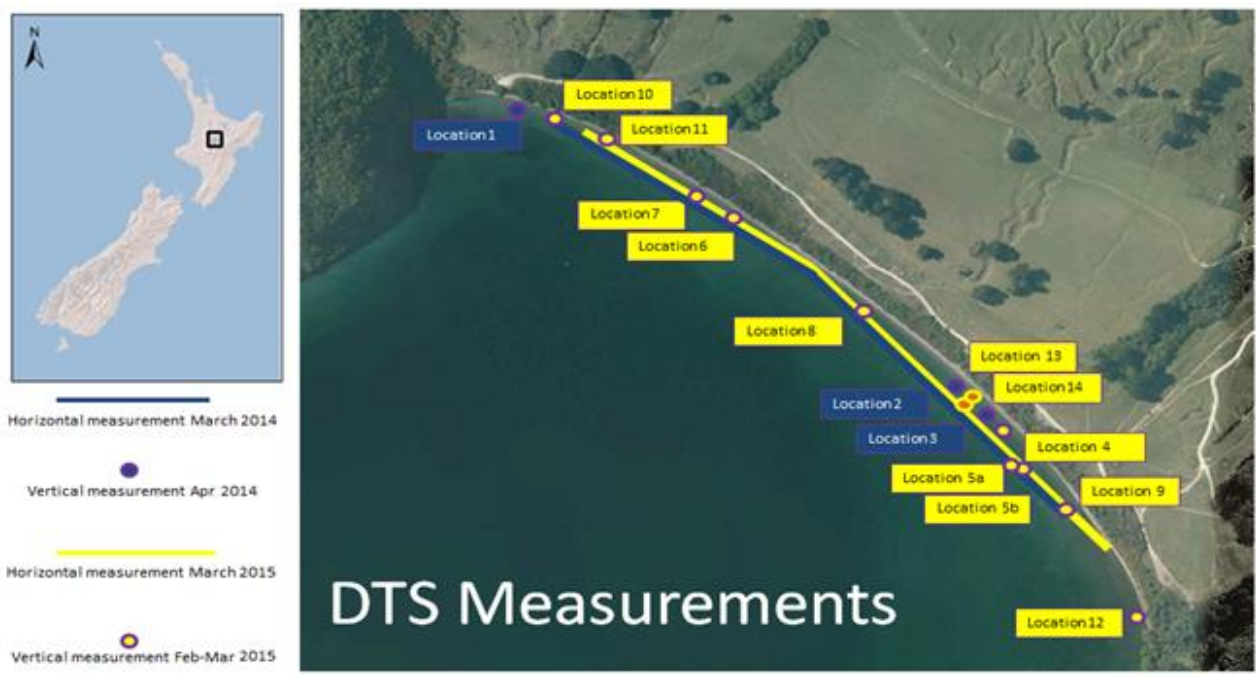

Figure 31: Overview of locations of V-DTS measurements and H-DTS near-shore deployments

The details of these measurements are shown in Table 4.

Table 4: Details of V-DTS measurements

LOC	Date	Daypart	Depth in m	Average temp ºC	Groundwater expected based on temperature H-DTS	Algae
1	2/4/14	Afternoon	1.20	18.0	No	No
2	10/4/14	Early afternoon	1.10	17.8	Yes	No
3	10/4/14	Late morning	1.20	18.5	Yes	Yes
4	13/2/15	Morning	1.40	18.7	Maybe	No
5a	13/2/15	Afternoon	1.60	20.4	Maybe	Yes
6	19/2/15	Early morning	1.20	18.5	No	No
7	19/2/15	Early afternoon	1.25	19.7	No	No
8	19/2/15	Late afternoon	1.10	21.3	No	No
5b	25/2/15	Morning	1.10	19.3	Maybe	Yes
9	25/2/15	Afternoon	1.10	20.6	Maybe	Yes
10	10/3/15	Morning	1.25	19.4	No	No
11	10/3/15	Early afternoon	1.20	19.4	No	No
12	*10/3/15*	*Late afternoon*	*0.37*	*8.4*	*Maybe*	*No*
13	20/3/15	Morning	1.50	14.7	Yes	No
14	20/3/15	Early afternoon	1.25	16.1	Yes	No

As can be seen in Table 4, the average temperatures differs between T = 8.4 °C and T = 21.3 °C. When the divergent result of LOC12 is not taken into account, the minimum average temperature of all locations is T = 14.7 °C . The minimum and maximum temperatures at each location are displayed in Figure 32.

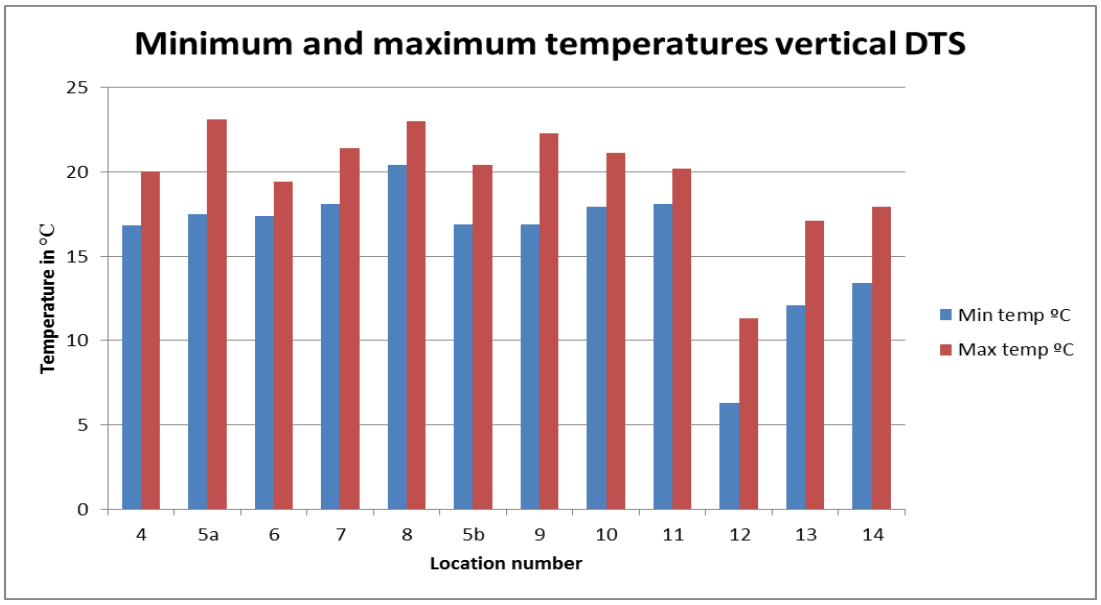

Figure 32: Minimum and maximum temperatures at each location by V-DTS

In Figure 33 a location of V-DTS surrounded by algae (LOC5B) and a location in a dug hole (LOC12) are shown.

Figure 33: A) V-DTS at LOC5B, among algae. B) V-DTS in dug shallow hole at LOC12

The measurement results are visualised using MATLAB software. The DTS set-up for each location is shown in Appendix F. Seepage is thought to happen at locations where a layer of cold water is developing at the base of the graph, which represents the SWI.

Figure 34: Measured water temperatures in °C at LOC4 by V-DTS

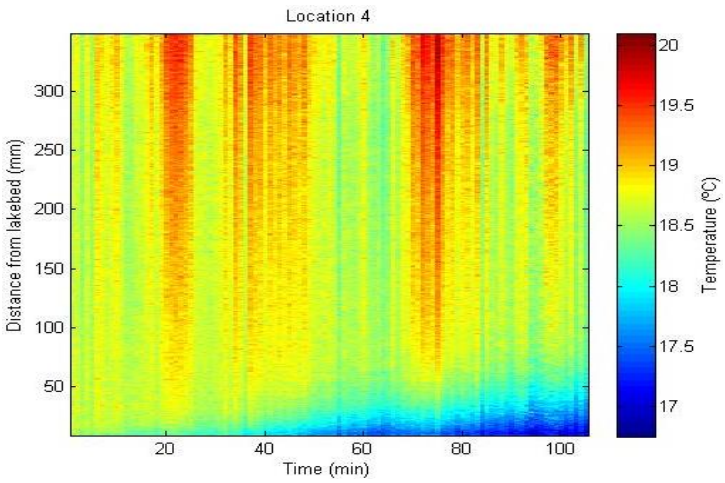

***LOC4** (Figure 34)*

Growth of cold water layer after 50 minutes

Seepage: Yes

Figure 35: Measured water temperatures °C at LOC5A by V-DTS

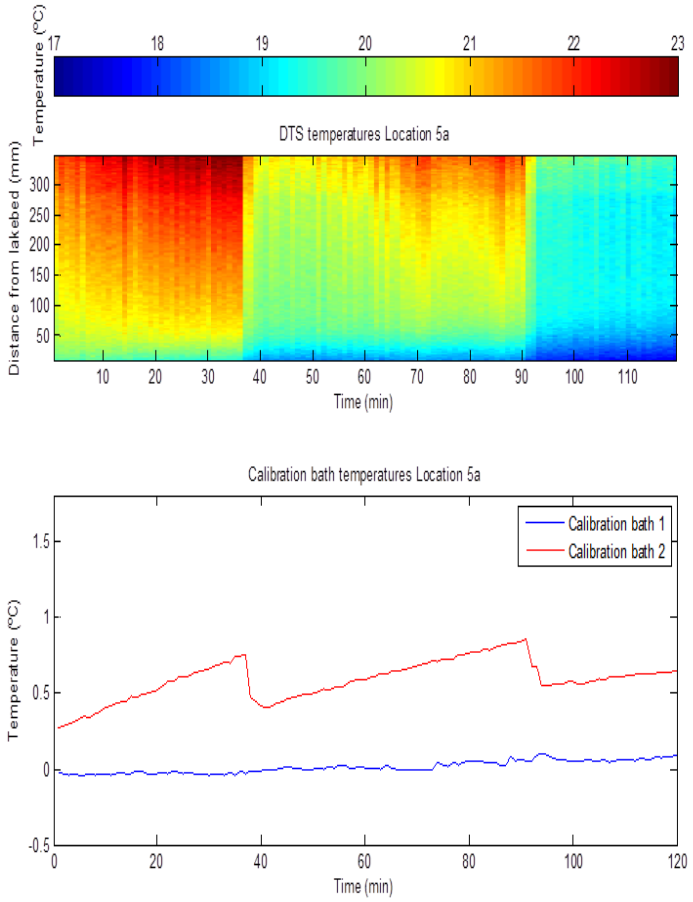

LOC5A *(Figure 35)*

Decrease of 1 °C over 5 minutes time after 35 minutes and a decrease of 1 °C over 10 minutes after 90 minutes

Decreasing of 0.3 °C of water in calibration bath 2 of for both situations

Probably caused by a sudden (re-) start of the aquarium bubbler in the calibration baths. The temperature of the water in calibration bath 2 shows sudden changes and this supposedly heavily affects the measurement data

Seepage: Probably not, as the water temperatures are decreasing due to the effect of the calibration baths.

Figure 36: Measured water temperatures in °C at LOC5B by V-DTS

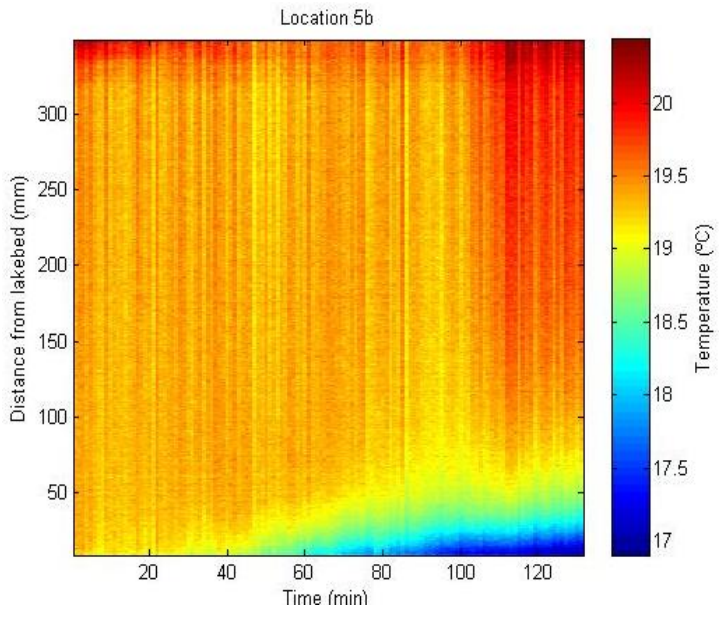

LOC5B *(Figure 36)*

7 meters distance from LOC5A

Growth of cold water layer after 60 minutes

Temperatures of upper water layers increased significantly in the last 20 minutes. This warming is probably due to sunlight in the late afternoon.

Seepage: yes

Figure 37: Measured water temperatures in °C at LOC6 by V-DTS

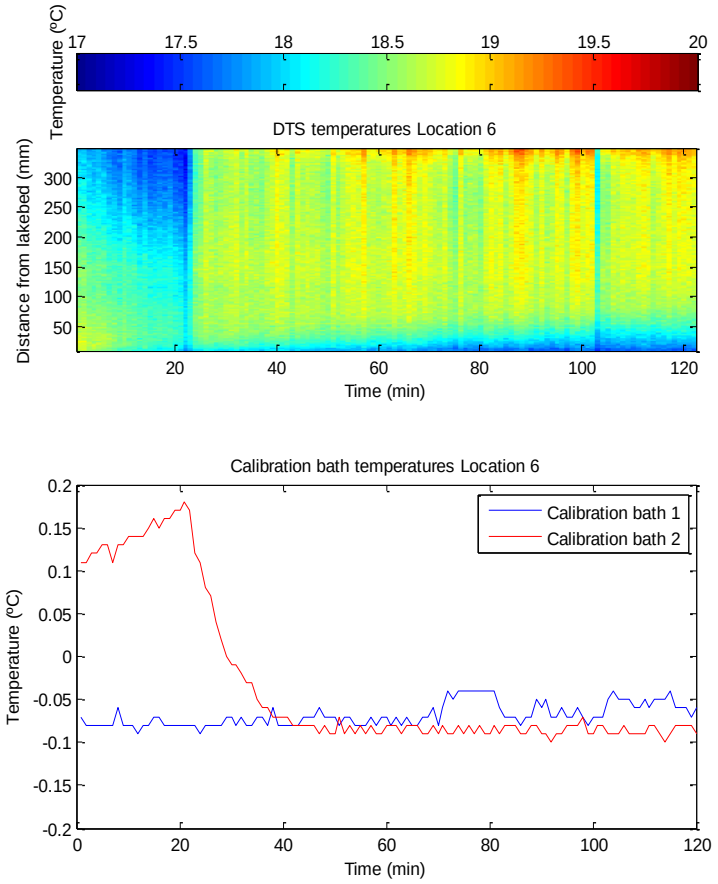

LOC6 *(Figure 37)*

Increase of 0.7 ºC after 22 minutes

Probably due to a decreasing temperature of the water in calibration bath 2 of 0.27 ºC between 21 and 40 minutes, with the largest part of the drop (0.17 ºC) in the first 7 minutes

Temperature of the water in calibration bath 2 does not decrease that much like the decrease in bath 2 at LOC5B.

Water temperatures increased rather than decreased

Growth of a tiny cold layer after 60 minutes

Seepage: Possibly, although the cold water layer is small

Figure 38: Measured water temperatures in °C at LOC7 by V-DTS

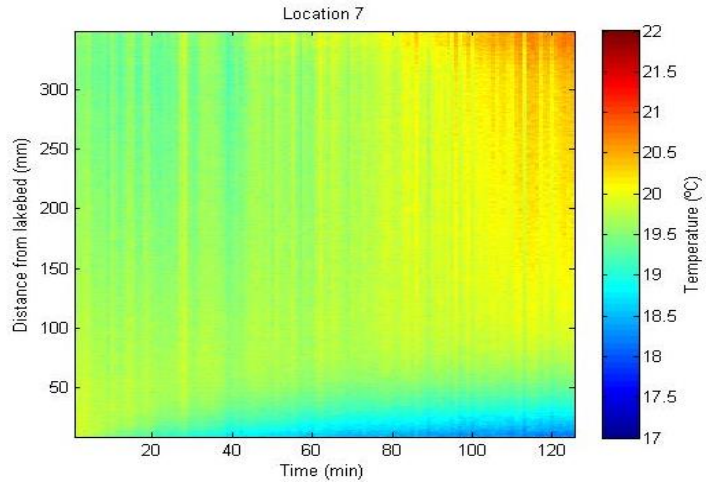

LOC7 *(Figure 38)*

Growth of a tiny cold layer at SWI after 60 minutes

Seepage: Possibly, although the cold water layer is small

Figure 39: Measured water temperatures in °C at LOC8 by V-DTS

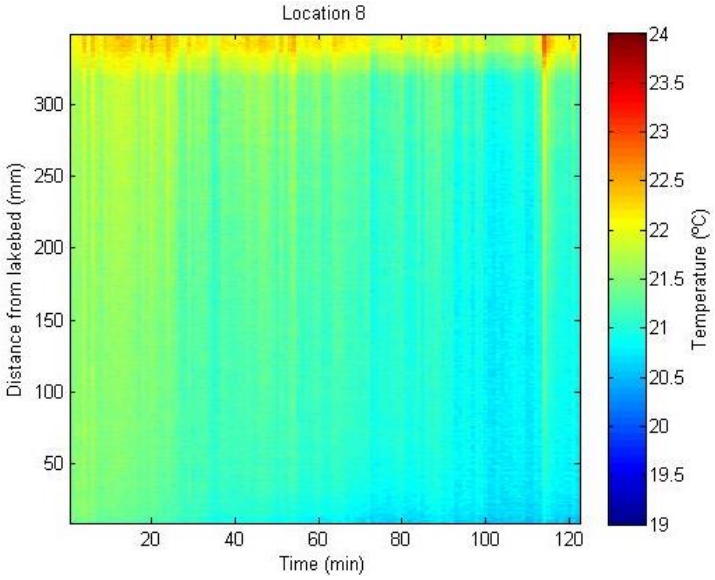

LOC8 *(Figure 39)*

No cold layer growing at SWI

Temperatures drop over time, as the measurement was conducted in late afternoon

Between lake bed and lake surface almost no variations in temperature visible, except for the last 20 minutes

Seepage: No

Figure 40: Measured water temperatures in °C at LOC9 by V-DTS

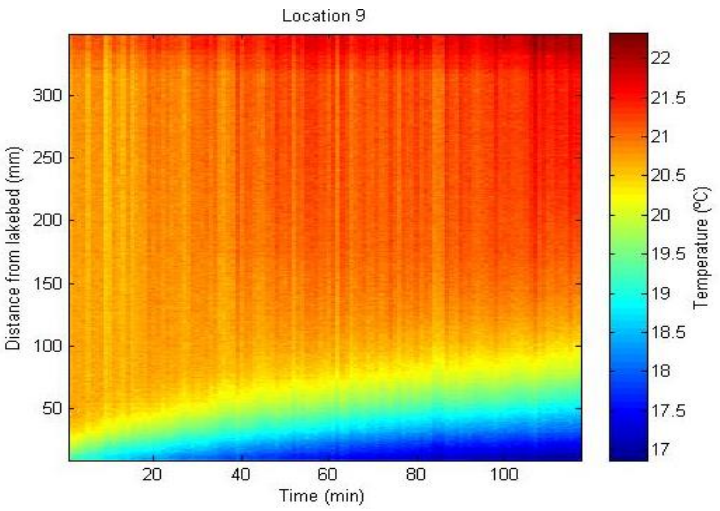

LOC9 *(Figure 40)*

5 meter from algae area

Clear layer of groundwater at SWI grew after 20 minutes

Seepage: Yes

Figure 41: Measured water temperatures in °C at LOC10 by V-DTS

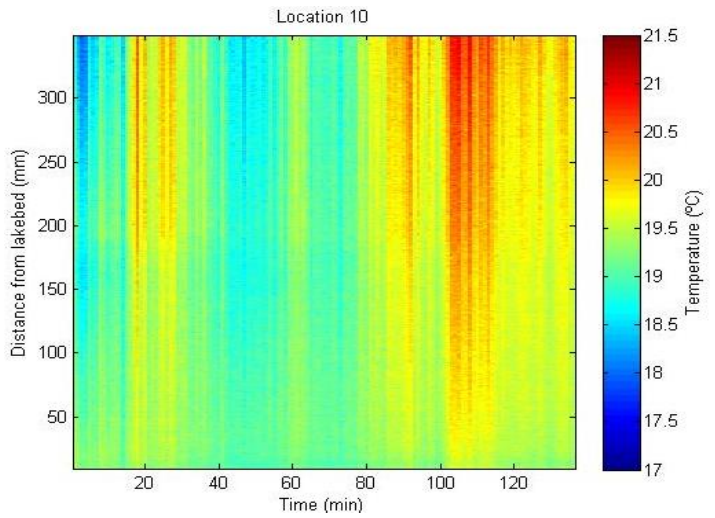

LOC10 *(Figure 41)*
In warm area of H-DTS

No cold layer developed at SWI

Temperature variation probably due to turbulence. Abrupt changes due to a temperature decrease of the water in calibration bath 2.

Seepage: No

Figure 42: Measured water temperatures in °C at LOC11 by V-DTS

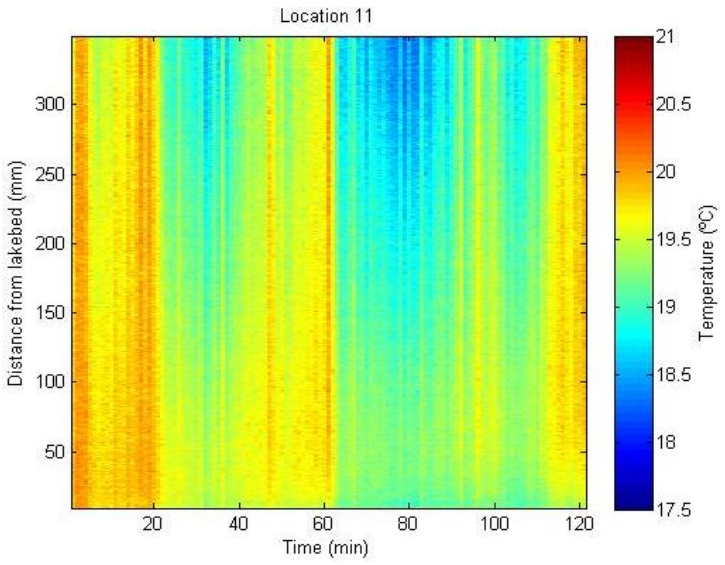

LOC11 *(Figure 42)*

In warm area of H-DTS

No cold layer growing at SWI

Temperature variation probably due to turbulence. Abrupt changes due to a temperature decrease of the water of calibration bath 2.

Seepage: No

Figure 43: Measured water temperatures in °C at LOC12 by V-DTS

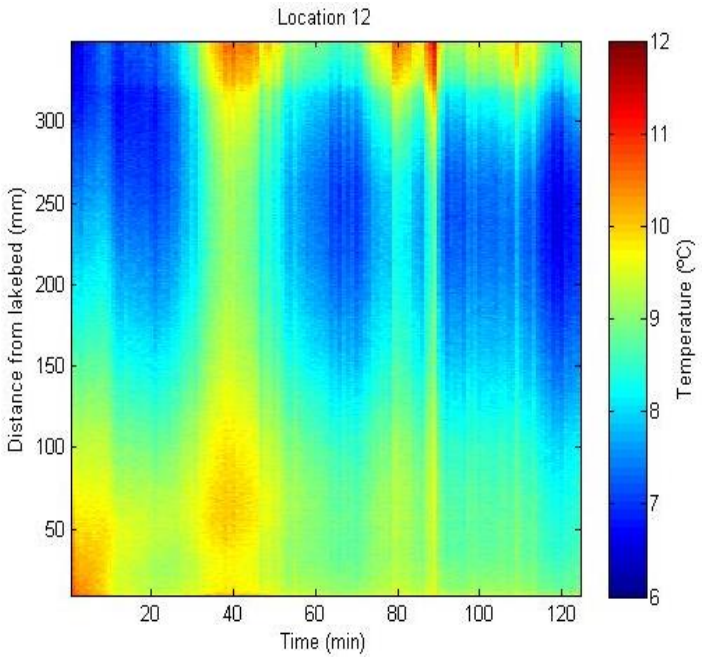

LOC12 *(Figure 43)*

Next to the outlet of the stream, 1.5 meter off the current in a dug hole

DTS was submerged under water, but the cylinder was not.

Temperature totally dependent on the temperature of the water in calibration bath 1, which fluctuated for unknown reasons.

Very cold temperatures, between 6 °C and 9 °C.

Seepage: Unknown

Figure 44: Measured water temperatures in °C at LOC13 by V-DTS

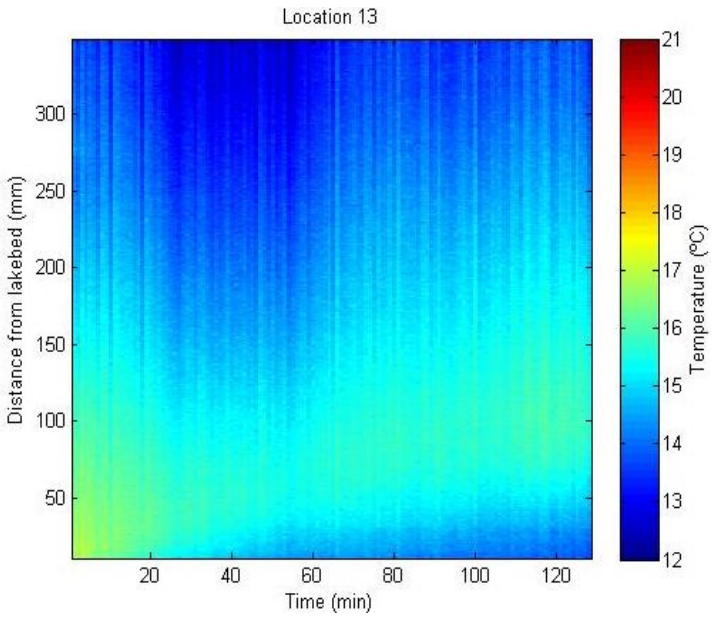

LOC13 *(Figure 44)*

Located at the coldest H-DTS spot

The temperature of the overlying surface water was cold, which is credible because the air temperature was low

Growth of cold water layer after 60 minutes

Seepage: Yes

Figure 45: Measured water temperatures in °C at LOC14 by V-DTS

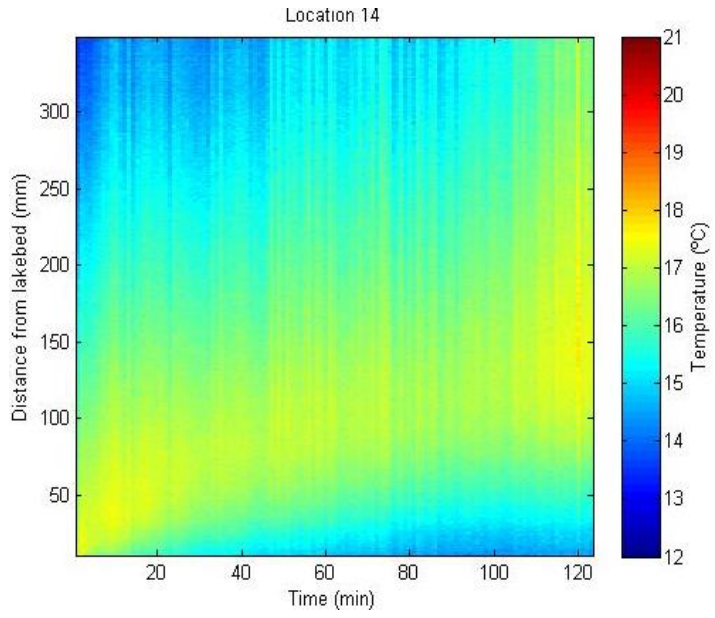

LOC14 *(Figure 45)*

At 5 meter distance of LOC13

Temperature of the overlying lake water was quite low, as air temperature was cold.

A small cold-water layer developed at the SWI.

Seepage: Yes

Flows

The seepage flow at each location was calculated using the displacement calculation method of Equation 2 and is shown in Table 5.

$$Q\ (cm/h) = Depth\ of\ groundwater\ layer\ at\ t_1\ (cm) * \frac{60}{Measurement\ time\ (min)}$$

The depth of the groundwater layer is the water depth above SWI where average water temperature at $t_1$is lower than average water temperature at SWI at t_0.

Table 5: Groundwater fluxes and flows V-DTS by displacement calculation. The flow rate (Q) is calculated by multiplying the flux by the cylinder area of 1134 cm².

Location number	Flux q (cm/h)	Flow rate Q (cm³/s)
1	n.a.	n.a.
2	1.27	0.400
3	2.34	0.736
4	2.05	0.645
5a	n.a.	n.a.
5b	1.66	0.523
6	0.95	0.298
7	1.23	0.388
8	0.89	0.281
9	2.24	0.705
10	n.a.	n.a.
11	0.80	0.253
12	n.a.	n.a.
13	2.30	0.724
14	2.16	0.680

At some locations is unclear whether seepage occurs, because the depth of the cold water layer does not increase much. The seepage flow rates fluctuated between $0.253\ \mathrm{cm^3/m^2/s}$ and $0.736\ \mathrm{cm^3/m^2/s}$, whereas the average rate was $0.512\ \mathrm{cm^3/m^2/s}$.

Minimum time of measurement

A measurement period of 30 minutes was not enough to provide useful information about possible seepage. A measurement period of 60 minutes would make clear whether seepage occurs, whereas a measurement period of 90 minutes probably is necessary to be able to more accurately calculate the seepage flow, since a longer series of decreasing temperatures is acquired.

Pock-marked depressions

Small open patches in algae felt colder than the surrounding areas by manual inspection. The measurements that were intended to be placed in the algae were located in these open patches, as it was impossible to install the cylinder in the algae bottom. LOC5A and LOC5B were located in the open area within the algae pock-marked depressions zone. It was tried to conduct vertical measurements at LOC9 and LOC10 in the algae zone, but the DTS cable was too short. At LOC9 (5 meter from the algae), seepage was found, but at LOC10 (20 meter from the algae area) there was certainly no seepage. Based on this limited number of measurements, there is not enough prove to state that algae zones are an indication for seepage hotspots.

5.2.2 Loggers

Vertical DTS locations

Fixed loggers

At all locations where V-DTS was used to measure temperatures, loggers were attached to the upper and lower part of the device. Hence, the upper logger was located far from the SWI, but the lower logger was located 3 cm above the SWI. Although the absolute temperatures of the loggers were not considered of importance for comparing the results, the development of temperatures over time is. In Figure 46 can be seen that the logger temperatures probably depend on the moment of the day the measurement was taken.

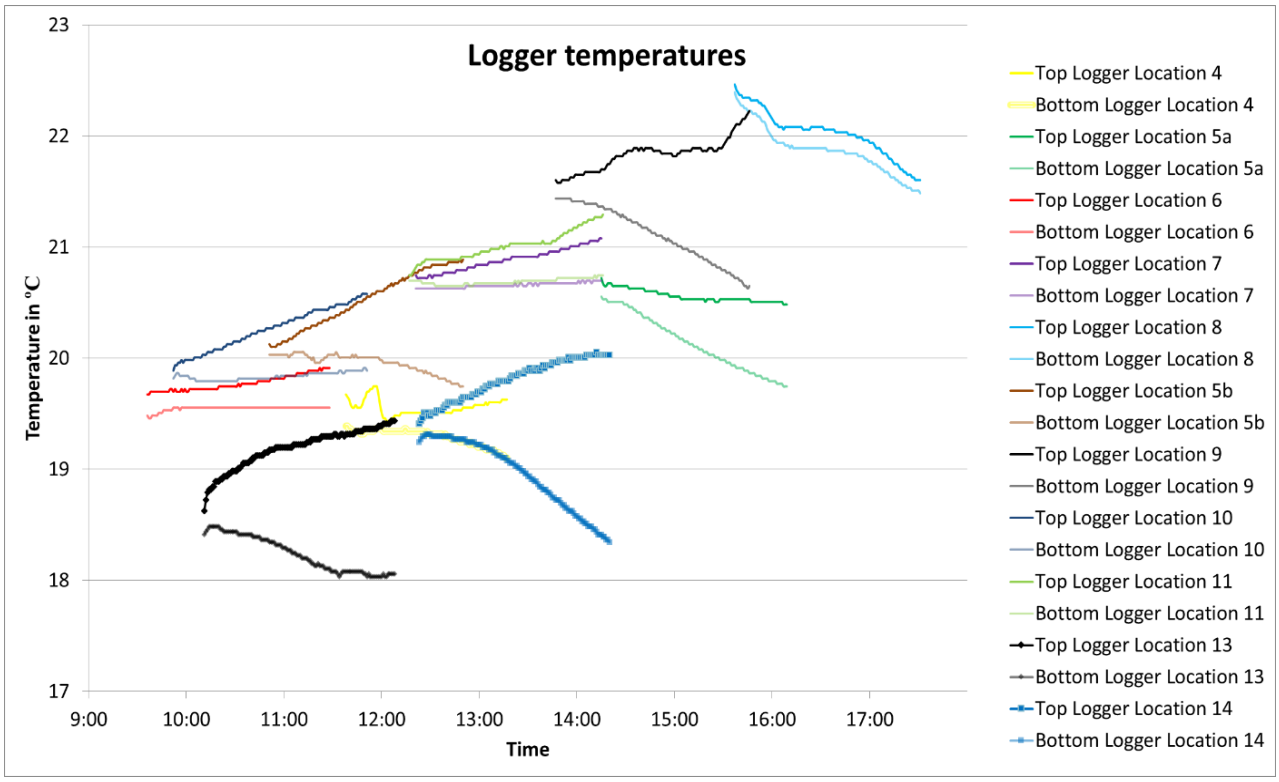

Figure 46: Logger temperatures at SWI (bottom logger) and top of V-DTS device (top logger) at each V-DTS location

The temperatures at LOC5A, LOC5B, LOC9, LOC13, LOC14 and LOC4 decreased at the lower logger level. These locations correspond with the locations where V-DTS found the highest seepage flow rates. At other locations, temperatures stayed constant (LOC6) or decreased. The logger temperatures of LOC12 are not shown in the figure as they were much lower than the other temperatures found. The bottom logger measured a decrease from 13°C to 12.5°C. The top and bottom logger temperature at LOC8 decreased. This is the only measurement that was taken during the late afternoon, when air temperatures were decreasing, which might also affect the lake water temperature. This is validated by the lake water temperatures of the V-DTS. A visualisation of logger temperatures per location is shown in Appendix F.

Logger device

As stated before, unknown is of seepage flows into Whakaipo Bay vary over the year. Logger measurements at the same locations as the V-DTS were conducted in late April, which was two weeks to two months later than the V-DTS measurements. The vertical logger device, which was shown in Figure 16, was used. The logger device shows a similar temperature decrease pattern at all locations as found with the fixed loggers. This is visualised in Figure 47 and Figure 48, which shows the temperature progression over time. Whilst the measurement at LOC3 (Figure 47) possibly was influenced by the decreasing air temperature by the end of the afternoon, the mid-afternoon measurement at LOC13 (Figure 48) shows a clear decreasing temperature at the SWI after a settlement period of 15 minutes. However, many locations showed a constant temperature rather than an expected temperature decrease.

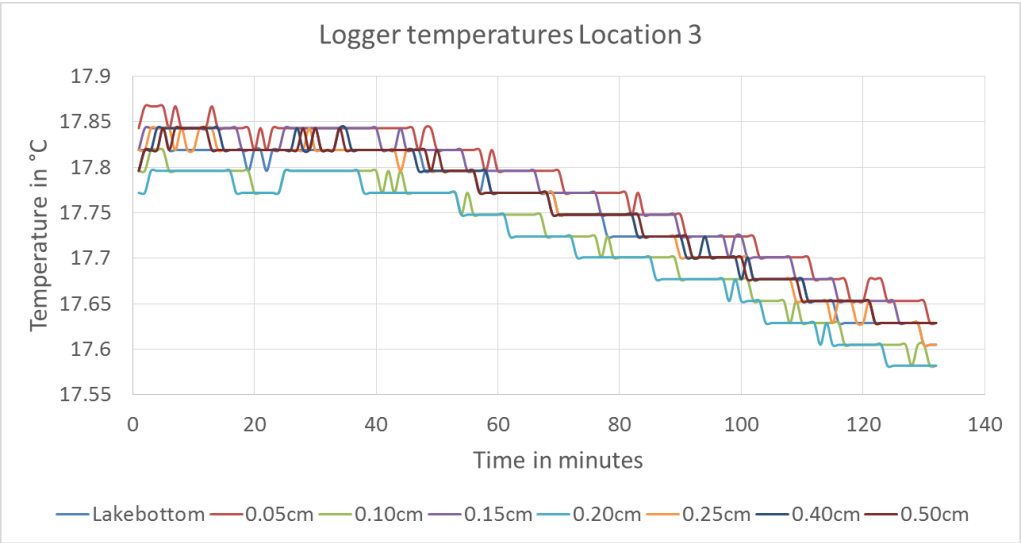

Figure 47: Logger device temperatures at LOC3.

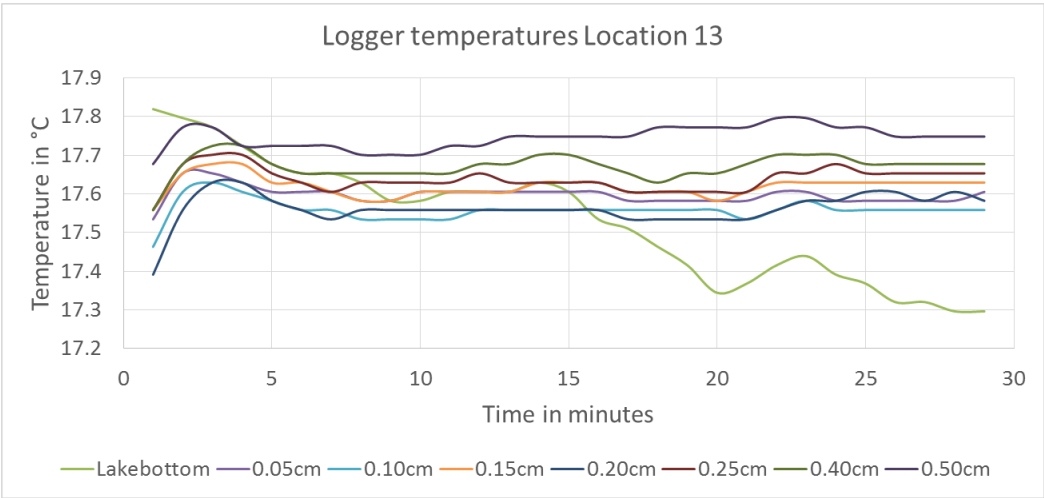

Figure 48: Logger device temperatures at LOC13

Loggers at distant locations

To be able to vertical profile the water column on off-shore locations, 12 off-shore locations between 3 and 9 meter water depth were chosen to conduct logger measurements on the off-shore H-DTS cable track. However, all the results did not show a cold-water layer growing on the SWI. Hence, it is likely that the handheld GPS was not accurate enough to track the exact cold-water areas. Another explanation might be that the rope anchor did not land at the intended location. Concluding, placement of loggers in deep water is not accurate enough to retrieve the exact locations detected by H-DTS.

Piezometer

The temperature loggers that were placed in the piezometer, measure groundwater temperatures at the groundwater level and the groundwater level itself. The piezometer was fixed in the beach by twisting and hammering until the groundwater was reached. Initially was tried to measure the groundwater temperatures slightly than at the groundwater level, but it was impossible to fix the piezometer deeper due to resistance. The loggers recorded the temperatures every minute. The measurements were taken at the on-shore beach location closest to each V-DTS measurement on April 14th and April 16th and are shown in Figure 49.

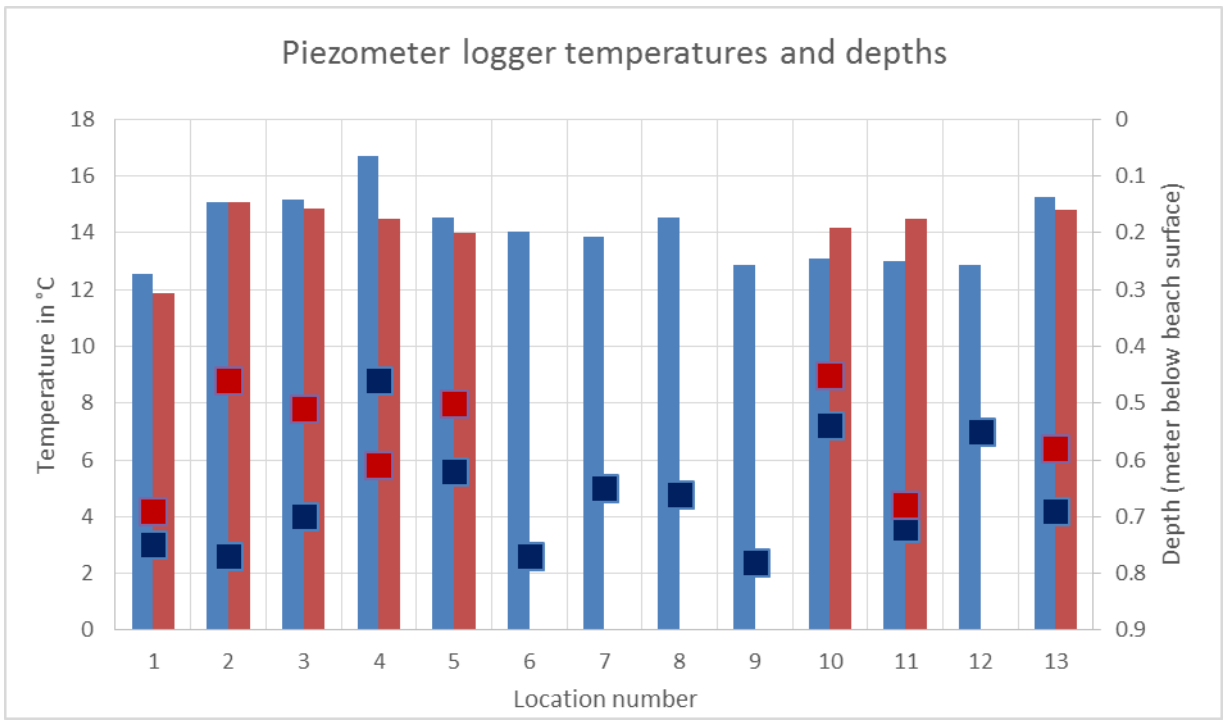

Figure 49: Piezometer logger temperatures and depths at each on-shore V-DTS location

After two rainy nights the groundwater table had increased on the latter day. The changes in groundwater level in the warm northwest area of the bay were less than 10 cm in depth, but the increase in groundwater level in the southeast cold part of the bay was between 10 cm and 31 cm in depth. The average depth increased with 14 cm to 54 cm below the surface. The temperatures found proved to be not useful, as the difference between these logger temperatures and the V-DTS temperatures at the SWI was almost 5 °C, from which the coldest logger temperatures were taken in the regions where no or little seepage flow occurs. This phenomenon might be due to the influence of both the lake and rainwater, which might be considerably on the upper groundwater layer.

Monitoring well

The temperature of the groundwater was measured with loggers in two monitoring wells close to the shore in Whakaipo Bay. Since these two measurements were conducted in the same period, the average temperature was used as for the variable groundwater temperature in the model. However, the groundwater temperature may fluctuate throughout the year. Hence it is advised that the groundwater temperature is measured during each V-DTS measurement, to improve the accuracy of the modelling results. Well 1 was located 42 meter from the shore in the western part of the bay. A groundwater level of 1.5 meter depth and an average temperature of 12.66 °C (5 May 2015) were found. Well 2 was located 82 meter from the shore at the east side of the bay. A groundwater level of 4.5m depth and an average temperature of 11.85 °C (23 April 2015) were found. Since the shallowest groundwater is most important for GW-SWI, a temperature value close to the western well value was taken for the model: 12.50 °C. Assumed is that the influence of air temperature was bigger in well 1 than in the well 2, as the groundwater level in well 1 was higher. The variability of deeper groundwater temperatures over the year is unknown. If this changes, measurements of the groundwater along the seepage measurements are likely necessary.

5.2.3 Direct seepage measurements

SPMs were used at the same locations as V-DTS. During the first measurements, rocks were put on the seepage drums to stabilize the SPM in the sandy SWI. In later measurements, twisting and turning ensured that the SPM was fixed in the sandy soil. During the first measurements, sticky seepage bags were unknowingly used, which caused a probable underestimation of seepage volumes in the seepage bags. Afterwards, measurements were conducted using a non-sticky seepage bag, prefilled with 50 mL water, and an empty non-sticky seepage bag. The prefilled bags also seemed to

underestimate the flow, such that only the non-sticky empty seepage bags were taken into account. When multiple empty seepage bags measurements were conducted, the highest measured flows were taken, since expected is that these flows were still underestimations of the total seepage flow.

The seepage rates are shown in cm³/s to compare them with the earlier calculated DTS flows and earlier research (Hector, 2004; Gibbs et al., 2005). The seepage volumes were read in mL (or cm³) during the measurement. This was converted to the same unit as the V-DTS flows (cm³/m²/s) and can be seen in Figure 50.

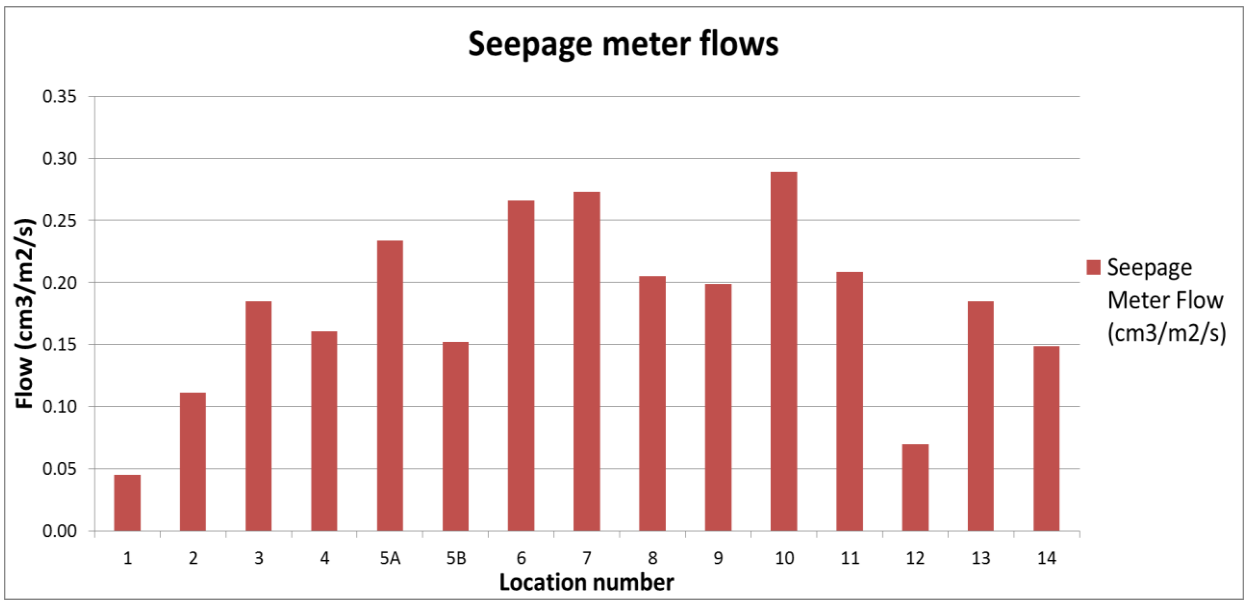

Figure 50: Seepage meter measured flows at each location (cm³/m²/s)

Notable are the differences in seepage flows, in the range of $0.045\ \mathrm{cm^3/m^2/s}$ to $0.289\ \mathrm{cm^3/m^2/s}$, whereas the average flow was $0.182\ \mathrm{cm^3/m^2/s}$.

5.2.4 Modelling

The heat-conduction model simulated a continuous seepage flow into the lake. The temperature at the locations where V-DTS recorded seepage was not continuously decreasing at the SWI. To be able to use the slope of these measurements, only the parts of the dataset where a linear decrease of temperatures occurs, are taken into account. Similar flow rates for the displacement calculation flow rate and modelling outflow rate were acquired. However, the V-DTS shows that a perfect continuous does not happen in reality and as a consequence, the flow rate in reality might be lower than calculated.

Modelling uncertainty analysis

The model investigated the effect, i.e. the discharge rate, of different initial lake and groundwater temperatures. The temperature of the lake water has a significantly large influence on the final outflow of the model. A slightly higher or lower lake water temperature usually results in completely different flow rates. The same applies to the groundwater temperature taken in the model. The flows for three scenarios, i.e. normal, low and high, were calculated. The three scenarios are the following:

1 *Normal*: Surrounding lake water temperature as calculated from the V-DTS data and the groundwater temperature by the logger in the monitoring well.
2 *Low*: Lake water temperature *Normal* -0.5 ºC and groundwater temperature 12 ºC
3 *High*: Lake water temperature *Normal* +0.5 ºC and groundwater temperature 13 ºC

The modelled flows for different scenarios and the flow calculated by V-DTS are visualised in Figure 51. The model results are given in fluxes (cm/h) but converted to flows ($cm^3/m^2/s$), to compare them with V-DTS.

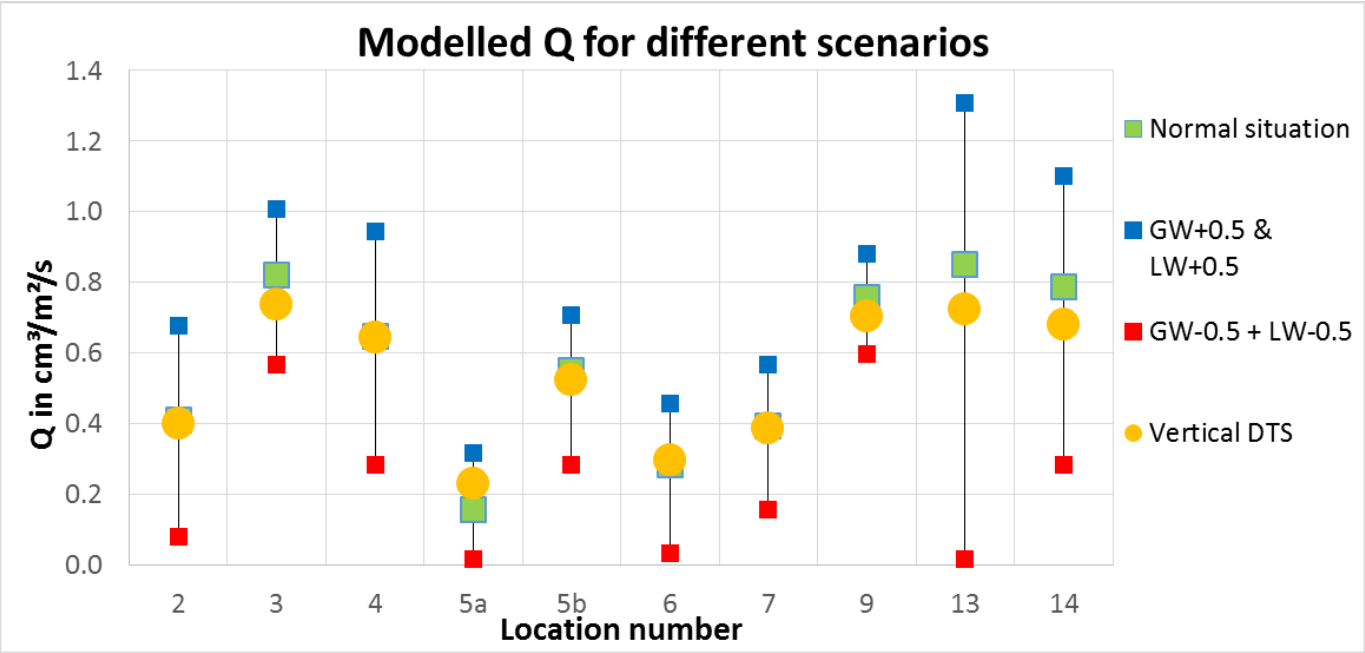

Figure 51: Modelled Q in $cm^3/m^2/s$ for the three scenarios compared to the flow by the displacement calculation of V-DTS. The squares indicate the modelled flow: Green for Scenario 1: Normal, red for Scenario 2: Low and blue for Scenario 3: High. The yellow dots indicate the seepage flows by the displacement method based on V-DTS.

The scenarios cause a large range of possible flows at LOC2, LOC4, LOC13 and LOC14. The duration of the modelling was chosen to be the same as the duration of the continuously decreasing temperatures at the V-DTS locations. At these four locations, the modelling duration was less than 70 minutes. At other locations, e.g. LOC5A and LOC9, the range of possible temperatures is quite small, probably due to long duration of the

modelling of more than 100 minutes. Concluded, the longer the duration of the modelling simulation, the smaller the range of temperatures found. In addition, the displacement method, which was used as an alternative to modelling, seems to work well as the flow rates found are similar to the flow rates found in Scenario 1: Normal. Although the modelling is sensitive to varying the parameters groundwater temperature and surrounding lake water temperature, the half degree variation between the scenarios is probably an overestimation of the uncertainty in observed temperatures.

5.2.5 Comparison of vertical profiling techniques

Large differences exist in the flow rates obtained by the SPM measurements and the rates obtained by the V-DTS measurements. This is visualised in Figure 52.

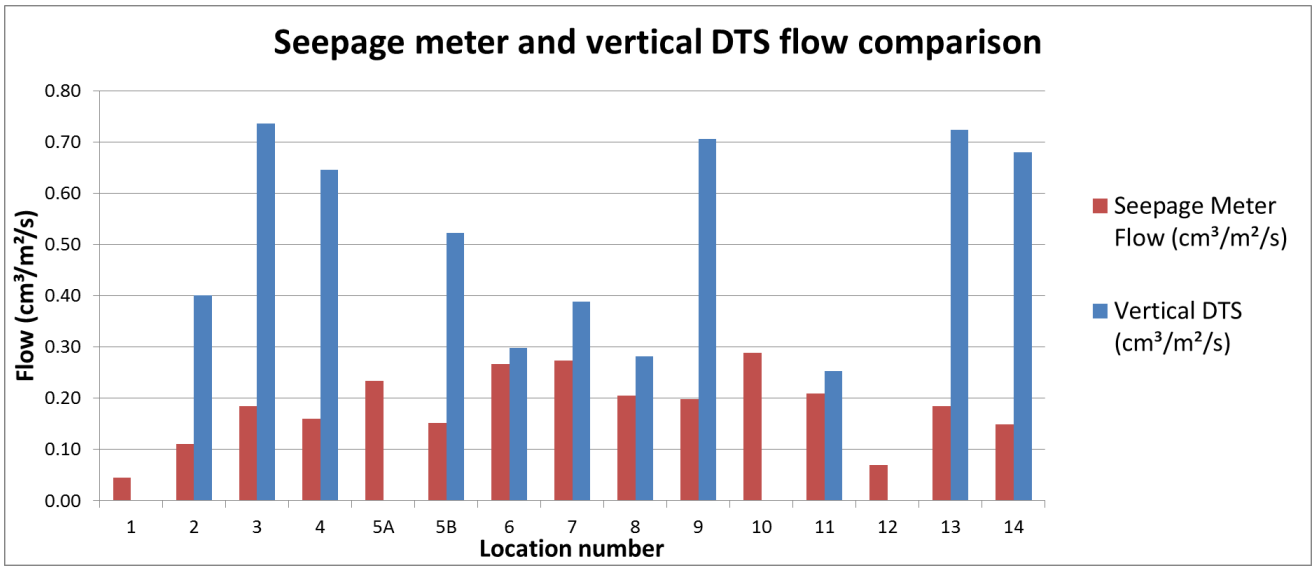

Figure 52: Differences between SPM flows and V-DTS flows by displacement calculation method

At LOC1, LOC5A, LOC10 and LOC12 it was impossible to calculate a flow using DTS measurements, but the SPMs measured small flows, except for LOC10. Strikingly, flows at locations where a little seepage flow was found by the DTS, the SPM approximates the same flow (LOC6, LOC7, LOC8 and LOC11). The average seepage flow by SPM at these locations was supposed to be $0.214\ \mathrm{cm}^3/\mathrm{m}^2/\mathrm{s}$, but was $0.305\ \mathrm{cm}^3/\mathrm{m}^2/\mathrm{s}$ by V-DTS. Thus, the average flow rate for these locations by V-DTS was 42% higher than the SPM flow rate.

At locations where V-DTS measured high seepage rates (LOC2, LOC3, LOC4, LOC5B, LOC9, LOC13 and LOC14), the SPM resulted in much lower flows. Whilst the average seepage flow of the SPMs was $0.163\ \mathrm{cm}^3/\mathrm{m}^2/\mathrm{s}$, the V-DTS resulted in $0.628\ \mathrm{cm}^3/\mathrm{m}^2/\mathrm{s}$. Thus, the average flow rate for these locations by V-DTS was 384% higher than the SPM flow rate.

In Figure 53 the SPM flows and V-DTS flows were sorted from the highest to the lowest values. In the left graph all flows are displayed, except the flows for which the displacement method did not yield a seepage rate. The rank order of the flows differs much between the V-DTS and SPM flow rates. In the right graph, only the high flow situations (>0.3 cm³/m²/s), as calculated by the displacement method, are shown. For this situation, the rank order is quite similar for both methods, as LOC3, LOC9 and LOC13 were characterised by the highest flows for both methods, whereas LOC2, LOC4, LOC5B and LOC14 were characterised by the lowest flows for both methods.

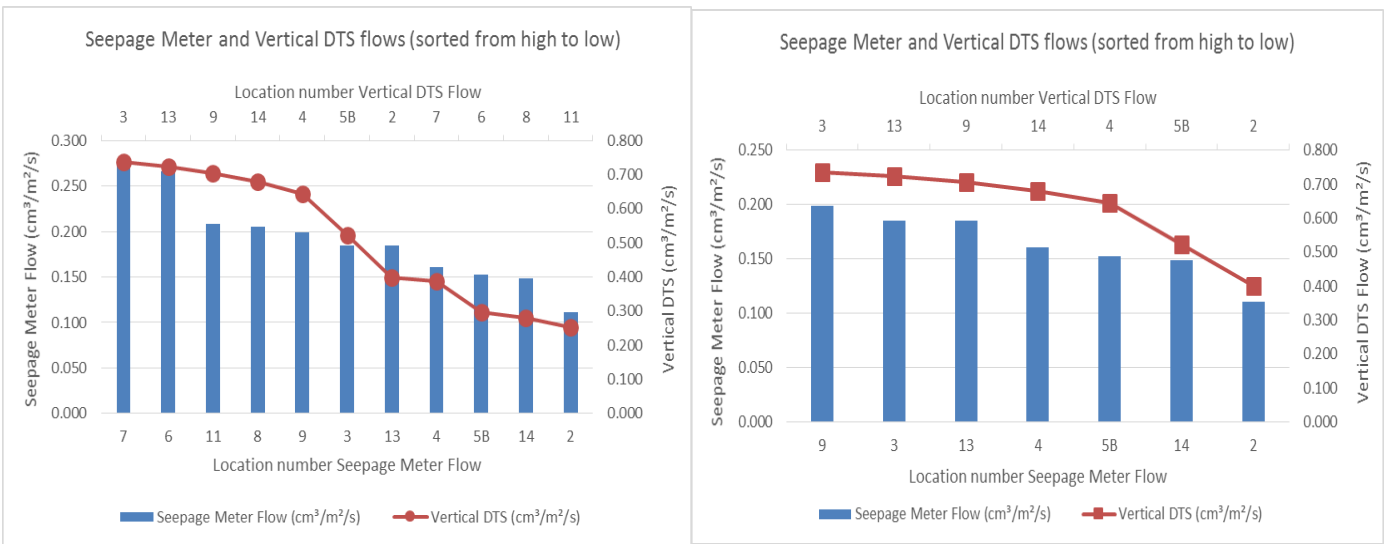

Figure 53: Seepage Meter and Vertical DTS flows. Left: Seepage meter flows at LOC1, LOC5A, LOC10 and LOC12 are left out as there are no corresponding V-DTS flowsRight: Only the high flow V-DTS seepage flows are shown.

Although the SPM results in low-seepage flow areas explained most of the seepage flow, on average 79% as calculated by the V-DTS, this cannot be said of the SPM results in high-seepage flow areas, which only explained 26% of V-DTS. This is visualised in Figure 54.

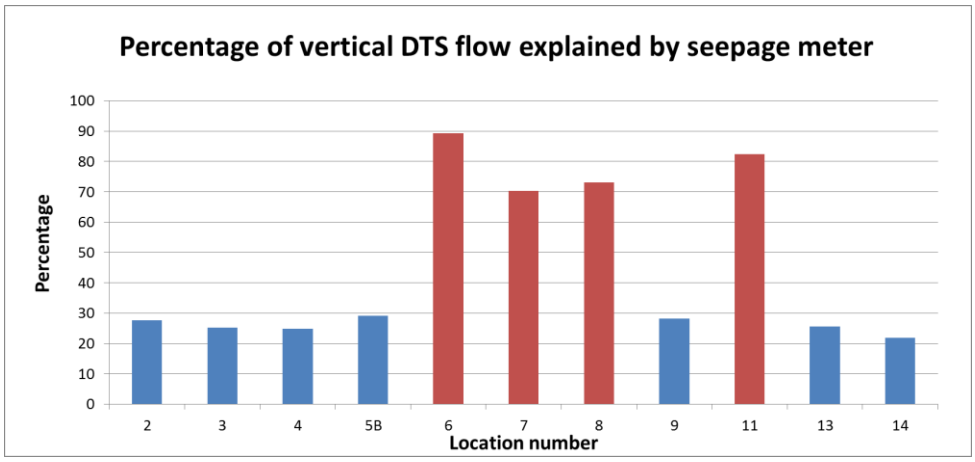

Figure 54: Percentage of SPM flow relative to V-DTS flow by displacement calculation

The share of V-DTS flow explained by the SPM seepage low-flow locations LOC6, LOC7, LOC8 and LOC11 is between 70% and 90%. The share of the V-DTS flow explained by the SPM seepage high-flow locations is between only 20% and 30%. It seems that SPMs can approximate the same seepage flow as found by the V-DTS at locations with a flow lower than 0.3 $cm^3/m^2/s$ (90% of flow explained) or 0.4 $cm^3/m^2/s$ (70% of flow explained). However, the SPMs highly underestimated the seepage flow for the higher V-DTS flows. This might be due to multiple causes, which will be described in the Discussion.

As seen in Figure 51, the modelling scenario 'Normal' approximates the flows found by V-DTS, as the flow rates are in a range of $0.160\ \mathrm{cm}^3/\mathrm{m}^2/s$ to $0.850\ \mathrm{cm}^3/\mathrm{m}^2/s$. The flows of this scenario were between 0.1% and 18% higher than the flows calculated by V-DTS, except for LOC5A and 7.

A comparison between seepage meter flows and vertical DTS flows shows that low flows seem hard to quantify using vertical DTS. Although still is uncertain about the accuracy of SPM's, for these low-flow situations seepage meters seem to be a more appropriate detection and calculation technique whereas vertical DTS seems to be more appropriate for high-flow situations. However, yet is unknown how accurate both methods. Besides, if the modelling is performed using a larger thermal diffusion coefficient, which accounts for turbulent exchange of heat, different or similar flux rates for both methods could be the outcome.

5.3 Linking horizontal and vertical DTS

RQ3: To what extent could horizontal DTS be improved to directly detect seepage areas and quantify seepage flows in lake environments?

Preferably, the amount and duration of measurements to gather useful results should be minimised to keep costs low. The measurements done in this research are rather time consuming, as can be seen in Table 6.

Table 6: Typical duration of temperature and seepage measurements in Whakaipo Bay

Measurement	Duration of measurement	Duration of whole measurement process	Total duration
Horizontal near-shore DTS	24 hour 2km cable	Deployment: 3 hour Monitoring: Often during day light, during night every couple of hours Un-deployment: 3 hour	30 hour
Vertical near-shore DTS	Measurement of 90 min	Deployment: 1 hour Monitoring: 1.5 hour Un-deployment 1 hour	3.5 hour
Seepage meter	Measurement of 30 min	Deployment: 5 minutes Settling: 10 minutes Monitoring: 30 minutes Measuring: 10 minutes Un-deployment: 5 minutes	1 hour

V-DTS results were used to calculate the seepage flow rate at one location. After combining the flow rates at several V-DTS locations, a relation between the average temperature and the flow rate at one location was made to calculate the flow rates along the H-DTS cable. This is a direct way of calculating flow rates along a cable by only measuring temperatures with H-DTS.

Regression formula

As can be seen in paragraph 5.4.1., the seepage flow rates along the H-DTS cable can be calculated using a regression relation. However, the relation was based on ten V-DTS measurements only and could become more trustworthy if more measurements were conducted. Furthermore, the new V-DTS results should be compared to further seepage meter measurements at locations where H-DTS and V-DTS results indicate seepage flows in Whakaipo Bay.

Testing the regression formula

Apart from an increased amount of V-DTS measurements that should be done in Whakaipo Bay, the regression relation should be tested in other environments. Conditions might differ, and the linear relation might even differ much from the relation used in Whakaipo Bay. However, if the relation is tested in multiple environments, different formulas can be constructed for different environments, such as rivers, bays, seas or for sandy, silty or clayey soils.

Bathymetry correction factor

A remaining issue is the movement of water following the downward sloped bathymetry of the lake. A possible solution to this might be the use of a correction factor, to correct the found flow for this phenomenon (Figure 1). However, this is dependent on the location of the measurement and the local bathymetry.

5.4 Spatial variability

RQ4: To what extent is DTS able to calculate the seepage component of the water balance by extrapolation of seepage inflow into Whakaipo Bay?

The spatial variability of seepage flows can be approximated by extrapolating the found seepage flows into the lake for the whole bay. The extrapolation is based on a regression between average temperature and associated flow rate. Cumulative flows following the extrapolation were compared against seepage flows from different water balances.

5.4.1 Regression

In order to retrieve a linear relation between temperature and flow rate, the vertical flow rates obtained by the displacement calculation of V-DTS are plotted against horizontal H-DTS temperatures at all V-DTS locations. The regression is based on Equation 7 and is shown in Figure 55.

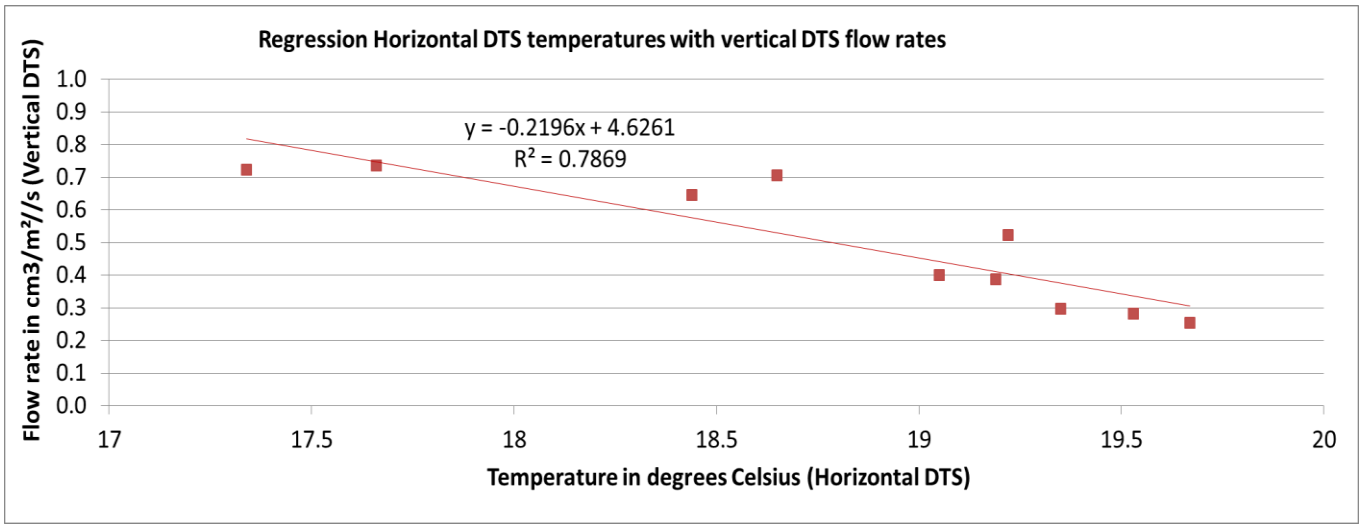

Figure 55: Relation H-DTS temperatures with V-DTS flow rates at each location showing the regression line

The goodness of fit (R^2), which shows what share of the variances are explained by the regression, which is 0.79 and is considered sufficient to use the linear relation for further extrapolation. The linear relation assigns flow rates on all temperatures lower than 21 °C. If higher temperatures were found, the negative flow rate is converted to a flow rate of $0\ \mathrm{cm^3/m^2/s}$. Due to this relation, temperatures in the range of 19-20 °C result in slightly higher flows than expected, as can be seen in Figure 55. However, as these flows are amongst the lowest flow rates of all locations, this was accepted. The linear relation is based on V-DTS measurements between 1 and 2 meter depth, and is suitable to extrapolate the flow. Since no other relation is available, this relation will also be used to extrapolate at other parts of Whakaipo Bay.

5.4.2 Extrapolation

The temperatures found by H-DTS were used for applying the linear relation. The total near-shore cable length of 1218 meter exists of the values found in 2015, extended with 85 meter of the H-DTS measurement by Meijer (2014). The temperatures from the period 14h-15h were taken for the 2015 measurement, combined with the anomalies of the complete 7-minute measurement of 2014. Noted should be that the near-shore H-DTS measurements of 2014 and 2015 were taken in different periods in late summer. Unfortunately, for the easternmost 171 meter of the bay no near-shore deployment was used. This extrapolation was based on extending the easternmost 20 meter of the near-shore measurement of 2015. However, the ultimate first and last parts of the bay were not taken into account.

When all flows for each point were calculated and summed using the regression relation, the total flow along the cable length resulted in $350\ \mathrm{cm}^3/\mathrm{m}^2/\mathrm{s}$. The extrapolations for areas 1, 2, 3 and 5 are visualised in Table 7, whereas the extrapolation of area 4 is shown in Table 8. The width of the areas into the bay is multiplied by the flow rates of the DTS cable.

Table 7: Width, size and extrapolated flow rates of different areas

Area	Area name	Width (m)	Size (m²)	Flow (m³/s)
1	DTS Cable	1	1200	0.00035
2	<1 meter depth (Hector, 2004)	6.5	38,000	0.023
3	1-2 meter depth (Bathymetry, 1966)	100	94,000	0.035
4	2-6.5 meter depth (Bathymetry, 1966)	Table 8	292,000	0.085
5	2-6.5 meter depth (Gibbs et al., 2005)	140	180,000	0.260

Table 8: Subdivision of Area 4 in 6 regions and their width, length and size

Region	Part of 2-6.5 meter depth area	Width (meter)	Length (meter)	Size (m²)
1	Far-west	300	160	48,000
2	Central-West	200	170	34,000
3	Middle-west	150	230	34,500
4	Middle-east	200	150	30,000
5	Central-east	250	160	40,000
6	Far-east	300	350	105,000

The size of areas 2 and 5 were based on Hector (2004) and Gibbs et al. (2005). The size of area 3 and 4 were determined by the water depth in Whakaipo Bay (LINZ, 1966, Figure 56). Area 3 consists of the region in which the water depth is less than 1 meter. As

indicated in Table 7, a subdivision of the 2-6.5 meter deep region, Area 4, was made in Appendix G. A few sub-regions were defined since the width of this area, which will be multiplied with the flow along the cable, differs much throughout the bay. The width of the six regions of Area 4 is estimated. The outer boundary for both area 3 and 4 was defined by the depth of 6.5 meter.

The bathymetry map (LINZ, 1966) validated that the large cold flows found in the horizontal off-shore measurement in 2014 by Meijer (Figure 30) are located at 3 locations, which are on a depth of 5 or 6 meter, on a depth of 2 meter closer to the shore and in an area in the western part of the bay, which is estimated to be 5 meter deep.

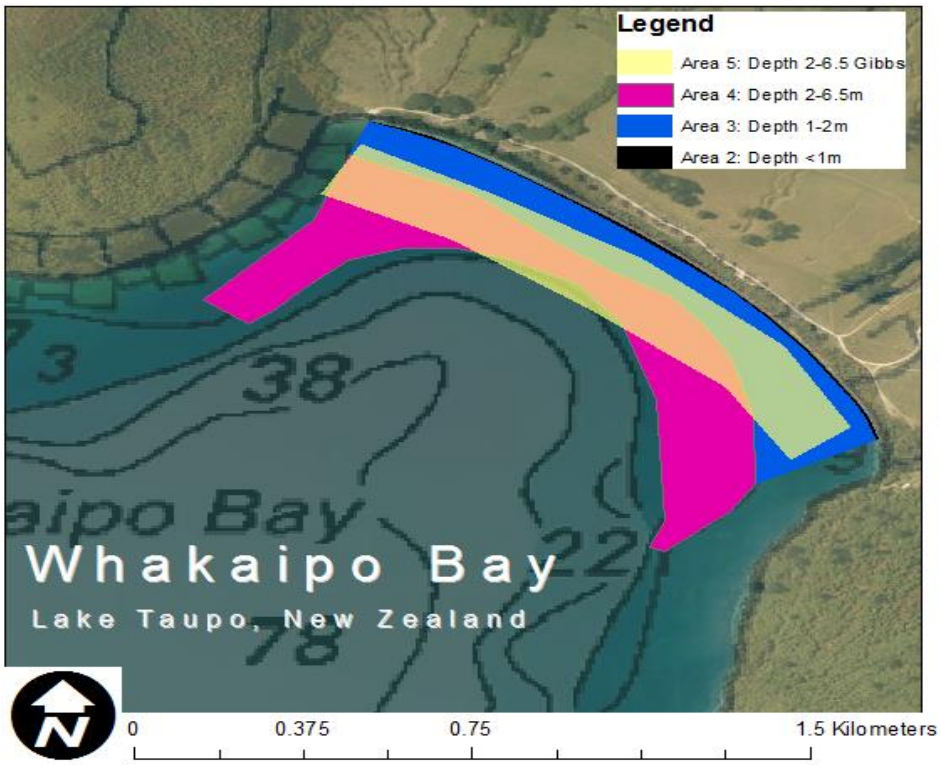

Figure 56: Bathymetry Map Whakaipo Bay with indicated areas 2 until 5 (LINZ, 2006). Area 2 is visible as a black strip along the lake edge. Because of the overlap, Gibbs <2-6.5 meter area is projected in a transparent yellow colour

5.4.3 Water balance

The water balance for the Mapara catchment is shown in Table 9. The data used to estimate its component are described in Appendix H. The total actual evapotranspiration is subtracted from the precipitation, which gives the precipitation surplus. After subtracting the discharge from the precipitation surplus, groundwater replenishment remains. Noted must be that 90% of the discharge of the Mapara Stream is considered base flow, which is groundwater that flowed into the stream before it reaches the lake. Hence, the total groundwater replenishment is slightly higher than the total seepage flow.

Table 9: Water balance Mapara catchment

Water balance component	m³/y	m³/s	Percentage of precipitation surplus
Precipitation	44,485,195 (Tait et al., 2006; Westerhoff, 2015a)	1.411	n.a.
Actual evapotranspiration	31,337,860 (Mu et al., 2011; Westerhoff 2015b)	0.994	n.a.
Precipitation surplus	13,147,336	0.417	100%
Discharge Mapara Stream	2,680,560 (Vant and Smith, 2004)	0.085	20%
Total seepage flow into lake	10,466,776	0.332	80%

The total seepage flow equals $0.332\ \mathrm{m}^3/\mathrm{s}$, which is 80% of the total precipitation surplus. This is a number close to the value of 81% found in the water balance study for Whakaipo Bay done by Piper (2004).

5.4.4 Discussion of estimated flows

The comparison of flows from different studies is presented in Table 10.

Table 10: Derived total average groundwater flow (m³/s) into Whakaipo Bay based on different studies

Area	Hector (2004)	Gibbs et al. (2005)	Piper (2004)	Klinkenberg
A. Shallow <1	0.021			0.002
B. Shallow-deep 1-2				0.035
C. Deep 2-6.5		0.24		0.085
Total extrapolated flow			*0.328*	*0.123*
Total extrapolated flow using Hectors shallow <1				*0.141*

As can be seen in Table 10, considerable differences exist in the results of the different studies. Piper's estimate of $0.328\ \mathrm{m}^3/\mathrm{s}$ for the total seepage flow is similar to the total seepage rate of $0.332\ \mathrm{m}^3/\mathrm{s}$ calculated by the water balance in this study. The extrapolation in this study results in a total flow of $0.123\ \mathrm{m}^3/\mathrm{s}$. In this study, the formula used for extrapolation in the area with a water depth of 0-1 meter, yielded much lower seepage rates than Hectors rate, who calculated a 10 times bigger flow. However, the assumption can be made that seepage flow in the area where water depth is between zero and one meter, is factor 10 bigger than the flow in the area with a water depth between one and two meter.

The extrapolation in this study showed seepage flow for the deep area which is factor 5 smaller compared to Gibbs et al. (2005): 0.05 m³/s instead of 0.25 m³/s. Gibbs et al. (2015) placed the two most easterly located benthic chambers in the middle of the area that appeared to be a large inflow zone (Meijer, 2014). However, other parts of the area in which Gibbs et al. (2004) estimated the flow rate, are supposed to be a no inflow zone,

according to the off-shore H-DTS measurement. For this reason, the estimates of Gibbs et al. (2015) for seepage into this part of the bay, which were based on these benthic chamber measurements, are supposedly too high.

It might be possible that cold locations can be found along the 5 meter deep isobaths in the bay, where currently no measurement has taken place. This would explain the missing seepage of the extrapolated seepage rate, as the researched regions cover only 35% (0.123 m^3/s) of the total seepage as calculated in the water balance (0.332 m^3/s). If Hectors reliable measurements for the shallow lake-edge area are taken into account, instead of the regression formula for area 2, the total seepage component would be 0.141 m^3/s and the percentage of the total extrapolated flow, with respect to the total seepage flow as calculated in the water balance, would rise to 41% (Table 10). There are areas close to the shore where no seepage measurements were conducted, such as in the western and the eastern part of Whakaipo Bay.

5.4.5 Uncertainty analysis of extrapolation and water balance method

The seepage component for the Mapara Stream catchment as calculated by the extrapolation method resulted in much lower rates than the as calculated by the water balance. In this paragraph an uncertainty analysis is performed, comparing the uncertainties in the results of the extrapolation method with the uncertainties in results of the water balance method, in order to investigate if the difference can be explained by the uncertainties in both methods.

Extrapolation method

1. All modelled minimum and maximum flows for each location are displayed in Table 11. As it was impossible to model both minimum and maximum flow rates at LOC8, LOC11 and LOC13, these locations were not taken into account in this analysis.

Table 11: Minimum and maximum modelled flow rates at each location. The 'Normal Flow rate' indicates the flow as calculated by the displacement method.

Location	Temperature °C	Flow rate ($cm^3/m^2/s$)		
Number	*H-DTS*	*Modelled Low*	*Normal*	*Modelled High*
2	19.05	0.08	0.4	0.68
3	17.66	0.57	0.74	1.01
4	18.44	0.28	0.65	0.95
5b	19.22	0.28	0.52	0.71
6	19.35	0.03	0.3	0.46
7	19.19	0.16	0.39	0.57
8	19.53	n.a.	0.281	n.a.
9	18.65	0.6	0.7	0.88
11	19.67	n.a.	0.253	n.a.
13	17.34	n.a.	0.72	n.a.

2. All flow rates from Step 1 were plotted against the average temperature at each location, as calculated by H-DTS and is shown in Figure 57.

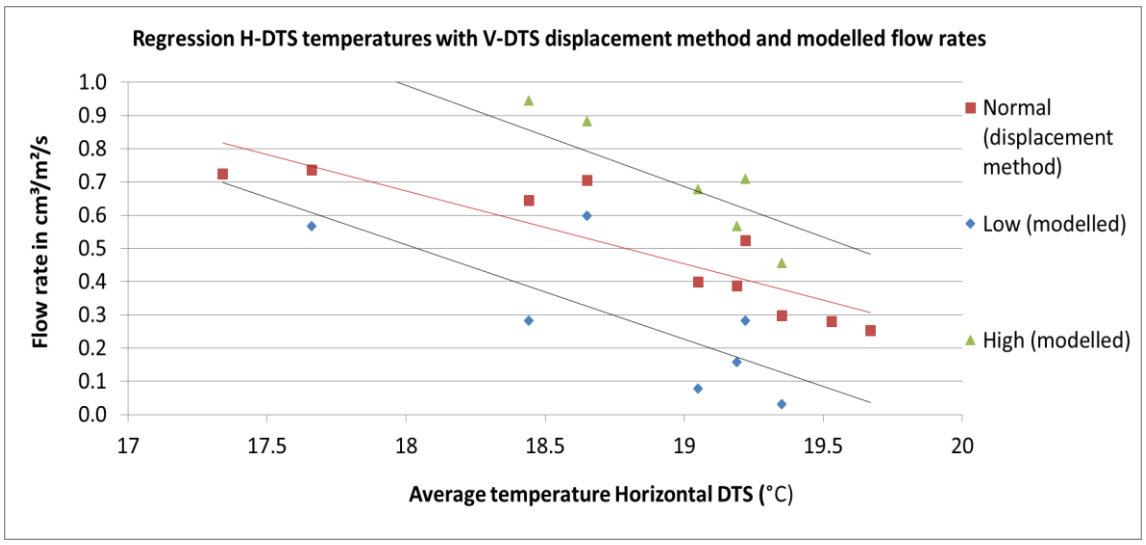

Figure 57: Regression of horizontal DTS temperatures with vertical DTS displacement method and modelled flow rates

The resulting regression formulas are shown in Table 12.

Table 12: Regression formulas for modelled minimum and maximum scenarios and for the displacement method (normal)

Scenario	Regression formula	Goodness of fit (R^2)
Minimum	Q ($cm^3/m^2/s$) = -0.284 * Temperature (°C) + 5.6243	R^2 = 0.5752
Normal	Q ($cm^3/m^2/s$) = -0.2196 * Temperature (°C) + 4.6261	R^2 = 0.7869
Maximum	Q ($cm^3/m^2/s$) = -0.341 * Temperature (°C) + 7.1654	R^2 = 0.8917

3. The bathymetry map widths that were used to calculate the minimum and maximum seepage rates by the regression formula are shown in Table 13.

Table 13: Subdivision of Area 4 for the minimum and maximum extrapolation scenario

Region	Part of 2-6.5 meter depth area	Estimated width (m)	Estimated width -50% (m)	Estimated width + 50% (m)
1	Far-west	300	150	450
2	Central-West	200	100	300
3	Middle-west	150	75	225
4	Middle-east	200	100	300
5	Central-east	250	125	375
6	Far-east	300	150	450

4. The extrapolated values for each of the areas are displayed in Table 14.

Table 14: Seepage rates (m³/s) for the three scenarios for the bathymetry map based areas. Hectors 0-1 meter depth extrapolation value is 0.021 m³/s.

Scenario	Seepage rate in area (m³/s)					
	Cable	*0-1 Bathymetry*	*1-2 Bathymetry*	*2-6.5 Bathymetry*	***Total***	***Total (Hector instead of 0-1 Bathymetry)***
Minimum	0.00004	0.0003	0.004	0.006	**0.010**	**0.031**
Normal	0.00035	0.0023	0.035	0.085	**0.123**	**0.141**
Maximum	0.00052	0.0034	0.052	0.190	**0.246**	**0.264**

Water balance

The uncertainties in the components of the water balance, other than groundwater replenishment, were evaluated. As observed in Figure 20, the minimum seepage rate scenario subtracts maximum actual evapotranspiration and maximum discharge from minimum precipitation, whereas the maximum seepage rate scenario subtracts minimum actual evapotranspiration and minimum discharge from maximum precipitation. The values for each single point measurement used are shown in Table 15.

Table 15: Values of water balance components used for the minimum and maximum seepage rate scenarios

Scenario	Precipitation (mm/y)	Actual Evapotranspiration (mm/y)	Discharge (L/s)
Minimum seepage rate	1144 (min)	910 (max)	85 (max, Vant and Smith, 2004)
Maximum seepage rate	1235 (max)	690 (min)	75 (min, Hadfield, 2007)

The water balances for the three different scenarios are shown in Table 16. All components were converted to m³/s and the precipitation and actual evapotranspiration rates were summed for the 37 locations. Two values for Mapara Stream discharge were found, i.e. minimum discharge $0.075\ \mathrm{m}^3/\mathrm{s}$ s (Hadfield, 2007) for the maximum seepage rate scenario and maximum discharge $0.085\ \mathrm{m}^3/\mathrm{s}$ (Vant and Smith, 2004) for the minimum seepage rate scenario. However, the discharge retrieved from Vant and Smith (2004) was used for the normal seepage rate scenario as well, so the discharge of the stream is the same for these two scenarios.

Table 16: Water balance for the minimum, normal and maximum seepage rate scenarios

Scenario	Minimum seepage rate scenario	Normal seepage rate scenario	Maximum seepage rate scenario
P (m³/s)	1.368	1.411	1.477
AET (m³/s)	1.088	0.994	0.825
P surplus (m³/s)	0.280	0.417	0.652
Q (m³/s)	0.085	0.085	0.075
Seepage (m³/s)	**0.195**	**0.332**	**0.577**
Percentage Seepage of P surplus (%)	70	80	88

Comparison of uncertainty analyses

In Figure 58 a comparison of the minimum, maximum and normal flow rate are shown for the extrapolation and water balance method. The first column for the extrapolation method indicates the minimum, normal and maximum flow of the extrapolation purely based on the bathymetry map, whereas the second column uses the seepage rate of 0.021 m³/s for the shallow 0-1 meter deep area as calculated by Hector (2004) to replace the bathymetry map based 0.003 m³/s for this region.

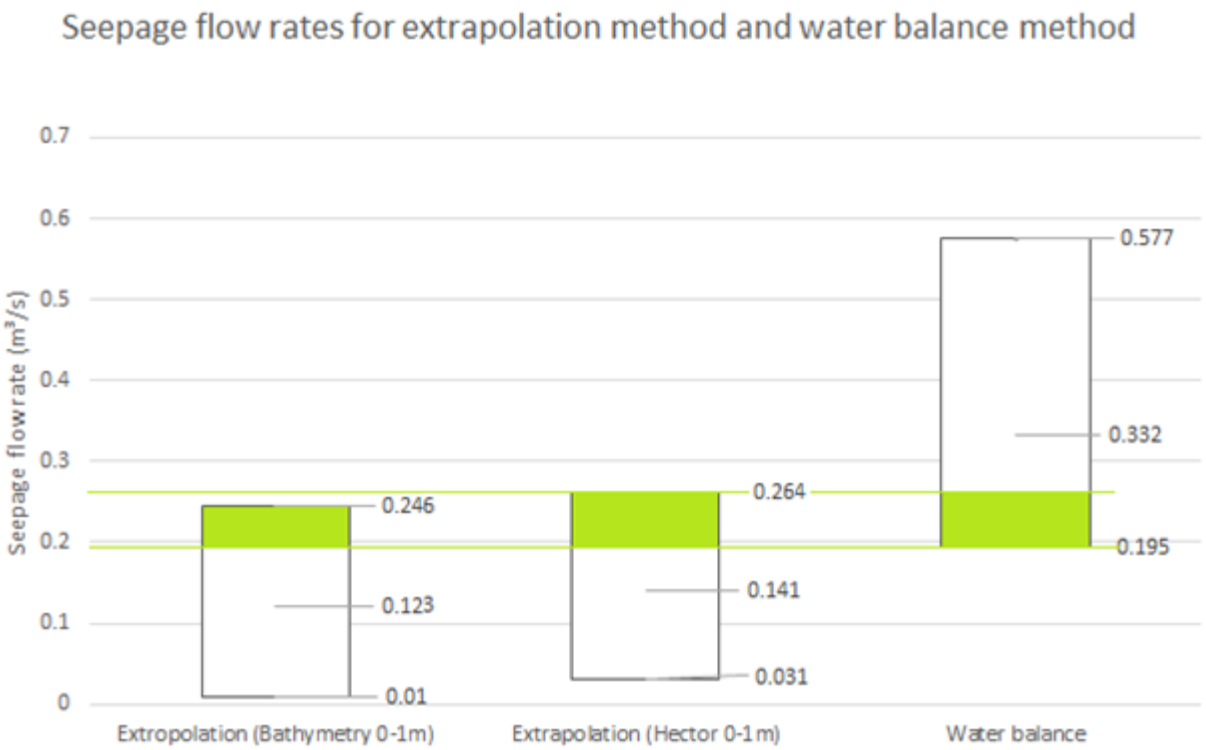

Figure 58: Seepage flow rates for extrapolation method and water balance method. The lowest number for each method indicates the minimum seepage rate and the highest number the maximum seepage rate, whereas the middle number indicates the 'normal' seepage rate which was calculated before. The green area indicates the range of seepage rates in which extrapolation is similar to water balance.

The maximum flow rates of the extrapolation scenarios are higher than the minimum flow rate of the water balance method. The uncertainty range of seepage rates for which the extrapolation method is similar to the water balance method is indicated by the green region (between $0.195\ \mathrm{m}^3/\mathrm{s}$ - $0.246\ \mathrm{m}^3/\mathrm{s}$ for the bathymetry based extrapolation and between $0.195\ \mathrm{m}^3/\mathrm{s}$ - $0.264\ \mathrm{m}^3/\mathrm{s}$ for the Hector based extrapolation).

Concluding from this uncertainty analysis, the seepage flow as calculated with the extrapolation might be similar to the seepage flow of the water balance. However, as the minimum extrapolation seepage rate is close to zero and the maximum water balance seepage rate approximates $0.60\ \mathrm{m}^3/\mathrm{s}$, the uncertainty analyses show that both the extrapolation and water balance calculated flow rates can be considerably different.

6 DISCUSSION

This chapter will discuss the accuracy and reliability of the methods and datasets used. The underlying assumptions that have been used throughout the research will be defined and evaluated.

6.1 Uncertainties and reliability of methods and data

Research on groundwater-surface water interaction is still subject to many open issues. Advanced methods using satellite data are available and attractive because they cover large areas, but might not gather results that area as accurate as in-situ measurements. Lowering the costs by conducting in-field research might be a solution, but increases the degree of uncertainty involved. Local environments, circumstances and limitations can impose a range of possible errors to every seepage zone detection technique. Horizontal DTS can largely overcome the mistakes made by traditional seepage detection techniques in an area, e.g. the extrapolation of seepage flow from a few seepage meters or benthic chambers. Clear water temperature differences close to the sediment-water interface in multiple environments are easily traceable by DTS. However, DTS is only able to detect relatively cold or warm water zones. To determine whether these zones are seepage zones and quantify the seepage, the use of other techniques is required or direct relations between temperature and flow rate should be made. The degree of uncertainty is even larger when measurements are used for further extrapolation of seepage over a larger area.

Horizontal and vertical DTS

Whereas DTS is a useful method to trace seepage zones, much uncertainty is involved. The configuration of DTS for the local environment is important for the most accurate measurements. Until now, not much effort has been put in investigating the ultimate DTS configuration for Whakaipo Bay, but rather a simple configuration is chosen for each DTS measurement. However, the configuration is one of the biggest influencing factors of the measurements' quality. During some measurements, the water temperature along the cable increased by an increasing distance from the Oryx. Due to the use of a cable length of a few kilometres for horizontal measurements, this sloping temperature caused unlikely high temperatures reaching 35 °C. By changing the channel and renewing the configuration more correct results could be obtained. However, this might take several hours of trial and error.

The use of multiple Oryx channels at the same time, the inclusion of zones and improved calibration baths might give more precise data. It was attempted to keep the temperature of the cable in the calibration baths constant during the complete measurement, by locating the baths in the shadow, using an aquarium bubbler to keep the water in the whole bath in movement and the fixation of the cables on the bottom of the bath. An improvement would be to create holes in the bath cover, to prevent the compression of the cables and the inflow of warm air. Nevertheless, the temperature of the coiled cables in the calibration baths changed abruptly during several measurements. This might be due to a sudden stop or (re-)start from the aquarium bubbler in the measurement. A change in calibration baths temperatures affects the measured temperatures along the whole DTS cable. Using a second bubbler as back-up might eliminate these problems.

Several factors might cause a larger uncertainty in vertical DTS compared to horizontal DTS. The vertical device was constructed to measure temperature every 0.9 millimetre, but the cable is not exactly wrapped evenly around the bamboo structure of the device. Measured temperatures might in reality come from locations slightly lower or higher on the device, which could affect the flow calculation. The location of the vertical DTS measurements was based on temperatures of the horizontal measurements. However, the GPS unit used occasionally caused minor deviations between the planned location and the actual location in the bay. Furthermore, a cloth was used to reduce, rather than restrict, the turbulence and inflow of water into the PVC cylinder. However, questionable is whether this yielded reliable results, or whether it is better not to use it.

A limitation of the vertical DTS is the spatial range for which it can be used. Since the DTS is attached to a black fibre cable with a length of 200 meter only, that should be attached to the Oryx in the car, deep areas are too far away to measure. Besides, the shallowest lake edge zones are hotspots for seepage (Hector, 2004), but are too shallow to measure by vertical DTS. LOC12 showed that when the vertical DTS device is not fully submerged under water, it remains unclear if a cold-water layer is increasing at the SWI.

As mentioned before, cold water originating from other locations might follow the bathymetry and flows down to pool at other locations, which were measured by DTS as cold seepage areas. Hence, it is necessary to remain using techniques than can measure seepage flows, such as vertical DTS or seepage meters. When vertical DTS shows that a cold water layer is growing on the sediment-water interface, this can only indicate seepage, as the measurement area is isolated.

Seepage meters

As mentioned in the results section, the seepage meter measurements are a delicate operation. Many factors can affect the seepage meter results, e.g. pressure changes, wave action and turbulence. No ventilation tube is used in the seepage drum, but air could be released by escaping through the valve. However, possible gas molecules originating in the seepage might affect the results.

During the first measurements the drums drifted away, although they were fixed in the sand. Hence, it was decided to use pegs or rocks to ensure they did not drift. The next field days less turbulence was noticed, so it was manageable to fix the drums in the sand.

During the first field day, the sides of the condoms stuck together. This complicated measuring the water volume, since some water stuck onto the valve. The operation to measure the water volume was conducted with care, but spills could not be prevented. Due to the sticking of the sides of the condom, an underestimation of the total seepage flow took place. It was therefore decided to use a start volume of water in the condom, since the sticking problem was solved when 50 mL water was used in the beginning. However, at most of the locations a starting volume seemed to generate a flow that was much lower than the flow measured when an empty condom was used. The second and third field day other seepage condoms were used, which prevented any sticking.

It would have been useful to conduct seepage meter measurements at the same moment as DTS measurements, to ensure no seasonal difference has to be corrected for (Lowry et al., 2007). Because of practical issues and labour-intensive measurements it was impossible to measure at the same day as DTS.

Flow calculation and modelling

As described in the flow calculation results, the rather simple displacement calculation method was used to calculate the seepage flow using the vertical DTS results. This method does not take heat-conduction into account. However, the results using the simple method were similar to the results from the vertical DTS and the model. The simple method did not take heat conduction between the layers into account, which is important for locations where a large temperature difference exists. The larger the temperature difference, the more important the conduction factor is in the process of heat transfer. Besides, the flow calculation in summer might not be representative for other seasons.

Some parts of the vertical DTS results showed stabilizing temperatures after 15 minutes. The model can be used only for decreasing temperatures with a constant rate, causing the flow rates to be maximum flow rates. The model seems not useful for small seepage flows.

Algae and pockmarked depressions

The relation between seepage flows and vegetation present in Whakaipo Bay is still based on speculations. However, this study showed that vegetation might be a useful indicator for seepage flow.

Bathymetry map

The bathymetry map (LINZ, 1966) showed a few areas where water depth is less than 10 meter. From conducting logger measurements using a 10 meter long cable, it appeared that in these areas the water depth is larger. Questionable is how accurate this map is between a depth of 1 and 6.5 meter, which was used for the extrapolation of flows.

Regression relation

The vertical DTS measurements were taken on different moments on different days and unknown is if the flows vary within this period. However, the horizontal temperatures that were chosen to relate to the vertical flows were all taken in the period between 14h-15h. This was done to facilitate the inclusion of the extension at the northwest side of the cable, based on Meijer (2014).

As for the calculation of the flows, the regression formula is only valid for the end of summer since seasonal fluctuations may result in different values. Furthermore, the temperature might not be the only effect of seepage. The regression formula could have been based on the normal modelling scenario only rather than on the simple V-DTS. It was decided not to do this, since there were fewer modelling results available and the vertical DTS results were close to similar to the modelling results. The regression relation could have been based on the seepage meter flows. As much uncertainty is involved with the seepage meter measurements, in this study the DTS flows were used.

Extrapolation

The extrapolation was based on the regression relation between temperature and flow rate. However, the use of this formula implied that all temperature differences along the horizontal cable were a consequence of seepage flows differences. As mentioned before, the downward flowing cold water following the bathymetry is still uncorrected for.

An uncertain factor in the extrapolation of flows was the width of the area. As mentioned before, this is dependent on the bathymetry (LINZ, 1966).

Water balance

The precipitation and evapotranspiration data in the water balance were based on point measurements. The total area sums up to 37,713 km², whereas the catchment's size is 34,641 km², thus overestimating the size by 8,8% procent. It was decided not to reduce the total amount of precipitation and evaporation relative to the size of the area, because unknown is at which exact locations the precipitation falls and evaporations occurs around these point measurements. Besides, there were considerable differences in precipitation data between the different points. The water balance was based on the discharge of the Mapara stream only, but other streams might also contribute during heavy precipitation events. Increased or decreased precipitation and evapotranspiration patterns as a result of climate change might affect the seepage flow rates as well.

Uncertainty analysis of extrapolation and water balance

In order to extrapolate the minimum and maximum seepage rates, the flow rates for each location were determined by modelling. The limitations on the modelled rates that were discussed before, are also applicable for these minimum and maximum seepage flow rates. The same applies to the discussion of the regression formula and the width of the extrapolation area.

In order to estimate the minimum and maximum seepage rates based on a water balance, assumptions were made on how the minimum and maximum precipitation rate, actual evapotranspiration rate and Mapara Stream discharge needed to be determined. The minimum and maximum values for precipitation and actual evapotranspiration in the Mapara Stream Catchment were taken as the lower and higher error value for the minimum and maximum seepage rate scenarios. The minimum or maximum rate for each location might differ much. The discharge of the Mapara Stream was purely based on values found in literature, but minimum and maximum rates possibly differ much.

6.2 Assumptions

- *Horizontal DTS:* All cold water spots measured by horizontal DTS were assumed seepage spots. Vertical DTS showed this is true at some locations, but it might not be true everywhere in the bay, because of the downward flows of cold water.
- *Vertical DTS*: To calculate the flow, all water colder than the water temperature at the start of the measurement was assumed groundwater in vertical DTS.
- *Model*: The thermal properties and parameters, such as porosity and specific heat in the model were based on literature and estimates. Local groundwater and lake water temperatures were derived separately for each measurement.
- *Regression*: Assumed was that temperature differences along the cable were a consequence of seepage flows.
- *Extrapolation*: The extrapolation was limited to 6.5 meter deep areas in Whakaipo Bay, as for deeper areas less data was available. However, the 2014 off-shore DTS measurement showed that cold spots had been found in deeper areas.
- *Water balance*: Assumed was that fluxes of the water balance components, such as precipitation and actual evapotranspiration, are equally divided over the year. This might not hold and it might influence the total or seasonal seepage. Further it is assumed that there is no groundwater storage change in the catchment.
- *Uncertainty analysis:* All the assumptions that were already described, regarding the model, regression, extrapolation and water balance were made. Further was assumed that the model is able to calculate minimum and maximum seepage rates at the locations used; assumed was that the extrapolation area sizes found in the bathymetry map could be half as large or small in order to determine the maximum and minimum extent of the seepage area; assumed was that the minimum and maximum precipitation and actual evapotranspiration rate were the values for respectively the lowest and highest value of the dataset; assumed was that found discharges of the Mapara Stream in literature describe the absolute minimum and maximum discharge.

7 CONCLUSIONS

This research has been undertaken using four research questions. The answers to these questions will be given here.

Research question 1

To what extent are seepage areas in Whakaipo Bay detectable by horizontal DTS?

During both on-shore and off-shore measurements, areas that were significantly colder than their environment were detected by horizontal DTS. Horizontal DTS is useful in distinguishing areas based on different temperatures. The vertical temperature profiles prove that significant colder areas are characterised by higher seepage flows than warmer areas. At locations where average temperatures were measured, generally average seepage flows occur. Still uncertain is if all cold areas are seepage zones or depressions in which cold water that originates from other areas, pools. Additional vertical DTS measurements are required to validate groundwater is seeping at these locations too.

Research question 2

To what extent is vertical deployment of DTS, validated with a numerical model, temperature loggers and seepage meters, able to quantify the seepage flow in different parts of Whakaipo Bay?

Vertical DTS is useful in validating seepage zones detected by horizontal DTS. It is able to quantify notable seepage flows using both a flow calculation displacement method and a convection-diffusion model. Based on the comparison between the seepage flow rates calculated by the displacement method and the rates calculated by the seepage meter measurements, low flows seem hard to quantify using vertical DTS. Vertical DTS seems appropriate to quantify the flow in high-flow situations. However, further measurements and validation by other techniques is necessary to give conclusions about whether seepage meters and the displacement method are accurate enough to quantify seepage in Whakaipo Bay. Temperature loggers, which were fixed to the vertical DTS device, validated the decreasing temperatures and seepage flows of the displacement method.

Research question 3

To what extent could horizontal DTS be improved to directly detect seepage areas and quantify seepage flows in lake environments?

The direct detection of seepage areas seems to be possible using horizontal DTS. In all areas where a water temperature was found that was considerably colder than the average lake bottom water temperature, vertical DTS showed that seepage flows are present. However, the downward flow of water following the bathymetry might influence the water temperatures in other areas. To correct for this, a locally dependent correction factor could be used. A direct quantification of seepage flows can be done using a regression relation between temperatures along the horizontal DTS cable and flow rates. This linear relation should be tested by relating more vertical DTS measurements to horizontal DTS temperatures and seepage meter results. Lastly, the relation should be tested in other areas.

Research question 4

To what extent is DTS able to calculate the seepage component of the water balance by extrapolation of seepage inflow into Whakaipo Bay?

A linear relation between temperatures found by horizontal DTS and seepage fluxes found by the displacement calculation can be used to calculate the seepage flow at locations where no measurements were taken. This method links temperatures along the horizontal fibre-optic DTS to flows calculated by vertical DTS. Extrapolation of these flows into the medium-deep part of Whakaipo Bay yields credible total seepage flow rates, if compared to other studies and the total seepage component of the water balance. The uncertainty in both methods might explain the difference in seepage rate found.

8 RECOMMENDATIONS

In this chapter recommendations will be given about further research. The main objectives for further research that were deducted from this thesis are:

- Increase the knowledge about DTS and its applicability in various environments. This is useful for every actor involved in the SAC project.
- Obtain a more thorough understanding of the groundwater systems and its interaction with surface water in the Mapara catchment. This is useful for research institutes such as GNS Science.
- Improve the estimates of seepage flows and nutrient flows into Whakaipo Bay. These rates are useful for local authorities such as the regional council.

The recommendations are broken down for the different subjects.

General

- A better understanding of the relevance of pockmarked depressions as indicators for groundwater seepage should be acquired when nutrient loads in groundwater at these locations are measured and compared to nutrient loads in groundwater at locations where no pockmarked depressions are situated.
- New research, e.g. seepage meter measurements in shallow areas and shallow horizontal DTS and vertical DTS deployments should be undertaken to test if Hectors measurements for the shallow area in Whakaipo Bay were reliable.

DTS

- A better understanding of the configuration of DTS, such as the effect of the inclusion of zones and an improvement in calibration baths, should be obtained for multiple locations in Whakaipo Bay.
- For a better understanding of the configuration, measurements should be taken at multiple locations using a similar configuration.
- Both horizontal and vertical DTS measurements should be conducted in other seasons to research the seasonal variability of seepage flows into Whakaipo Bay. Due to temperature differences summer and winter are the most suitable seasons for DTS. Lake level and groundwater level data combined with groundwater models might extrapolate seepage rates for other seasons.

- Yet, 59% of the total seepage needs to be explained, following the comparison between the extrapolation and water balance in this study. Horizontal DTS measurements in Whakaipo Bay, in areas with a depth of 5 meter and deeper and at the utter western and eastern part of Whakaipo Bay, should be conducted to obtain knowledge whether cold areas exist in these regions.

Vertical DTS

- More vertical DTS measurements should be done at cold locations to test if the regression relation holds. Preferably, these measurements should be conducted at locations where many algae are present.
- Groundwater temperature at each vertical DTS location should be measured by a in order to improve the accuracy of the modelling results, since groundwater temperature is one of the most sensitive parameters in the heat-conduction model.
- A shallow vertical DTS device should be created in order to validate Hectors seepage meter measurements in shallow areas.
- Cold off-shore locations found by Meijer (2014) should be examined, in order to see if these deep areas are locations where water is pooling or where seepage is flowing into the lake. To enable this, another new vertical DTS device for far off-shore locations should be created. The use of this technique in a deep cold area and at a location on a slope close-by can give an indication of the difference due to cold-water pooling. This comparison needs to be repeated at other locations in Whakaipo Bay.

Seepage meter

- A ventilation tube on top of the seepage meter should be created in order to conduct more accurate measurements.
- More seepage meter measurements should be conducted. The measurements that were already done should be repeated at the exact same location and new seepage meter measurements should be conducted in the shallowest area of the bay, alongside new shallow vertical DTS measurements. However, in order to do this a more accurate GPS unit is necessary.
- Seepage meter and monitoring well measurements should be conducted at the same moment and as close as possible to the vertical DTS measurement, to eliminate seasonal or diurnal variability.

Extrapolation

- The regression relation should be tested, based on an increased number of vertical DTS measurements. This should be applied in different areas to see if the relation holds and if the relation can be transferred to other environments.
- An exploration of the bathymetry in Whakaipo Bay should be done to create a more detailed bathymetry map. This can be used to include a bathymetry correction factor in the regression formula at locations where water might pool in depressions.

Uncertainty analysis of the extrapolation and water balance methods

- A more advanced uncertainty analysis of both methods should be undertaken. In this study, many assumptions were made regarding the minimum and maximum seepage flow rates. A critical review on the regression formulas and a more accurate bathymetry map are required to improve the uncertainty analysis. Data on the climatologic variability of the precipitation, actual evapotranspiration and Mapara Stream discharge should be acquired in order to calculate a more accurate water balance.

9 REFERENCES

Anderson, M.P. (2005). Heat as a ground water tracer. Ground Water 43(6), pp. 951-968. Doi: 10.1111/j.1745-6584.2005.00052.x

Blume, T., Krause, S., Meinikmann, K., Lewandowski, J. (2013). Upscaling lacustrine groundwater discharge rates by fiber-optic distributed temperature sensing. Water Resources Research, 49(12), pp. 7929-7944. Doi: 10.1002/2012WR013215

Briggs, M.A., Lautz, L.K., McKenzie, J.M. (2012). A comparison of fibre-optic distributed temperature sensing to traditional methods of evaluating groundwater inflow to streams. Hydrological Processes, 26(9), pp. 1277-1290. Doi: 10.1002/hyp.8200

Brodie, R.S., Baskaran, S., Ransley, T., Spring, J. (2009). Seepage meter: Progressing a simple method of directly measuring water flow between surface water and groundwater systems. Australian Journal of Earth Sciences, 56(1), pp. 3-11. Doi: 10.1080/08120090802541879

Environment Waikato. (2003). Protecting Lake Taupo: A Long Term Strategic Partnership. Environment Waikato, Hamilton

Elsawwaf, M., Feyen, J., Batelaan, O., Bakr, M. (2014). Groundwater-surface water interaction in Lake Nasser, Southern Egypt. Hydrological Processes. 28(3), pp. 414-430. Doi: 10.1002/hyp.9563

Gibbs, M., Clayton, J., Wells, R. (2005). Further investigation of Direct Groundwater Seepage to Lake Taupo. NIWA report to Environment Waikato, Hamilton. Technical Report 2005/34. 27pp.

GNS Science (2011). Proposal Smart Aquifer Characterisation.

González-Pinzón, R., Ward, A.S., Hatch, C.E., Wlostowski, A.N., Singha, K., Gooseff, M.N., Haggerty, R., Harvey, J.W., Cirpka, O.A., Brock, J.T. (2015). A field comparison of multiple techniques to quantify groundwater-surface-water interactions. Freshwater Science, 34(1), pp.139–160. Doi: 10.1086/679738

Hadfield, J.C., Nicole, D.A., Rosen, M.R., Wilson, C.J.N., Morgenstern, U. (2001). Hydrogeology of Lake Taupo Catchment – Phase 1. Environment Waikato, Hamilton. Technical Report 2001/01. 52pp.

Hadfield, J. (2007). Groundwater Flow and Nitrogen Transport Modelling of the Northern Lake Taupo Catchment. Environment Waikato, Hamilton. Technical Report 2007/39. 62pp.

Hadfield, J., Morgenstern, U., Piper, J.J. (2007). Delayed impacts of land-use via groundwater on Lake Taupo, New Zealand. WIT Transactions on the Ecology and the Environment. 103, pp. 292-303. Doi: 10.2495/WRM070281

Hamblin, W.K., Christiansen, E.H. (1995). Earth's Dynamic Systems. Prentice Hall, Englewood Cliff, New Jersey. 740pp.

Harvey, F.E., Lee, D.R. (2000). Discussion of “The effects of bag type and meter size on seepage meter measurements” by Isiorho, S.A. and Meyer, J.H. Ground Water 38(3), pp. 326-327. Doi: 10.1111/j.1745-6584.2000.tb00214.x

Hausner, M.B., Suarez, F., Glander, K.E., Van de Giesen, N., Selker, J.S., Tyler, S.W. (2011). Calibrating single-ended fiber-optic Raman spectra distributed temperature sensing data. Sensors 2011(11), pp. 10.859-10.879. Doi: 10.3390/s111110859

Hector, R.P. (2004). Investigation of direct groundwater and nutrient seepage to Lake Taupo. MSc thesis, University of Waikato.

Isiorho, S. A. & Meyer, J. H. (1999). The effects of bag type and meter size on seepage meter measurements. Ground Water, 37(3), pp. 411-413.

Kalbus, E., Reinstorf, F., Schirmer, M. (2006). Measuring methods for groundwater – surface water interactions: a review. Hydrology and Earth System Sciences, 10(6), pp. 873–887. Doi: 10.5194/hess-10-873-2006

Lee, D. R. (1977). Device for measuring seepage flux in lakes and estuaries, Limnology and Oceanography, 22(1), pp. 140–177

Lock, M.A., and John, P.J., (1978). The measurement of groundwater discharge into a lake by direct method. Internationale Revue der gesamten Hydrobiologie, 63(2), pp. 271–275. Doi: 10.1002/iroh.19780630212

Lovett, A., Reeves, R., Verhagen, F., Westerhoff, R., Cameron, S., Meijer, E., Van der Raaij, R., Moridnejad, M. (2015). Characterisation of groundwater – surface water interaction at three case study sites within the Upper Waikato River Catchment, using temperature sensing and hydrochemistry techniques. GNS Science Report 2014/64. 83pp.

Lowry, C.S., Walker, J.F., Hunt, R.J., Anderson, M.P. (2007). Identifying spatial variability of groundwater discharge in a wetland stream using a distributed temperature sensor. Water Resources Research, 43(10), 9pp. Doi: 10.1029/2007WR006145

Matheson, F.E., Tank, J.L., Costley, K.J. (2011). Land use influences stream nitrate uptake in the Lake Taupo catchment. New Zealand Journal of Marine and Freshwater Research, 45(2), pp. 287-300, Doi: 10.1080/00288330.2011.562143

Meijer, E.C. (2014). Using fibre-optic distributed temperature sensing and heat modelling to characterize groundwater-surface water interaction in Whakaipo Bay, Lake Taupo, New Zealand. 33pp.

Martinez, C.J. (2013a). Seepage Meters for Measuring Groundwater-Surface Water Exchange. University of Florida.

Martinez, C.J. (2013b). Mini-Piezometers for measuring Groundwater to Surface Water Exchange. University of Florida.

McBride, M.S., Pfannkuch, H.O. (1975). The distribution of seepage within lakebeds. US Geological Survey. Journal of Research, 3(5), pp. 505-512.

Morgenstern, U. (2007). Lake Taupo Streams: Water Age Distribution, Fraction of Land-Use Impacted Water, and Future Nitrogen Load. Environment Waikato, Hamilton. Technical Report 2007/26.

Morgenstern, U. (2008). Lake Taupo Catchment Groundwater Age Distribution and Implications for Future Land-Use Impacts. Environment Waikato, Hamilton. Technical Report 2007/49.

Morgenstern, U., Daughney, C.J. (2012). Groundwater age for identification of baseline groundwater quality and impacts of land-use intensification – The National Groundwater Monitoring Programme of New Zealand. Journal of Hydrology 456-457, pp. 79–93. Doi: 10.1016/j.jhydrol.2012.06.010

Mu,Q., Zhao, M., & Running, S. (2011). Running, improvements to a MODIS global terrestrial evapotranspiration algorithm. Remote Sensing of Environment, 115(8), pp. 1781–1800. Doi: 10.1016/j.rse.2007.04.015

Mwakanyamale, K., Day-Lewis, F.D., Slater, L.D. (2013). Statistical mapping of zones of focused groundwater/surface-water exchange using fiber-optic distributed temperature sensing. Water Resources Research, 49(10), pp. 6979-6984, Doi: 10.1002/wrcr.20458

Newson, J.A., (1993). Geothermal and groundwater Hydrology of the Reporoa-Waiotapu Basin. Master of Philosophy Engineering Thesis, University of Auckland.

Petch, T., Young, J., Thorrold, B., Vant, B. (2003). Protecting an icon managing sources of diffuse nutrient inflow to Lake Taupo, New Zealand. Water Resources Management. Diffuse Pollution Conference, Dublin 2003.

Piper, J.J. (2004). Surface / groundwater interaction and catchment influence on waters entering Lake Taupo, New Zealand. MSc Thesis. Victoria University, Wellington.

Rahman. T., Kohli, M., Megdal, S., Aradhyula, S., Moxley, J. (2009). Determinants of environmental compliance by public water systems. Contemporary Economic Policy, 28(2), pp. 264-274. Doi: 10.1111/j.1465-7287.2009.00150.x

Rosenberry, D.O., LaBaugh, J.W., Hunt, R.J. (2008). Use of monitoring wells, portable piezometers and seepage meters to quantify flow between surface water and groundwater. U.S. Geological Survey. Techniques and Methods 4(2), pp. 39-70.

Rudnick, S., Lewandowski, J., Nützmann, G. (2015). Investigating groundwater-lake interactions by hydraulic heads and a water balance. Groundwater 53(2), pp. 227-237. Doi: 10.1111/gwat.12208

Schincariol, R.A., McNeil, J.D. (2002). Errors with small volume elastic seepage meter bags. Groundwater, 40(6), pp. 640-651. Doi:10.1111/j.1745-6584.2002.tb02551.x

Sebok, E., Duque, C., Kazmierczak, J., Engesgaard, P., Nilsson, B., Karan, S., Frandsen, M. (2013). High-resolution distributed temperature sensing to detect seasonal groundwater discharge into Lake Vaeng, Denmark. Water Resources Research, 49(9), pp. 5355-5368. Doi: 10.1002/wrcr.20436

Selker, J.S., Thévenaz, L., Huwald, H., Mallet, A., Luxemburg, W., Van de Giesen, N., Stejskal, M., Zeman, J., Westhoff, M., Parlange, M.B. (2006). Distributed fiber-optic temperature sensing for hydrologic systems. Water Resources Research, 42, 8pp. Doi: 10.1029/2006WR005326

Sensornet. (2007). Oryx DTS User Manual.

Shaw, R.D., Prepas, E.E. (1990). Groundwater-surface water interactions: accuracy of seepage meter estimates of lake seepage. Journal of Hydrology, 119, pp. 105-120.

Siebert, C., Rödiger, T., Mallast, U., Gräbe, A., Guttman, J., Laronne, J.B., Storz-Peretz, Y., Greenman, A., Salameh, E., Al-Raggad, M., Vachtman, D., Ben Zvi, A., Ionescu, D., Brenner, A., Merz, R., Geyer, S. (2014). Challenges to estimate surface- and groundwater flow in arid regions: The Dead Sea catchment. Science of the Total Environment, 485–486(1), pp.828–841. Doi: 10.1016/j.scitotenv.2014.04.010.

Sophocleous, M. (2001). Interactions between groundwater and surface water: the state of science. Hydrogeology Journal, 10(1), pp 52-67. Doi: 10.1007/s10040-001-0170-8

Steckis, R.A., Potter, I.C., Lenanton, R.C.J. (1995). The commercial fisheries in three southwestern Australian estuaries exposed to different degrees of eutrophication. Eutrophic Shallow Estuaries and Lagoons. pp. 186-203. CRC Press, Boca Raton, FL.

Stein, M.L. (1999). Interpolation of spatial data: some theory for kriging. New York. 249pp. Doi: 10.1007/978-1-4612-1494-6

Stronestrom, D., Constantz, J. (2003). Heat as a tool for studying the movement of ground water near streams. Reston, Virginia: USGS. 96pp.

Tait, A., Henderson, R., Turner, R., Zheng, X. (2006). Thin plate smoothing spline interpolation of daily rainfall for New Zealand using a climatological rainfall surface. International Journal of Climatology 26(14), pp. 2097-2115. Doi: 10.1002/joc.1350

Thoreau, H.D. (1854). Walden; or, Life in the Woods. Boston: Ticknor & Fields. Doi: 10.5962/bhl.title.38999

Tyler, S.W., Selker, J.S., Hausner, M.B., Hatch, C.E., Torgersen, T., Thodal, C.E., Schladow, S.G. (2009). Environmental temperature sensing using Raman spectra DTS fiber-optic methods. Water Resources Research, 45, 11pp. Doi:10.1029/2008WR007052

Vant, B., Smith, P. (2004). Nutrient concentrations and water ages in 11 streams flowing into Lake Taupo. Environment Waikato, Hamilton. Technical Report, 2002/18R. 20pp.

Vogt, T., Schneider, P., Hahn-Woerle, L., Cirpka, O.A. (2010). Estimation of seepage rates in a losing stream by means of fiber-optic high-resolution vertical temperature profiling. Journal of Hydrology, 380, pp. 154-164. Doi: 10.1016/j.jhydrol.2009.10.033

Westerhoff, R.S. (2015b). Using uncertainty of Penman and Penman–Monteith methods in combined satellite and ground-based evapotranspiration estimates. Remote Sensing of Environment, 169, pp. 102–112. Doi:10.1016/j.rse.2015.07.021

Wetzel, R.G. (2001). Limnology. 3rd Edition Orlando: Academic Press. 1006pp.

Wildland Consultants Ltd. (2013). History of Land Development in the Lake Taupo catchment. Environment Waikato, Hamilton. Technical Report 2013/26.

Winter, T., Harvey, J., Lehn Franke, O., & Alley, W. (1998). Ground Water and Surface Water a Single Resource. Denver: U.S. Geological Survey.

Wilson, C.J.N. (2001). The 26.5 ka Oruanui eruption, New Zealand: an introduction and overview. Journal of Volcanology and Geothermal Research, 112(1), pp. 133-174. Doi: 10.1016/S0377-0273(01)00239-6

Wilson, C.J.N., Blake, S., Charlier, B.L.A., Sutton, A.N. (2006). The 26.5 ka Oruanui Eruption, Taupo Volcano, New Zealand: Development, Characteristics and Evacuation of a Large Rhyolitic Magma Body. Journal of Petrology, 47(1), pp. 35-69. Doi:10.1093/petrology/egi066

Yang, Z., Zhou, Y., Wenninger, J., Uhlenbrook, S., Wan, L. (2015). Simulation of Groundwater-Surface Water Interactions under Different Land Use Scenarios in the Bulang Catchment, Northwest China. Water, 2015(7), pp.5959-5985. Doi: 10.3390/w7115959

Data

LINZ (1966). Bathymetry Map Lake Taupo. Chart NZ232. Navy survey. Hydrographic Systems Technical Lead New Zealand Hydrographic Authority, Land Information New Zealand.

Rainfall data: Source data is rainfall according to Tait et al. (2006), which were then regridded to the local setting by Westerhoff (2015a).

Evapotranspiration data: Data is from the MOD16 data from the MODIS satellite (Mu et al., 2011). Data has been regridded, applied and tested in a New Zealand setting by Westerhoff (2015b).

Personal communication

Gibbs, M. Personal communication. Water quality scientist NIWA.

Verhagen, F. (2014). Personal communication.

Westerhoff, R.S. (2015a). Personal communication. Geophysicist at Deltares.

Equipment

Oryx and further DTS equipment. GNS Science Wairakei. Hydrogeology Department.

Piezometer and temperature loggers. GNS Science Wairakei. Hydrogeology Department.

Seepage meter valves. NIWA Hamilton. Max Gibbs.

APPENDICES

Appendix A: Configuration Oryx

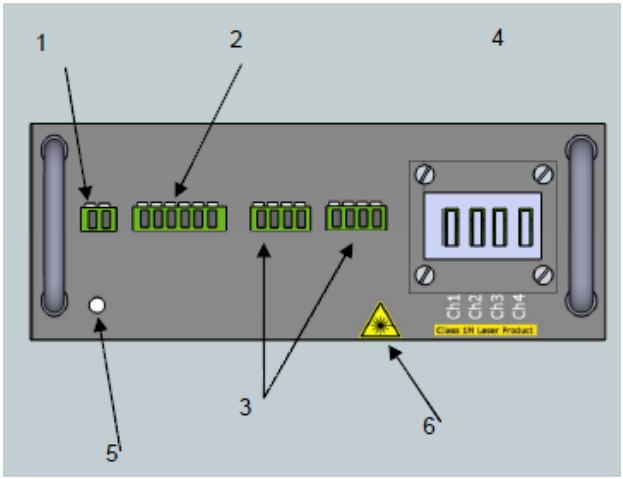

LIST OF CONNECTIONS:

1. Input power
2. Serial RS232 communications ports, Com1 & Com2
3. PT100 external probe connections
4. Fibre Optic connector panel
5. Earthing point
6. Laser emission warning symbol

Figure 59: Oryx DTS (Oryx DTS User Manual)

Repetition time:	1 minute
Number of measurements:	60, continuous
Channel:	Only channel 2 has been used during the measurements
Time averaging :	No
Length scaling parameter:	1
Temperature slope:	Temperature reference sections → T1/T2 probes as source for calibration baths temps.
Temperature offset:	Fixed
Zones:	No
Spatial averaging:	No

Appendix B: Schematised DTS operating system in air-conditioned car

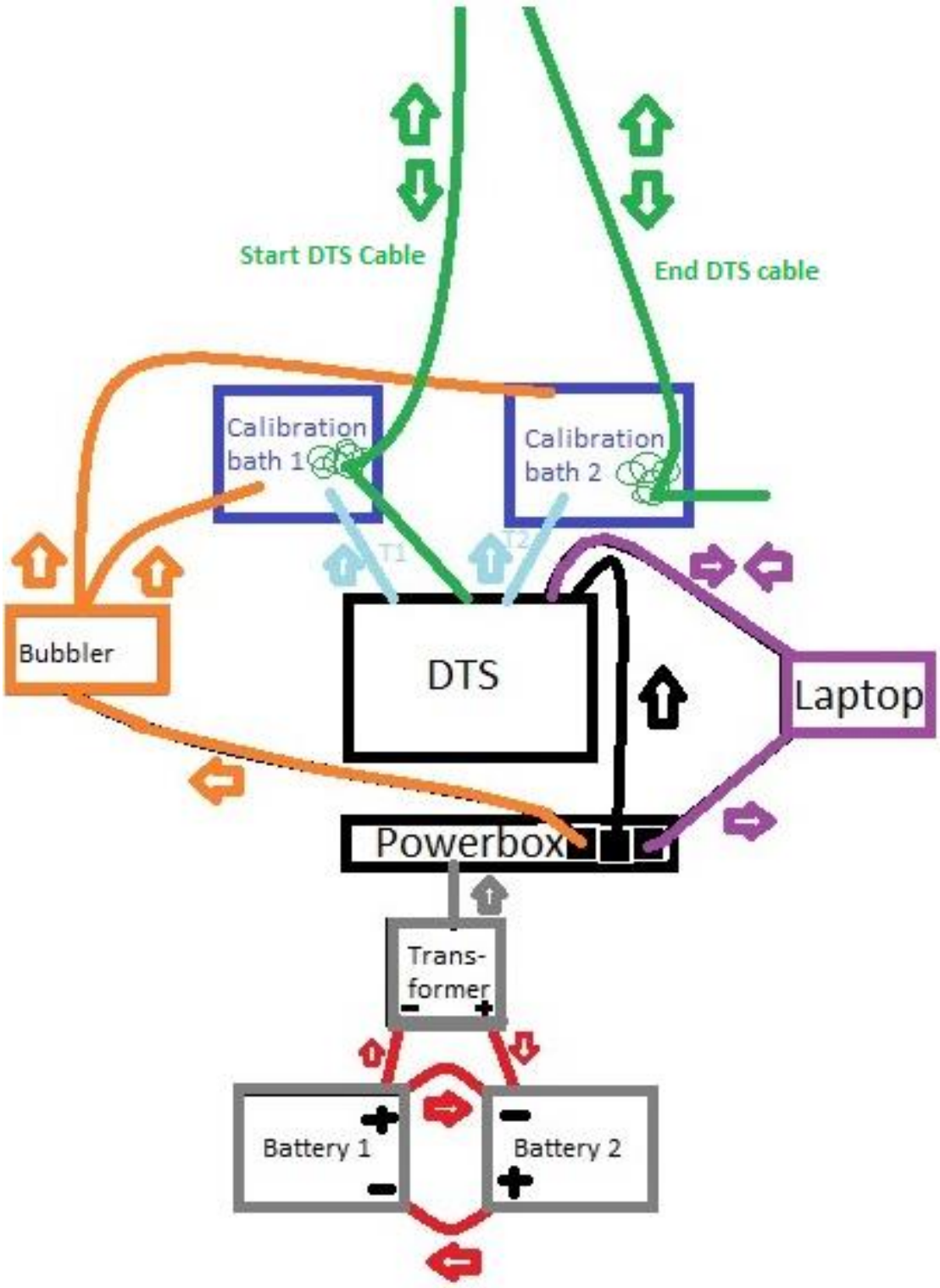

Figure 60: DTS Collection system

Appendix C: Flux Determination Model

```
%%%%%%%%%%% Initialisation
%%%%%%%%%%%%%%%%%%%%%%%%%%%%%%%%%%%%%%%%%%%%%%%%%%%%%%%%%%%%%%%%%%%%%%%%%%%%%%%%
%

clear all
close all

% Control Constants
StartTime = 0;                                  % [min]
dt = 0.001;                                     % [min]
EndTime = 144;                                  % [min]
PlotStep = 1;                                   % [min]
StoreStep = 1;                                  % [min]
ThickL = 0.001;                                 % [m]
NrLayerSoil = 100;                              % [-]
NrLayerWater = 350;                             % [-]
NrLayer = NrLayerSoil + NrLayerWater;                   % [-]

% General Paramaters
TempGW = 12;                                    % [°C]
TempLW = 19;                                    % [°C]
TempBottom = 12;                                % [°C]
OutflowWater = 1.3;                             % [cm/hour]

% System Parameters Water-part
ConducWater = 34.8;                             % [J/°C m min]
SpecHeatWater =  4.1855;                        % [J/g °C] based on water of 15°C
MassDensityWater = 0.999*10^6;                  % [g/m3] based on water of 15°C
eWater = 1;                                     % Porosity: ratio liquid/total volume
uWater = OutflowWater/(60*100);                 % [m/min] velocity
aWater = ConducWater/(SpecHeatWater*MassDensityWater);  % diffusion coefficient

% System Parameters Soil-part
ConducSoil = 132;                               % [J/oC m min] check, bron van Floris
MassDensitySoil = 2*10^6;                       % [g/m3]
SpecHeatSoil = (2.5*10^6)/MassDensitySoil;              % [J/g°C] (Source: 2.5 MJ/m3,K)
eSoil = 0.4;                                    % Porosity: ratio liquid/total volume
uSoil = (1/eSoil)*uWater;                       % [m/min] velocity
aSoil = ConducSoil/(SpecHeatSoil*MassDensitySoil);      % diffusion coefficient

% Control Variables
NrStore = 1;
PlotTime = PlotStep;
StoreTime = StoreStep;
Time = StartTime;

Stabil1 = 1-((2*aWater*dt)/(ThickL^2));
Stabil2 = 1-((2*aSoil*dt)/(ThickL^2));
Stabil3 = (aWater/(ThickL^2))-((eWater*uWater)/(2*ThickL));
Stabil4 = (aSoil/(ThickL^2))-((eSoil*uSoil)/(2*ThickL));
Stabil5 = ((2*aSoil)/(eSoil*uSoil))-ThickL;
```

```
Stabil6 = ((2*aWater)/(eWater*uWater))-ThickL;

% Initial temperature distribution on soil.
A = linspace(TempBottom,12,100);

% System Variables
TempOld = ones(1,NrLayer)*TempLW;
TempOld(1:100) = A;
TempNew = TempOld;


%~~~~~~~~~~~~~~~~~~~~~~DYNAMIC
LOOP~~~~~~~~~~~~~~~~~~~~~~~~~~~~~~~~~~~~~~~~~~~~~~~~
while Time < EndTime
    % ------------------ Soil part --------------------------------------
    % Layer 1 always stays a stable temperature --> TempBottom
    TempOld(1) = TempBottom;
    TempNew(1)= TempBottom;
    % Lakebed Layers
    for k = 2:100
    I = (1-((2*aSoil*dt)/(ThickL^2)))*TempOld(k);
    II = (((aSoil*dt)/(ThickL^2))+ ((eSoil*uWater*dt)/(2*ThickL)))*TempOld(k-1);
    III = (((aSoil*dt)/(ThickL^2))- ((eSoil*uWater*dt)/(2*ThickL)))*TempOld(k+1);
    TempNew(k) = I + II + III;
    end

%     for k = 2:100
%       TempOld(k) = TempNew(k);
%     end

    % ------------------ Water part --------------------------------------

    % water Layers
    for k = 101:(NrLayer-1)
    I = (1-((2*aWater*dt)/(ThickL^2)))*TempOld(k);
    II = (((aWater*dt)/(ThickL^2))+ ((eWater*uWater*dt)/(2*ThickL)))*TempOld(k-1);
    III = (((aWater*dt)/(ThickL^2))- ((eWater*uWater*dt)/(2*ThickL)))*TempOld(k+1);
    TempNew(k) = I + II + III;
    end

   TempNew(NrLayer)=TempNew(NrLayer-1);

    for k = 1:NrLayer
    TempOld(k) = TempNew(k);
    end

    Time = Time+dt;

  %%%%%%%%%%%%%%%%%%%% Storing and Visiualisation
%%%%%%%%%%%%%%%%%%%%%%%%%%%%%%%%
    StoreTime = StoreTime - dt;
if StoreTime <= 0
```

```
    StoreTemp(NrStore,:) = [TempOld];
    NrStore = NrStore+1;
    StoreTime = StoreStep;
End

% figure (1)
% PlotTime = PlotTime-dt;
% if PlotTime <= 0
%     ImTemp = rot90(TempOld,1);
%     imagesc(ImTemp,[TempBottom TempLW]), colorbar
%     xlabel(Time)
%     pause(0.1)
%     PlotTime = PlotStep;
% end
end

figure (2)
ImMod = rot90(StoreTemp,1);
imagesc(ImMod); title('Outflow of 1.3 cm/hour'); caxis([TempBottom TempLW]);

yLimits = [0,NrLayer];                  %# Get the y axis limits
yTicks = yLimits(2)-get(gca,'YTick');       %# Get the y axis tick values and
                                        %# subtract them from the upper limit
set(gca,'YTickLabel',num2str(yTicks.'));    %# Convert the tick values to strings
                                        %# and update the y axis labels

line([0,450],[350,350],'Color','k','LineWidth',2)
colorbar
xlabel('Time (min)')
ylabel('Distance from lakebed(mm)')

figure (3)


ImMod = rot90(StoreTemp,1);
waterpart = ImMod(1:350,:);
imagesc(waterpart); title('Outflow of 1.3 cm/hour'); caxis([15 21]);

yLimits = [0,NrLayer];                  %# Get the y axis limits
yTicks = yLimits(2)-get(gca,'YTick');       %# Get the y axis tick values and
                                        %# subtract them from the upper limit
set(gca,'YTickLabel',num2str(yTicks.'));    %# Convert the tick values to strings
                                        %# and update the y axis labels

%line([0,450],[350,350],'Color','k','LineWidth',2)
colorbar
xlabel('Time (min)')
ylabel('10 cm soil + 35 cm lake')
```

Table 17: Specific parameters of the heat-conduction model (Meijer, 2014)

Property	**Units**	**Sym**	**Value**
Porosity	Dimensionless	ϵ	0.22 [a]
Specific heat water	J g^{-1} °C^{-1}	c_w	4.1855 [b]
Specific heat sediment	J g^{-1} °C^{-1}	c_s	2.5253 [c]
Mass density water	g m^{-3}	ρ_w	0.99 x 10^6 [d]
Mass density sediment	g m^{-3}	ρ_s	2 x 10^6 [e]
Thermal conductivity water	J min^{-1} m^{-1} °C-	λ_w	34.8 [f]
Thermal conductivity sediment	J min^{-1} m^{-1} °C-	λ_s	132 [g]

a Estimated for Whakaipo Bay

b The International Committee for Weights and Measures, Paris, 1950, accepted W. J. de Haas's recommended value of 4.1855 Jg−1 °C−1 for the specific heat capacity of water at 15 °C

c Based on typical value for saturated medium coarse to medium fine sand sediment (Nederlandse organisatie voor energie en milieu, 2003)

d Value at 15 °C

e (Sekellick, Banks, & Myers, 2013)

f Value at 15 °C

g Based on typical value for saturated medium coarse to medium fine sand sediment (Nederlandse organisatie voor energie en milieu, 2003)

Appendix D: Overview of all measurements

Table 18: Overview of all measurements done in Whakaipo Bay. Orange = measurements done in 2014. Yellow = measurements done in 2015.

Overview measurements Whakaipo Bay

	Temperature					Direct seepage
Horizontal DTS	***Vertical DTS***	***Logger Piezometer***	***Logger DTS***	***Logger Deep***	***Logger Wells***	***Seepage meter***
Whakaipo off-shore	a	1_1	1_1	1	West well	1_1
Whakaipo near-shore 1	b	1_2	2_1	2	East well	1_2
Whakaipo near-shore 2	c	2_1	3_1	3		2_1
	d	2_2	3_2	4		2_2
	e	3_1	4_1	5		3_1
	f	3_2	4_2	6		3_2
	1	4_1	5A_1	7		3_3
	2	4_2	5B_1	8		4_1
	3	5A5B_1	6_1	9		4_2
	4	5A5B_2	7_1	10		4_3
	5a	6_1	8_1	11		5A_1
						5A_2
	5b	7_1	9_1	12		5A_3
	6	8_1	9_2	13		5B_1
						5B_2
	7	9new_1	10_1	14		5B_3
	8	10_1	11_1	15		6_1
	9	10_2	12_1	16		6_2
	10	11_1	1314_1	17		7_1
2014	11	11_2		18		7_2
2015	12	12_1		19		8_1
	13	1314_1		20		8_2
	14	1314_2				9_1
						9_2
						9_3
						10_1
						10_2
						11_1
						11_2
						12_1
						12_2
						12_3
						1314_1
						1314_2

Table 19: Overview of date when measurements are conducted in Whakaipo Bay. Orange = measurements done in 2014. Yellow = measurements done in 2015.

			DTS		Loggers				Seepage
			Horizontal	*Vertical*	*Logger Deep*	*Logger DTS*	*Logger Piezometer*	*Wells*	*Seepage meters*
2014	**FEB**	**12**	Near-shore 1	a/b/c					
		18			1/2/3/4/5				
		24		d/e/f	8				
		26			6/7				
	MAR	**11/12**	Off-shore 1						
	APR	**2**		1					
		10		2/3					
2015	**FEB**	**13**		4/5a					
		19		6/7/8					
		25		5b/9					
	MAR	**3/4**	Near-shore 2						
		10		10/11/12					
		20		13/14					
	APR	**14**				1_1/2_1/3_1/ 4_1/5A_1	All_1 1_2/2_2/3_2/ 4_2/5A5B_2		
		16					10_2/11_2/1314_2		
		21				5B_2/6_1/7_1/ 8_1/9_1 10_1/11_1/ 12_1/1314_1			
		23						East	3_1/3_2/3_3/ 4_1/13_1
	MAY	**1**			9 until 18				
		5						West	2_1/2_2/4_2/4_3/ 5A_1/5A_2/5A_3/5B_1/5B_2/5B_3 9_1/9_2/12_1/12_2/ 13_2/14_1/14_2
		8			19/20				1_1/1_2/6_1/ 6_2/7_1/7_2 8_1/8_2/9_3/10_1/ 10_2/11_1/11_2/12_3

Appendix E: Horizontal near-shore measurement

Figure 61: Lay-out of horizontal near-shore DTS measurement of 2015

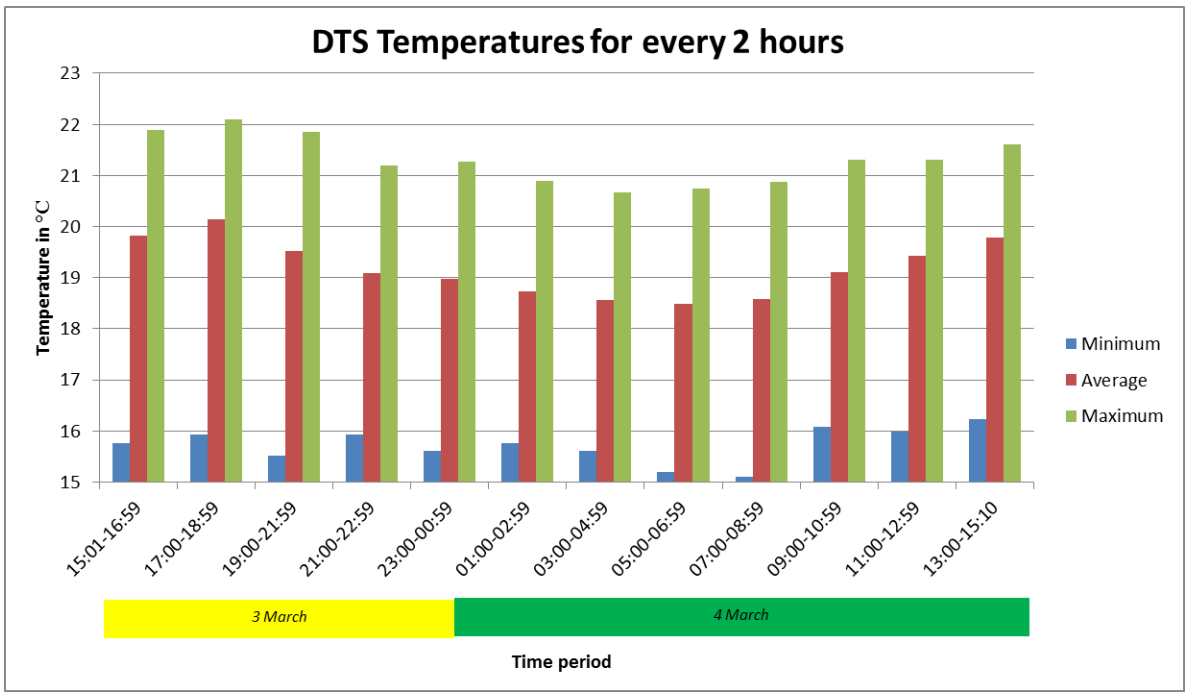

Figure 62: Horizontal near-shore DTS temperatures for each 2 hour period.

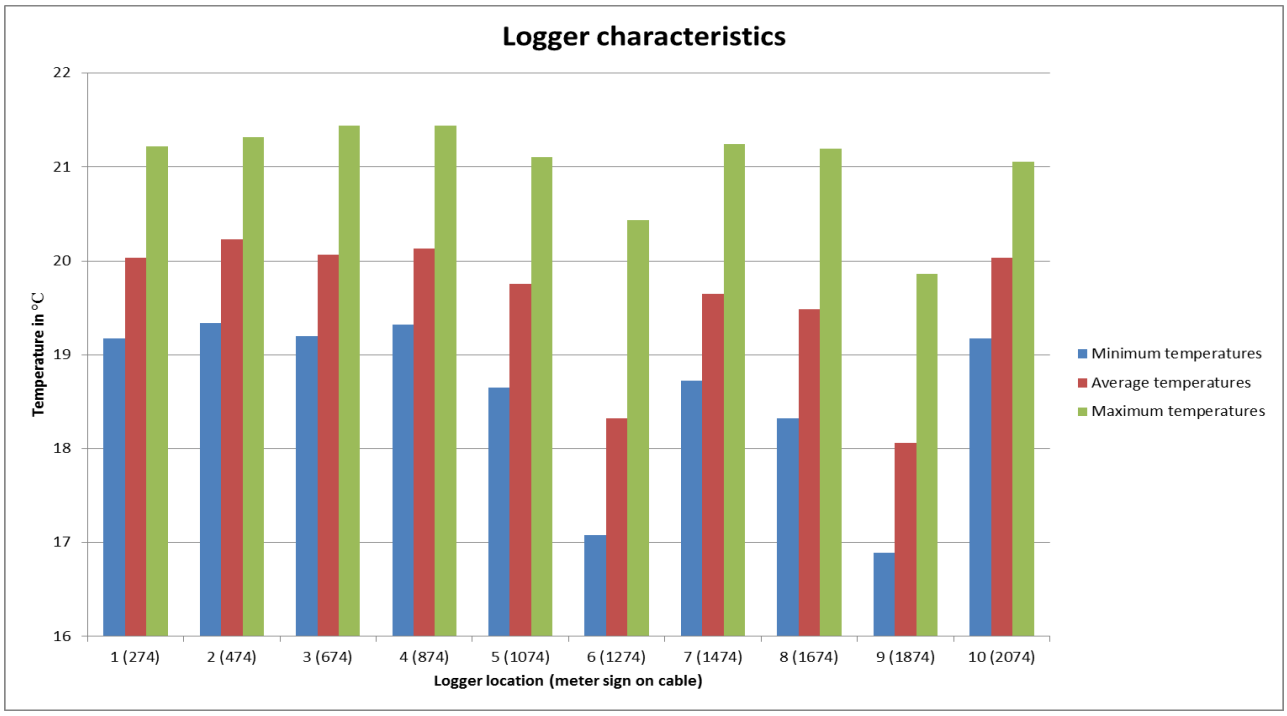

Figure 63: Found temperatures by the loggers. Location 6 and 9 were located in the cold area in the south east of Whakaipo Bay

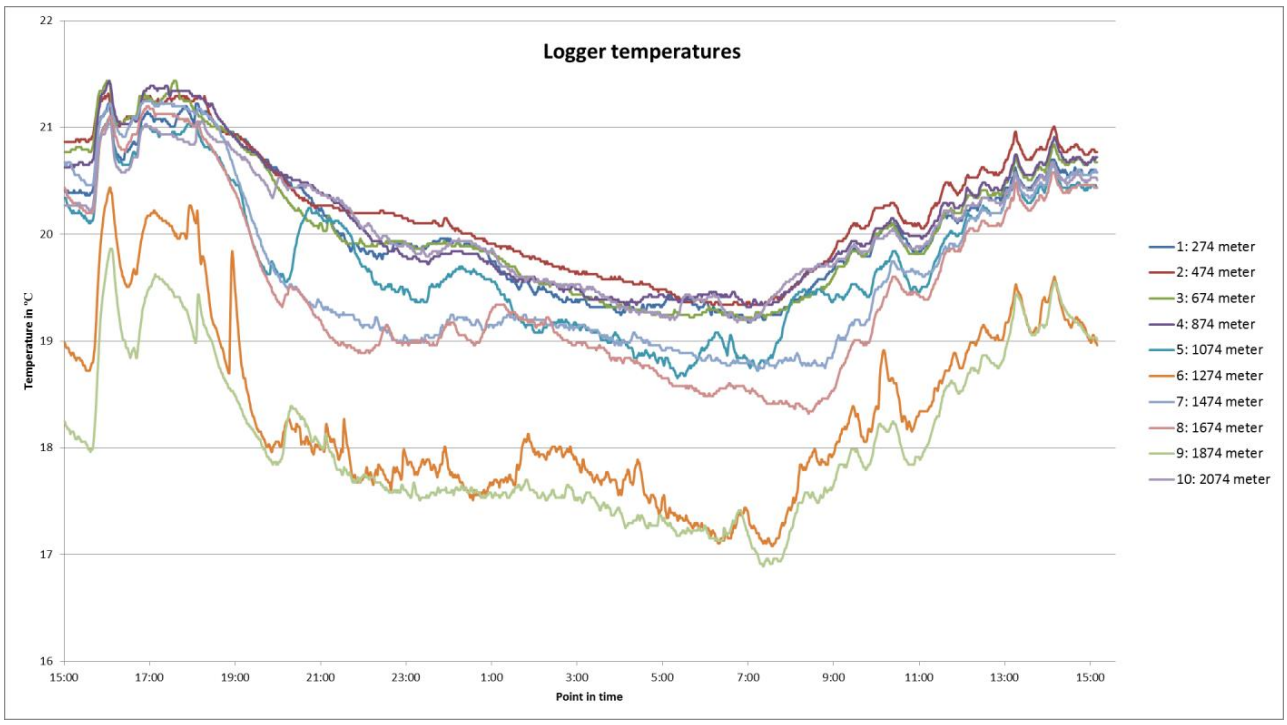

Figure 64: Logger temperatures for each logger location on near-shore horizontal DTS cable

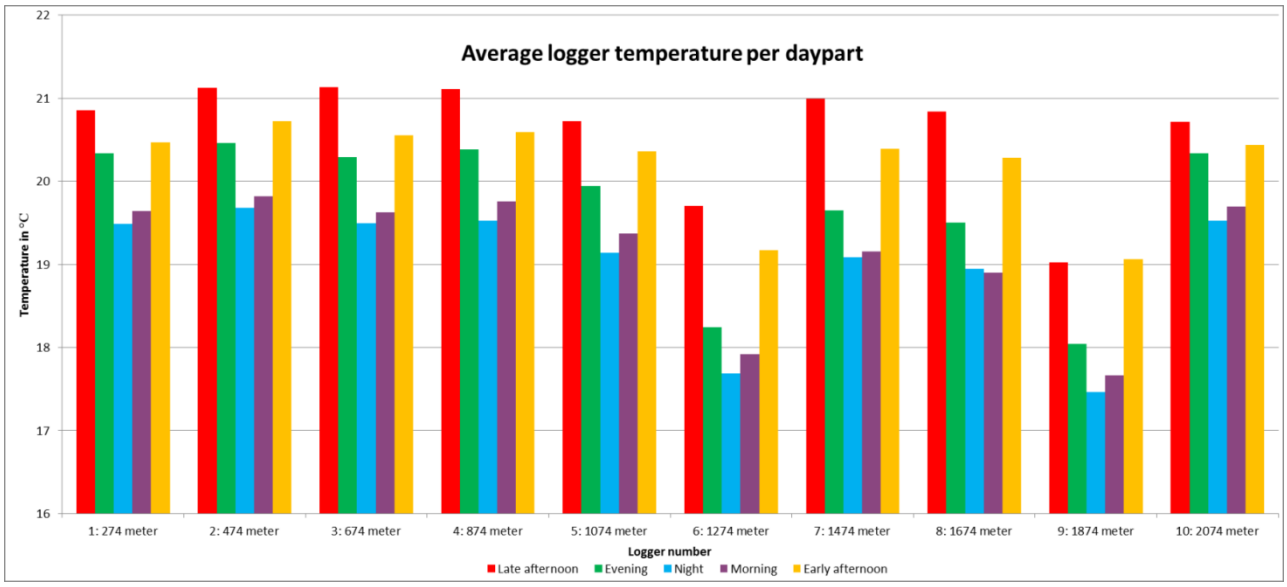

Figure 65: Average logger temperatures per day-part on near-shore horizontal DTS logger locations

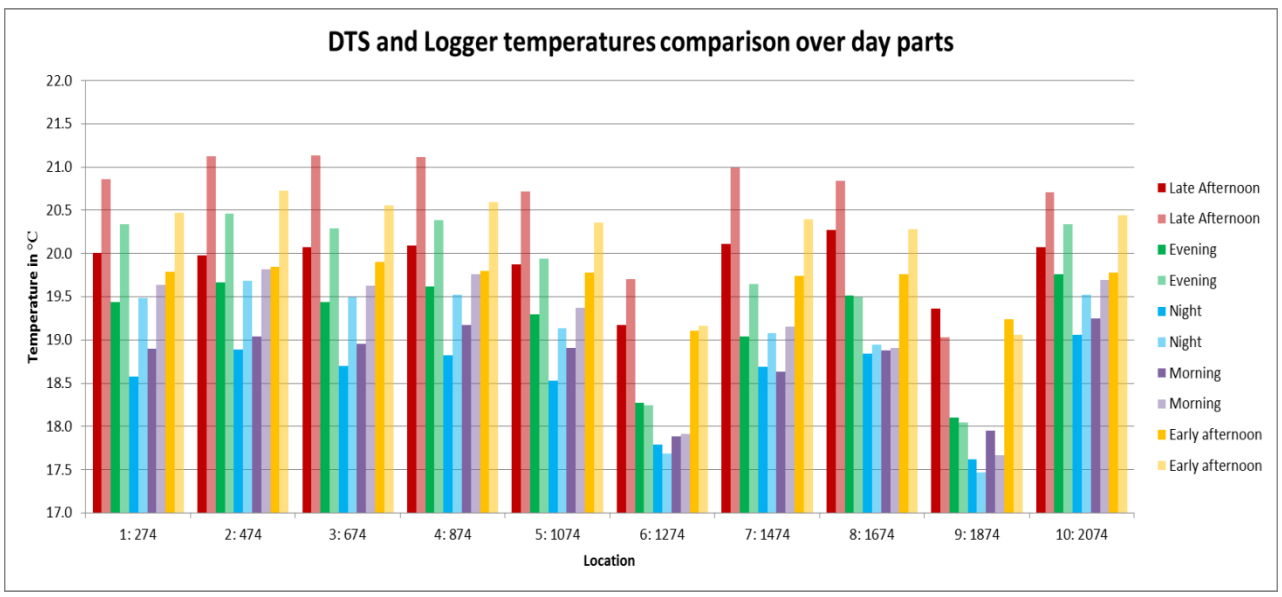

Figure 66: Comparison between DTS and logger temperatures of the near-shore horizontal DTS measurements. Bright = DTS, 50% transparent = Logger

Appendix F: Vertical DTS measurements

Table 20: Coordinates of Vertical DTS locations

Nr	Date	Day part	Coordinates S	Coordinates E	WP nr	Depth
1	2/4/14	Afternoon	38°40'57.67"S	175°57'20.96"E	248	1.20
2	10/4/14	Early afternoon	38°41'11.06"S	175°57'46.32"E	245	1.10
3	10/4/14	Late morning	38°41'13.28"S	175°57'48.43"E	247	1.20
4	13/2/15	Morning	38°41'13.61"S	175°57'49.31"E	332	1.40
5a	13/2/15	Afternoon	38°41’14.81”S	175°57’50.36”E	333	1.60
6	19/2/15	Early morning	38°41’02.99”S	175°57’34.08”E	341	1.20
7	19/2/15	Early afternoon	38°41’02.31”S	175°57’32.81”E	342	1.25
8	19/2/15	Late afternoon	38°41’07.00”S	175°57’40.29”E	344	1.10
5b	25/2/15	Morning	38°41'14.81"S	175°57'50.63"E	346	1.10
9	25/2/15	Afternoon	38°41'17.93"S	175°57'53.32"E	348	1.10
10	10/3/15	Morning	38°40'58.12"S	175°57'24.90"E	No	1.25
11	10/3/15	Early afternoon	38°40'58.89"S	175°57'27.01"E	No	1.20
12	*10/3/15*	*Late afternoon*	*38°41'23.79"S*	*175°57'57.44"E*	*No*	*0.37*
13	20/3/15	Morning	38°41'12.43"S	175 57' 47.44"E	349	1.50
14	20/3/15	Early afternoon	38°41'12.33"S	175 57' 47.64"E	350	1.25

Figure 67: Set-up Vertical DTS measurements for all locations. A: LOC4 and LOC5a. B: LOC5B and 9. C: LOC6, LOC7 and LOC8. D: LOC10 and LOC11. E: LOC12. F: LOC13 and LOC14.

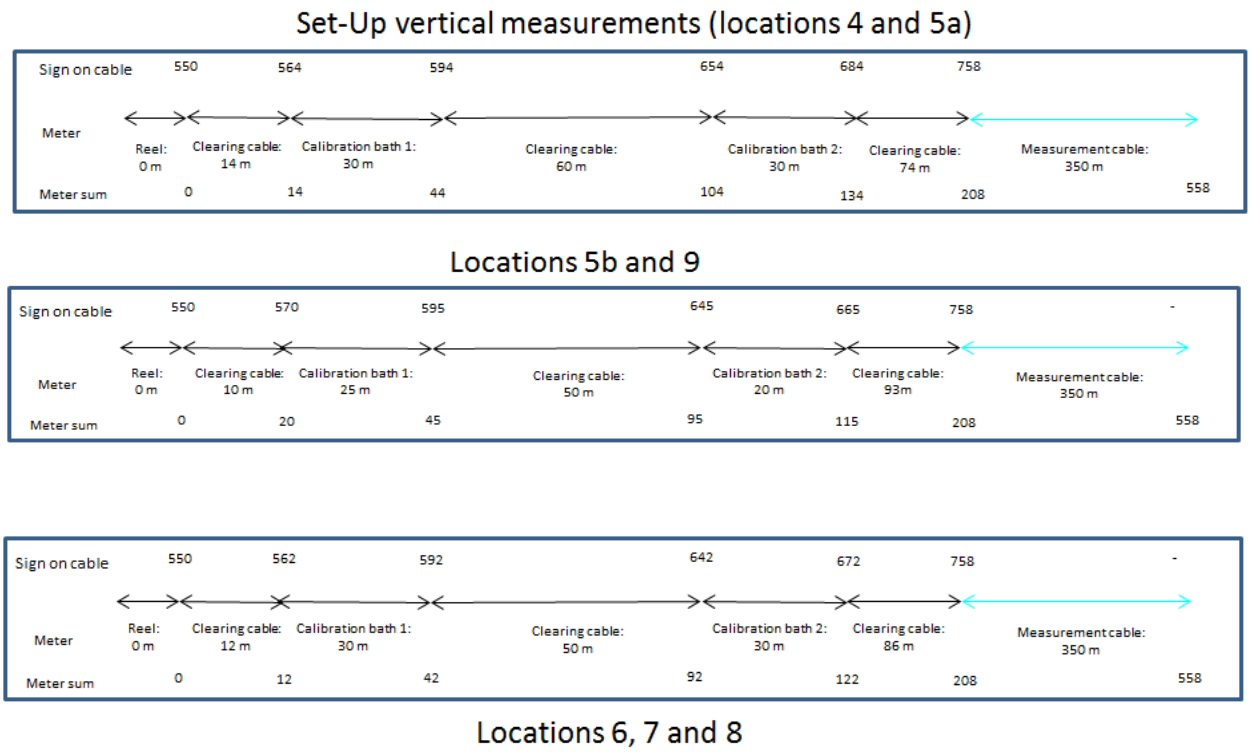

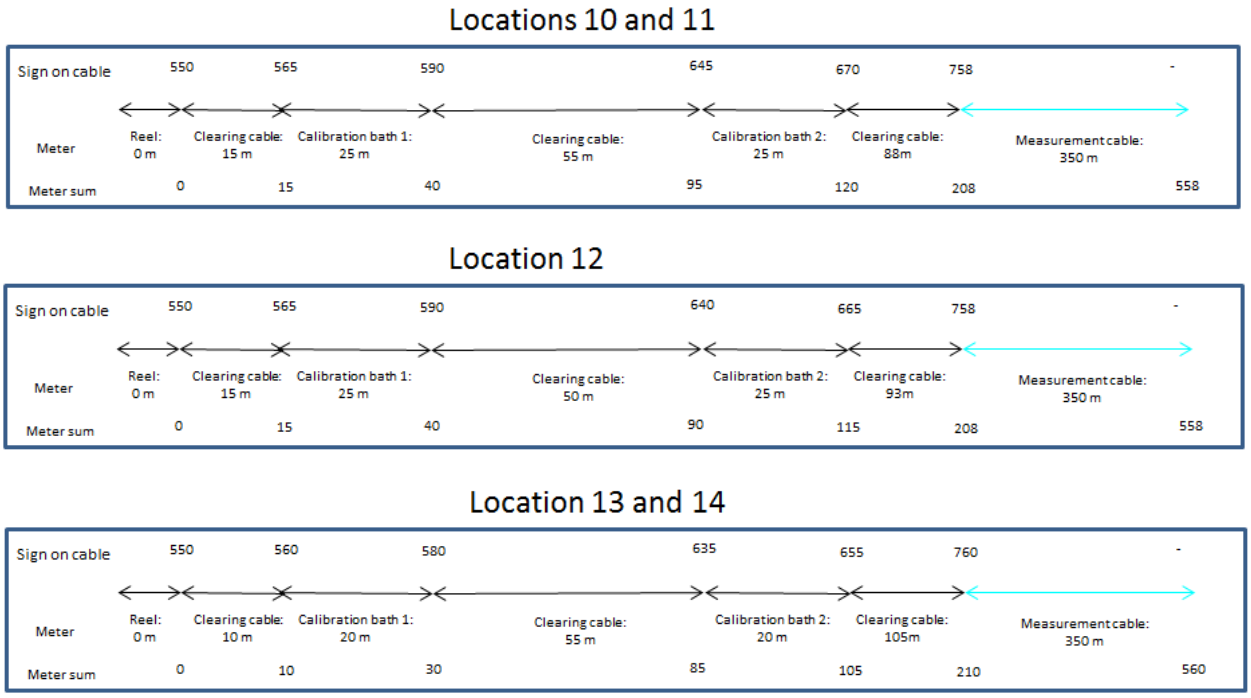

Figure 68: Top and bottom logger temperatures visualization for each location during vertical DTS measurement.

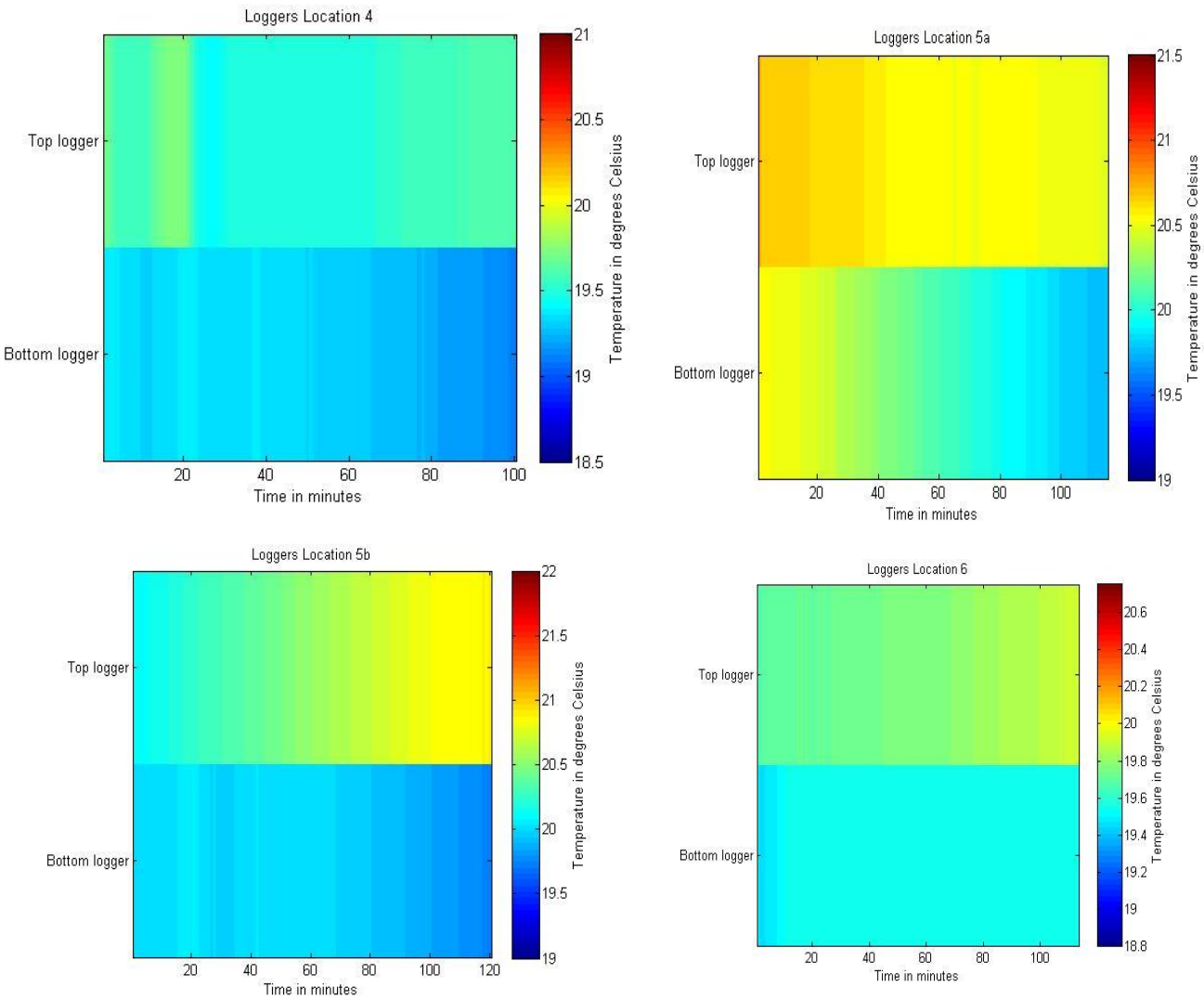

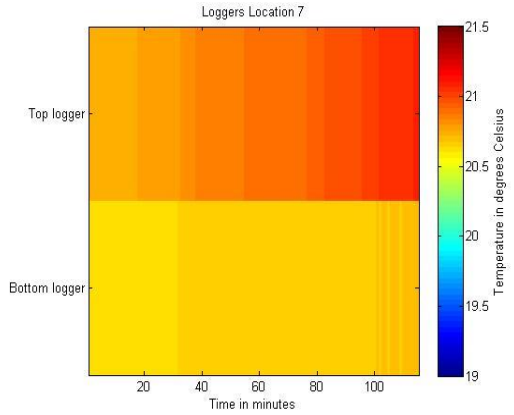
Loggers Location 7
Top logger
Bottom logger
20
40
60
80
100
Time in minutes
21.5
21
20.5
20
19.5
19
Temperature in degrees Celsius

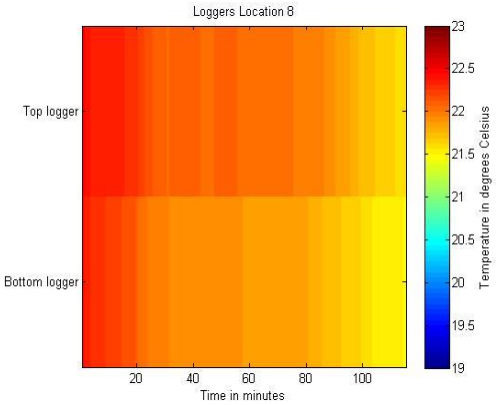
Loggers Location 8
Top logger
Bottom logger
20
40
60
80
100
Time in minutes
23
22.5
22
21.5
21
20.5
20
19.5
19
Temperature in degrees Celsius

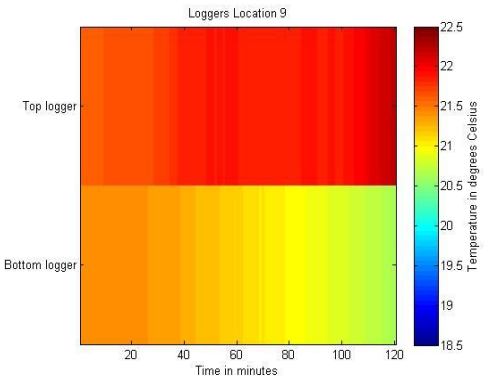
Loggers Location 9
Top logger
Bottom logger
20
40
60
80
100
120
Time in minutes
22.5
22
21.5
21
20.5
20
19.5
19
18.5
Temperature in degrees Celsius

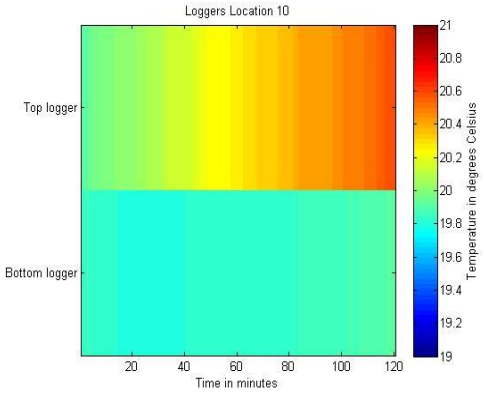
Loggers Location 10
Top logger
Bottom logger
20
40
60
80
100
120
Time in minutes
21
20.8
20.6
20.4
20.2
20
19.8
19.6
19.4
19.2
19
Temperature in degrees Celsius

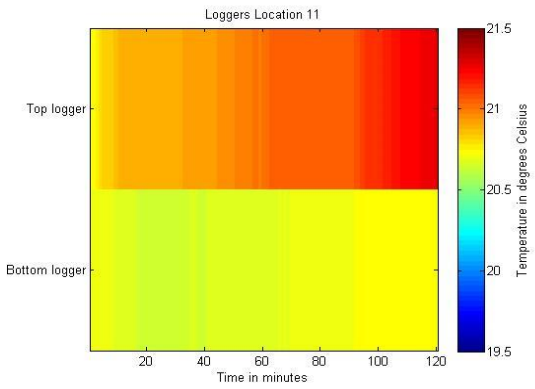
Loggers Location 11
Top logger
Bottom logger
20
40
60
80
100
120
Time in minutes
21.5
21
20.5
20
19.5
Temperature in degrees Celsius

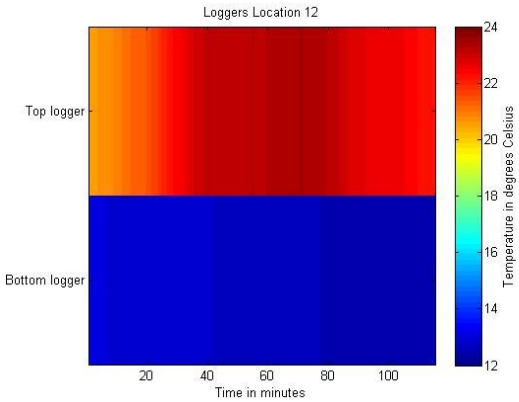
Loggers Location 12
Top logger
Bottom logger
20
40
60
80
100
Time in minutes
24
22
20
18
16
14
12
Temperature in degrees Celsius

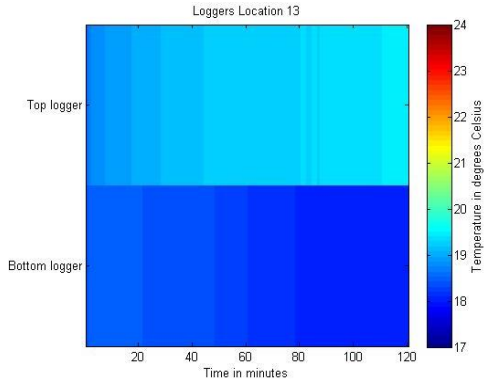
Loggers Location 13
Top logger
Bottom logger
20
40
60
80
100
120
Time in minutes
24
23
22
21
20
19
18
17
Temperature in degrees Celsius

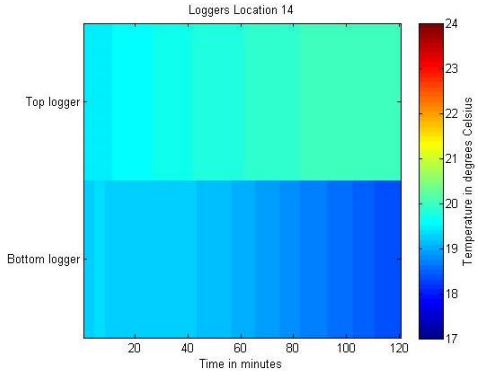
Loggers Location 14
Top logger
Bottom logger
20
40
60
80
100
120
Time in minutes
24
23
22
21
20
19
18
17
Temperature in degrees Celsius

Appendix G: Precipitation and evaporation data Mapara catchment

Table 21: Precipitation and evapotranspiration data (Mu et al., 2011; Tait et al., 2006; Westerhoff, 2015a; Westerhoff 2015b)

Nr	Coordi-nates E	Coordi-nates S	Precip. (mm/y)	Precip. (m/y)	Precip. area (m^3/y)	Actual evapotransp. (mm/y)	Actual evapotransp. (m/y)	Actual evapotransp. area (m^3/y)	Precipitation – Actual evapotranspiration
0	175,9242	-38,6936	1193	1.193	1,216,154	836	0.836	851,749	364,405
1	175,9245	-38,7027	1184	1.184	1,206,767	725	0.725	738,873	467,894
2	175,9354	-38,6842	1193	1.193	1,216,154	888	0.888	905,541	310,613
3	175,9466	-38,6749	1193	1.193	1,216,037	880	0.880	897,312	318,725
4	175,947	-38,684	1193	1.193	1,216,154	783	0.783	798,563	417,591
5	175,9578	-38,6655	1186	1.186	1,208,570	825	0.825	840,911	367,660
6	175,9582	-38,6746	1186	1.186	1,208,473	813	0.813	828,855	379,618
7	175,9593	-38,7018	1170	1.170	1,193,047	726	0.726	739,648	453,399
8	175,9694	-38,6652	1186	1.186	1,208,473	910	0.910	928,006	280,466
9	175,9698	-38,6743	1186	1.186	1,208,473	862	0.862	878,411	330,061
10	175,9702	-38,6834	1186	1.186	1,208,473	843	0.843	859,638	348,835
11	175,9706	-38,6925	1186	1.186	1,208,473	808	0.808	823,589	384,883
12	175,9806	-38,6558	1186	1.186	1,208,473	706	0.706	719,600	488,872
13	175,981	-38,6649	1186	1.186	1,208,473	846	0.846	861,878	346,595
14	175,9814	-38,674	1186	1.186	1,208,473	852	0.852	868,821	339,652
15	175,9818	-38,6831	1186	1.186	1,208,473	854	0.854	870,383	338,089
16	175,9822	-38,6922	1186	1.186	1,208,473	866	0.866	882,737	325,735
17	175,9919	-38,6464	1235	1.235	1,258,454	690	0.690	703,745	554,709
18	175,9922	-38,6555	1185	1.185	1,207,837	814	0.814	829,793	378,044
19	175,9926	-38,6646	1184	1.184	1,206,970	832	0.832	848,481	358,489
20	175,993	-38,6737	1184	1.184	1,207,045	860	0.860	877,100	329,945
21	175,9934	-38,6828	1185	1.185	1,207,476	838	0.838	854,034	353,441
22	175,9938	-38,6919	1185	1.185	1,207,681	825	0.825	840,585	367,097
23	176,0034	-38,6461	1227	1.227	1,250,670	841	0.841	857,377	393,293
24	176,0038	-38,6552	1157	1.157	1,179,314	834	0.834	850,586	328,728
25	176,0042	-38,6643	1157	1.157	1,179,314	830	0.830	846,422	332,892
26	176,0046	-38,6734	1157	1.157	1,179,314	822	0.822	837,440	341,873
27	176,005	-38,6825	1157	1.157	1,179,314	822	0.822	837,799	341,515
28	176,0054	-38,6916	1157	1.157	1,179,314	840	0.840	856,248	323,066
29	176,0057	-38,7007	1144	1.144	1,166,474	840	0.840	855,961	310,513
30	176,015	-38,6458	1219	1.219	1,242,528	905	0.905	922,217	320,311
31	176,0154	-38,6549	1157	1.157	1,179,314	882	0.882	898,761	280,553
32	176,0158	-38,664	1157	1.157	1,179,314	893	0.893	910,716	268,598
33	176,0162	-38,6731	1157	1.157	1,179,314	851	0.851	867,619	311,695
34	176,0166	-38,6822	1157	1.157	1,179,314	789	0.789	804,249	375,064
35	176,027	-38,6546	1157	1.157	1,179,314	851	0.851	867,416	311,898
36	176,0274	-38,6637	1157	1.157	1,179,314	860	0.860	876,794	302,519
37		**SUM**	**43,643**	**44**	**44,485,195**	**30,745**	**31**	**31,337,860**	**13,147,336**
		AVERAGE	**1180**	**1.180**	**1,202,303**	**831**	**0.831**	**846,969**	**355,333**

Q Mapara (L/s)	85
Q Mapara (m^3/y)	2,365,200
Number of points	37
Area m^2	1,019,292
Total area m^2	37,713,810
Area catchment	34,641,000
Total seepage flow Mapara catchment P-AET-Q (m^3/y)	**10,782,136**
% GW of total P-ET (Klinkenberg)	82
% GW of total P-ET (Hadfield)	81

Source of precipitation and evapotranspiration data:

Discharge Mapara Stream: Vant and Smith (2004)

Evapotranspiration data: Data is from the MOD16 data from the MODIS satellite (Mu et al., 2011). Data has been regridded, applied and tested in a New Zealand setting by Westerhoff (2015b).

Rainfall data: Source data is rainfall according to Tait et al. (2006), which were then regridded to the local setting by Westerhoff (2015a).